UNIVERSITY OF CALIFORNIA
RIVERSIDE

Roles of the RRM Domain Proteins EDM3 and IBM2 in Coordinating Immunity and Development in Arabidopsis

A Dissertation submitted in partial satisfaction
of the requirements for the degree of

Doctor of Philosophy

in

Plant Biology

by

Jianqiang Wang

December 2022

Dissertation Committee:
Dr. Thomas Eulgem, Chairperson
Dr. Xuemei Chen
Dr. Meng Chen

The Dissertation of Jianqiang Wang is approved:

_____

_____

_____

Committee Chairperson

University of California, Riverside

Acknowledgements

I would like to express my deepest gratitude to everyone who helped me during my PhD study. This endeavor would not have been possible without their help and support.

First and foremost, I would like to thank my advisor Dr. Thomas Eulgem for his guidance, patience, continuous support, and encouragement not only in the project but also in my daily life. He is one of the most knowledgeable scientists I have ever met. I would also like to thank my dissertation committee members Dr. Xuemei Chen and Dr. Meng Chen for their valuable advice and all the guidance they gave me. My special thanks to Dr. Xuemei Chen for generously providing us all the vectors for CRISPR/Cas9 system and the yeast strain AH109 that being used in this research project. I also appreciate all the support I received from the current and former members in Eulgem lab.

I would also like to express my sincere appreciation to all the committee members of my qualifying exam: Drs. Isgouhi Kaloshian, Xuemei Chen, Meng Chen, Carolyn Rasmussen, and Fedor Karginov; and the members of my guidance committee: Drs. Linda Walling and Daniel Koenig. In addition, I would also like to express my deep gratitude to my master advisor Dr. Zonghua Wang who has given me a lot of help, advice, and support

Finally, I would like to thank my parents, my sister, and my grandparents for their love, unceasing support, and encouragement throughout so many years.

ABSTRACT OF THE DISSERTATION

Roles of the RRM Domain Proteins EDM3 and IBM2 in Coordinating Immunity and Development in Arabidopsis

by

Jianqiang Wang

Doctor of Philosophy, Graduate Program in Plant Biology
University of California, Riverside, December, 2022
Dr. Thomas Eulgem, Chairperson

Abstract

The PHD finger protein EDM2 and the two RRM domain proteins EDM3 and IBM2 were shown to preferentially target genes that contain heterochromatin. In my thesis research, I found that only the longer IBM2 isoforms, IBM2L, interacts with both expressed EDM3 isoforms, EDM3S and EDM3L. These interactions positively regulate flowering time and negatively regulate basal immunity. Mutants of *EDM3* and *IBM2* exhibit a delay of gradually declined expression of the floral suppressor gene *FLC* during the progression of development. This is negatively correlated with a gradual increase of the transcript levels of the interacting EDM3 and IBM2 isoforms. Moreover, both EDM3L and IBM2L directly target certain defense-associated genes and suppress basal immunity. Lastly, these isoforms are also found to coordinate the

floral transition with a gradual repression of basal immunity. Collectively, these findings suggest a functional link between basal immunity and flowering time control. Both processes are clearly coordinated by EDM3L and IBM2L.

I further found that only IBM2L can co-localize with both EDM3 isoforms at the *COPIA-R7* retrotransposon within the plant immune receptor gene *RPP7*. Consistently, only IBM2L can rescue RPP7-mediated resistance against *Hyaloperonospora arabidopsidis* (*Hpa*) Hiks1 and expression levels of the full-length RPP7-coding transcripts.

Like mutants of *EDM2*, *edm3* and *ibm2* mutants also exhibit growth defects. We found that *EDM2*, *EDM3* and *IBM2* negatively regulate peroxidase activity by downregulating the expression levels of peroxidases. I further found that all three genes promote growth and negatively regulate basal immunity partly by inhibiting peroxidase activity. As growth defects in *edm2*, *edm3* and *ibm2* mutants are only partially rescued by suppression of peroxidase activity, there may exist other mechanisms coordinating immunity and growth. By crossing with the *sid2-2* and *pad4* mutants, which are deficient in SA-mediated immunity, and the transgenic *NahG* line, which cannot accumulate SA, growth defects in all three mutants are fully or partly rescued. Lastly, we also found that growth defects and enhanced basal immunity can be partly rescued by the longer IBM1 isoform, IBM1L. Collectively, my results show that EDM2, EDM3 and IBM2 have complex roles in coordinating immunity and developmental processes in Arabidopsis.

Table of Contents

List of Figures

List of Tables

Chapter 1

General Introduction

The Plant Immune System

Plant innate immunity depends on a network of functionally interconnected genes involved in the regulation and execution of defense reactions (Glazebrook *et al*, 2003; Tsuda *et al*, 2009). Two classes of plant immune receptors are critical for defense-activation (Jones & Dangl, 2006; Dodds & Rathjen, 2010). Pattern recognition receptors **(**PRRs**)** directly interact with microbe associated molecular patterns (MAMPs) activating pattern-triggered immunity **(**PTI**)** (Segonzac & Zipfel, 2011; Zipfel, 2014). PTI can be attenuated or blocked by effector molecules that are secreted into host cells by microbial pathogens (Abramovitch & Martin, 2004). The remaining weakened host immunity is called basal defense (Glazebrook *et al*, 2003). While it limits the spread of virulent pathogens/pests in their hosts, basal defense is often insufficient to fully prevent disease. A second class of plant immune receptors, encoded by disease resistance (*R*)-genes, recognize the presence of effectors and induce effector-triggered immunity **(**ETI**)**, a manifestation of gene-for-gene or race-specific resistance (Flor, 1956, 1971). R-genes typically encode nucleotide binding site & leucine-rich repeat-containing immune receptors (NLRs) (Jones *et al*, 2016). MAMPs are often critical for pathogen fitness and virulence. Thus, these

molecular patterns and their cognate receptors are typically widely conserved. In contrast, effectors and R-proteins/NLRs evolve quickly and are often specific for certain races of pathogens or plants, respectively.

Epigenetic Regulation of Intragenic Heterochromatin

Typically, DNA repeats and transposable elements (TEs) are primarily found in pericentromeric areas. They are heavily methylated at position 5 of their cytosines (Du *et al*, 2015), resulting in a tightly packed and transcriptionally silent chromatin state called heterochromatin. However, TEs and repetitive sequences can also be interspersed within euchromatin, gene-rich regions that are less-tightly packed and can be actively expressed. Such heterochromatic patches can be inserted in promoter regions, introns or intergenic regions (Lippman *et al*, 2004; Henderson & Jacobsen, 2008; Le *et al*, 2015). TEs can be deleterious if their expression and transposition is not inhibited. To maintain genome stability, they are usually enriched with cytosine methylation and silencing histone modifications (Erdmann & Picard, 2020). DNA methylation can occur in contexts of CG, CHG and CHH (where H is A, T or C). In *Arabidopsis thaliana* (Arabidopsis), the well-known RNA-directed DNA methylation (aka RdDM) pathway is employed to initiate methylation of cytosines at unmethylated DNA. This is mediated by heterochromatic siRNAs derived from repeats and TEs guiding RdDM to targeted regions converting them into silenced heterochromatic patches (Chen, 2009). Although intragenic TEs can be targeted by RdDM, their

silencing state can also be maintained in an RdDM independent manner (Le *et al*, 2015). Maintenance of DNA methylation requires different methyltransferases. Methyltransferase 1 (MET1) (Kankel *et al*, 2003) catalyzes methylation at CG sites through DNA replication independent of histone modifications (Stroud *et al*, 2013). Chromomethylase 2 (CMT2) is responsible for DNA methylation at CHH sites (Stroud *et al*, 2014), while chromomethylase 3 (CMT3) functions to maintain CHG methylation (Lindroth *et al*, 2001; Bartee *et al*, 2001). Both CMT2 and CMT3 are recruited by the histone mark H3K9me2 (di-methylation at lysine 9 of histone 3) to deposit DNA methylation. Meanwhile, methylated DNA can be recognized by KYP/SUVH4, a histone methyltransferase, which then catalyzes the methylation at lysine 9 of histone 3, thereby establishing a self-reinforcing loop (Du *et al*, 2015). Besides KYP/SUVH4, another two histone methyltransferases, SUVH5 and SUVH6, are also responsible for methylation of histone 3 lysine 9 (Jackson *et al*, 2002; Ebbs & Bender, 2006). On the contrary, IBM1 (short for Increase in BONSAI Methylation 1), a histone demethylase, exclusively removes H3K9me2 from genes but not transposons (Saze *et al*, 2008).

EDM2/EDM3/IBM2 Regulate Alternative Polyadenylation at Genes Containing Intragenic Heterochromatin

TEs, though transcriptionally silenced, can still influence surrounding genes affecting their expression and/or transcript processing (alternative splicing

or polyadenylation). Thus, mechanisms limiting such effects of TEs on gene expression appear to be very important. In Arabidopsis, around 3% of TEs reside within genes (Le *et al*, 2015). TEs located in or near genes can affect expression of these genes, by recruiting silencing DNA or histone modifications or creating new *cis* regulatory elements such as promoter elements, and polyadenylation signals. TEs can even duplicate genes and transfer them into different genomic contexts (Cowley & Oakey, 2013; Lisch, 2013). Consequently, TEs are believed to be major drivers of adaptive plant evolution. Although TEs are capable of benefiting genome evolution (Bennetzen & Wang, 2014), they can cause adverse effects by disrupting coding regions of genes or disturbing their proper expression control. Thus, restraining the transposition of TEs and maintaining normal expression of genes near TE insertions appears to be very important. Plants have evolved sophisticated mechanisms to properly express genes containing TE associated intragenic heterochromatin (see details below).

A protein complex, comprising Enhanced Downy Mildew 2 (EDM2), EDM3/AIPP1 (referred to as EDM3 hereafter) and IBM2/ASI1/SG1 (referred to as IBM2 hereafter), was identified to regulate genes that contain heterochromatic sequences (Tsuchiya & Eulgem, 2013b; Wang *et al*, 2013; Saze *et al*, 2013; Lei *et al*, 2014; Coustham *et al*, 2014; Duan *et al*, 2017; Lai *et al*, 2019). Originally EDM2 was found to be a critical regulator of the Arabidopsis NLR-type immune receptor RPP7. Both EDM2 and RPP7 are required for strong race-specific resistance of the Arabidopsis accession Col-0 to the Hiks1 isolate of the

pathogenic oomycete *Hyaloperonospora arabidopsidi*s (*Hpa*Hiks1) (Eulgem *et al*, 2007). The EDM2 protein bears an N-terminal replication foci domain (RFD), followed in its central parts by three PHD domains and a N6-adenine methyltransferase-like domain (Eulgem *et al*, 2007; Tsuchiya & Eulgem, 2010b). The PHD domain is capable of binding certain triple modifications of histone H3 *in vitro* (Tsuchiya & Eulgem, 2014). These histone marks are either associated with active transcription (H3K4me1, H3K4me2 or H3K4me3) or transcriptional repression (H3K9me2). EDM2 was further found to bind the H3K9me2-marked Long Terminal Repeat (LTR)-containing retrotransposon *COPIA-R7* within the first intron of the *RPP7* gene as well as heterochromatic repeats in the largest intron of the H3K9 demethylase gene *IBM1* (Tsuchiya & Eulgem, 2013b; Lei *et al*, 2014). Recruitment of EDM2 to these heterochromatic areas prevents the usage of promoter-proximal polyadenylation (poly(A)) sites located there, while promoting the usage of distal ones. At *RPP7* selection of the proximal poly(A) site results in expression of the long non-coding ECL (Exon1-containing LTR-terminated) transcript, while selection of the distal one in the 3'UTR of the gene leads to transcription of the full-length RPP7-coding transcript. TEs and repetitive sequences are enriched with the silencing marks H3K9me2 and methylated cytosine. As expected, high levels of these silencing marks are observed at *COPIA-R7* and the heterochromatic repeats at *IBM1* (Tsuchiya & Eulgem, 2013b; Saze *et al*, 2013; Lei *et al*, 2014). These marks have further spread into the intronic regions surrounding their source. In the *suvh4/5/6* triple mutant, which is

deficient in all three H3K9 methyltransferases, H3K9me2 levels at *COPIA-R7* and the surrounding intronic sequences are decreased resulting in increased use of poly(A) sites located in the 5'LTR of this transposon. Consequently, as in *edm2* mutants, levels of ECL transcripts are enhanced, levels of full-length RPP7 coding transcripts are reduced and resistance against *Hpa*Hiks1 is lost in this triple mutant (Tsuchiya & Eulgem, 2013b). While the *COPIA-R7* insertion into the first intron of *RPP7* is widely conserved among natural Arabidopsis accessions, it is absent in a small number of them, such as Krazo-2 and Koch-1. There is no H3K9me2 detectable in the first *RPP7* intron of these accessions. Although a functional Poly(A) site is conserved in Krazo-2 and Koch-1, its use and expression of *RPP7* are independent of EDM2 (Tsuchiya & Eulgem, 2013b). Clearly, insertion of *COPIA-R7* recruited an EDM2-and H3K9me2-dependent mechanism that fine-tunes *RPP7* expression by alternative polyadenylation. As stated above, EDM2 also regulates alternative polyadenylation at *IBM1* by binding to the heterochromatic repeats in its largest intron. Deletion of this heterochromatic repeats rescue the expression levels of the longer isoform of IBM1 (IBM1L) in *edm2* mutants (Lei *et al*, 2014), confirming that EDM2 controls IBM1 expression also dependent on the heterochromatic repeats.

Besides EDM2, the IBM2 protein was also reported by two groups to regulate *IBM1* and *RPP7* expression (Saze *et al*, 2013; Wang *et al*, 2013). IBM2 contains a N-terminal BAH (short for Bromo Adjacent Homology) domain and a C-terminal RRM (RNA Recognition Motif) domain. Like the EDM2 PHD domain,

the BAH domain was also reported to bind to certain histone marks such as H3K9me2 (Du *et al*, 2012) and H3K27me3 (Qian *et al*, 2018). Also like EDM2, IBM2 directly targets the heterochromatic repeats at *IBM1*, thereby suppressing the expression of the shorter isoform of IBM1 (IBM1S) and promoting the expression of IBM1L. Deletion of the heterochromatic repeats rescues IBM1L expression as well as DNA hypermethylation of IBM1 target genes in mutants of *IBM2*, indicating that, like EDM2, IBM2 regulates *IBM1* expression dependending on the intronic heterochromatic repeats. Besides *RPP7* and *IBM1*, EDM2 and IBM2 also regulate multiple other genes, such as AT3G05410 and AT1G11270, that contain intragenic heterochromatin by directly binding to them.

An additional RNA recognition motif (RRM)-containing protein, EDM3, was identified to join EDM2 and IBM2 in directly regulating *RPP7* and *IBM1* expression (Duan *et al*, 2017; Lai *et al*, 2019). EDM3 was shown to be a bridge protein that mediates physical interactions between EDM2 and IBM2. Moreover, like EDM2, EDM3 is required for *RPP7*-mediated *Hpa*Hiks1 resistance. As expected, EDM3 as well as EDM2 and IBM2 all co-localize at *COPIA-R7* within *RPP7* and the heterochromatic repeats at *IBM1* (Wang & Eulgem, unpublished), suppressing the usage of the proximal poly(A) site and facilitating preferential selection of the distal one (Lai et al., 2020). Furthermore, EDM3 as well as EDM2 were shown to physically associate with the RPP7 RNA segment that contains 5' LTR of the retrotransposon, where the proximal poly(A) signal is located (Lai et al., 2020). As mentioned above, EDM2 has a putative N^6-adenine

methyltransferase domain, which suggests a possible role on 3' end formation of mRNAs (Parker *et al*, 2020). Therefore, it is possible that EDM2 suppresses the promoter-proximal poly(A) site by affecting the 3'end processing of the *ECL* transcript. However, more research on details of this putative mechanism is needed. Another possible explanation could be that EDM2, EDM3 and IBM2 facilitate passing of the transcription machinery through the H3K9me2 marked retrotransposon at *RPP7* and heterochromatic repeats at *IBM1*. In mutants of *EDM2* and *IBM2*, the ratio of total RNA polymerase II (Pol II) occupancy between regions upstream and downstream of the heterochromatic regions of *RPP7* and *IBM1* was shown to be similar to that in their wild type parents (Saze *et al*, 2013; Lei *et al*, 2014), suggesting that both EDM2 and IBM2 do not affect transcriptional read-through in these heterochromatic areas. However, Lai and co-workers (Lai *et al*, 2019) showed that occupancy of Pol II C-terminal domain (CTD) ser2 phosphorylation (Ser2p) instead of total Pol II is increased around the 3'end of the *ECL* region in mutants of *EMD2* and *EDM3* by using an Anti-Pol II antibody that specifically recognizes phosphorylated Ser2 of the Pol II CTD, a form that is typically actively elongating transcripts. It was reported that Ser2p levels increase throughout gene bodies and peak at their 3'end (Chen *et al*, 2018). It was also reported that Pol II pauses in human cells after transcription of poly(A) signals, causing phosphorylation of Ser2 by Cdk12 (Davidson *et al*, 2014). Thus, an increase of Pol II CTD Ser2p might imply Pol II pausing around

the *ECL* poly(A) site. Consequently, EDM2/EDM3/IBM2 may inhibit the pathway that causes Pol II to pause.

Overall, these data have established that EDM2/EDM3/IBM2 preferentially target genes that contain intragenic heterochromatin to suppress proximal transcript polyadenylation and to facilitate the usage of the distal poly(A) site by an unknown mechanism.

Genome Wide Effects of EDM2/EDM3/IBM2 on CHG Methylation and H3K9me2

EDM2, EDM3 and IBM2 all have similar effects on genome-wide levels of CHG methylation, which were found to overall increase in mutants of each of these three genes (Tsuchiya & Eulgem, 2013a; Saze *et al*, 2013; Wang *et al*, 2013; Lei *et al*, 2014; Coustham *et al*, 2014; Duan *et al*, 2017). For each of the tested mutants the majority of differentially methylated regions identified by genome-wide bisulfite sequencing were hypermethylated, while only a few were found to be hypomethylated. The majority of CHG-hypermethylated regions are located within genes, suggesting that EDM2, EDM3 and IBM2 prevent CHG methylation mainly in gene bodies. Similarly, increased levels of CHG methylation and H3K9me2 in gene bodies were also reported for *ibm1* mutant plants (Saze *et al*, 2008). In contrast, levels of CHG and CHH methylation at TEs in mutants of *EDM2*, *IBM2* and *IBM1* were found to decrease, while there is no pronounced difference of DNA methylation of TEs in *edm3* mutants compared to

wild type plants. *EDM2*, *IBM2* and *EDM3* share most of the hypermethylated regions with *IBM1* (90% in *edm2-4* and 81% in *ibm2*). Since EDM2, EDM3 and IBM2 promote the expression of IBM1L by directly targeting its intronic heterochromatin, these observations suggest that all three genes likely prevent CHG methylation via IBM1L. In fact, when proper IBM1L expression levels were restored by deletion of the heterochromatic repeat in this gene in the mutants of *EDM2* and *IBM2*, DNA hypermethylation at some tested genes were suppressed, indicating that EDM2 and IBM2 function upstream of IBM1 to prevent CHG methylation in gene bodies. Besides *ibm1-4*, *edm2* and *ibm2* mutants also have some hypermethylated regions in common with a triple mutant, *ros1/dml2/dml3*, which are deficient in three related 5-methylcytosine DNA glycosylases preventing TEs and repeats from hypermethylation (Agius *et al*, 2006; Penterman *et al*, 2007; Ortega-Galisteo *et al*, 2008).

Accumulation of CHG methylation in mutants of *EDM2*, *IBM2* and *IBM1* requires KYP/SUVH4 and CMT3 (Tsuchiya & Eulgem, 2013a; Saze *et al*, 2013, 2008), which are known to maintain the self-reinforcement loop between CHG methylation and H3K9me2. Besides preventing ectopic accumulation of genic CHG methylation, EDM2 and EDM3 also affect the genome-wide distribution of H3K9me2 (Lai *et al*, 2019, 2020). Consistent with the effects of EDM2, EDM3 and IBM2 on genic CHG methylation (Tsuchiya & Eulgem, 2013a; Saze *et al*, 2013; Wang *et al*, 2013; Lei *et al*, 2014; Coustham *et al*, 2014; Duan *et al*, 2017), a large number of genes associated with H3K9 hyper-dimethylated regions were

identified (~98% in *edm2-2* and ~99% in *edm3-1*), while only a few genes associated with H3K9 hypo-dimethylation were observed. Although it remains unknown if genes that are surrounded by high levels of H3K9me2 in *edm2* and *edm3* mutants are also hypermethylated at CHG sites, it can be speculated that there is extremely likely a large overlap as CHG normally correlates with H3K9me2 (Inagaki *et al*, 2010). A large overlap of genes that are associated with high or low levels of H3K9me2 were found between *ibm1* and *edm2* mutants. However, while it seems EDM2 controls H3K9me2 indirectly via IBM1L, a large number of genes and TEs that are co-affected by IBM1 and EDM2 are directly targeted by EDM2, suggesting cooperative effects of IBM1 and EDM2 on H3K9me2 at some loci. Although IBM1 was reported to prevent CHG methylation mainly in gene bodies, many TEs were observed to have substantial changes in H3K9me2 levels in *ibm1* mutant plants. EDM2 and EDM3 affect H3K9me2 at TEs as well. Many of the TEs were observed to have higher levels of H3K9me2 in the *edm2-2* mutant, while only a few of them were found to have lower levels.

EDM2/EDM3/IBM2-Interacting Proteins and Their Effects on Plant Development and Immunity

EDM2 is not working alone but needs protein partners to exert its functions. EDM2 is found to interact in the nucleus with the serine/threonine protein kinase WNK8 (Tsuchiya & Eulgem, 2010b). The interaction between EDM2 and WNK8 is mediated by the EDM2 PGR domain (a plant G***γ***-like related

protein-protein interaction domain). Further experiment shows that WNK8 is capable of phosphorylating EDM2. Disruption of WNK8 causes early flowering compared to wild-type, while *edm2* mutants flowers later than wild-type. Consistently, the expression levels of *FLC*, encoding a floral repressor, is upregulated in *edm2* mutant but decreased in *wnk8* plants. An epistatic analysis shows that an *edm2*;*wnk8* double mutant flowered later than wild-type plants, but exhibited similar flowering times like *edm2*, indicating that WNK8 functions upstream of EDM2. In contrast, an *edm2*;*flc*, double mutant flowered earlier than wild-type mimicking the early flowering phenotype of *flc* single mutants, implying that FLC acts downstream of EDM2. Overall, WNK8 phosphorylates EDM2, possibly causing inactivation of EDM2, which releases inhibition of *FLC* expression, thereby delaying the floral transition. Besides regulating flowering time, EDM2 and WNK8 also have an effect on plant fitness as both mutants show lower fresh weight compared to wild-type plants. By looking closer into their leaf epidermis architecture, both mutants exhibited abnormal leaf pavement cells, lacking lobes and indentations (Tsuchiya & Eulgem, 2010a). Consequently, EDM2 and WNK8 positively regulate plant fitness and morphology of leaf pavement cells, which is in contrast to their counter-directional effects on the floral transition. Although EDM2 and WNK8 cooperate in some developmental processes, in other cases EDM2 functions independently from this protein kinase (Tsuchiya & Eulgem, 2010a). For example, vegetative phase transition is clearly delayed in *edm2* mutants while WNK8 has no effects on this process.

Furthermore, EDM2 promotes *RPP7*-mediated disease resistance against *Hpa*Hiks1 while WNK8 has no effects on this mechanism (Tsuchiya & Eulgem, 2010b).

EDM2 is also found to interact in plant nuclei with at least two EMSY-like proteins (EML), *At*EML1 and *At*EML2 (Tsuchiya & Eulgem, 2011). Interestingly, the central Agenet domain in *At*EML is likely involved in chromatin regulation like EDM2 (Maurer-Stroh *et al*, 2003; Ramos *et al*, 2006). Single mutants of either *AtEML1* and *AtEML2* show full resistance to *Hpa*Hiks1, while this immune mechanism is strongly compromised in *edm2* mutants. However, a *eml1*;*eml2* double mutant exhibits a remarkable decrease of *Hpa*Hiks1 resistance compared to wild-type. Moreover, three independent quadruple mutants, in which *AtEML3* and *AtEML4* are co-silenced via RNA interference (RNAi) in *eml1*;*eml2*, *eml-quad-1*, *eml-quad-2* and *eml-quad-3*, show more pronounced reduction of *Hpa*Hiks1 resistance than *eml1*;*eml2* double mutant, suggesting that *AtEML1*, *AtEML2* as well as *AtEML3* and/or *AtEML4* have redundant functions in regulating *RPP7*-mediated *Hpa*Hiks1 resistance. *AtEML* genes also positively regulate basal immunity since their quadruple mutants are more susceptible to *Hpa*Noco2, an *Hpa* strain that is virulent to Col-0. Because neither *AtEML* single mutants, nor the *eml1*;*eml2* double mutant show significant differences regarding basal defense against *Hpa*Noco2 compared to wild type plants, *AtEML* genes also play redundant roles on basal immunity. Thus, *AtEML* genes not only promote *RPP7*-mediated immunity but also enhance basal immunity, indicating

that *At*EMLs have a broad role in plant defense. It is interesting that EDM2, in contrast to *At*EMLs, suppresses basal immunity. EDM2 likely executes this role by down-regulating expression of a large number of NLR genes (Lai *et al*, 2020). It appears that *At*EMLs counteract EDM2 function on basal immunity. Thus, *At*EMLs and EDM2 may act as an "immune buffer" to prevent extremely high or extremely low overall levels of immune responses. An important question to be addressed in the future is how *At*EMLs and EDM2 maintain immune balance. Since *At*EMLs are also likely involved in chromatin regulation, their effects on basal immunity could be genome-wide.

Several interactors of IBM2 were also identified in the past (Duan *et al*, 2017). These include the Pol II CTD phosphatase CPL2, the plant homeodomain-containing protein AIPP2, and the BAH domain protein, AIPP3. These direct IBM2 interaction partners seem to counter the roles of IBM2, EDM2 and EDM3 in RNA processing (Duan et al., 2017). However, details of their roles in this context are still unknown.

EDM2/EDM3/IBM2 Homologs in Rice

There are eight *EDM2* orthologs in rice (Eulgem *et al*, 2007), termed *OsELP* (*EDM2-Like Protein*) *1-8*, among which *OsELP2* (You *et al*, 2021) and *OsELP3* (Ma *et al*, 2021) have been described. The *Os*ELP3 protein lacks the PHD-fingers and PGR domains characteristic for this group of proteins and contains only an N^6-adenine methyltransferase-like domain (Eulgem *et al*, 2007),

suggesting a possible function on N^6-methyladenosine (m^6A) modification of RNA. Both m^6A methylation assays and methylated RNA immunoprecipitation sequencing (MeRIP-seq), which were carried out in anthers at meiosis stage, show lower levels of m^6A in an *Oselp3* mutant compared to wild-type plants. Thus, *Os*ELP3 affects m6A modification in anthers. However, whether *Os*ELP3 has N6-adenine methyltransferase activity still needs to be addressed in future studies. Program cell death (PCD) of the tapetum of anther was observed to be delayed in *OsELP3* mutant plants, leading to defective pollen development, which is likely caused by downregulation of *EAT1* that controls tapetal programmed cell death (Niu *et al*, 2013). Further experiments show that *Os*ELP3 interacts with bHLH142 and TDR which regulate *EAT1* expression by targeting its promoter area (Ko *et al*, 2014). Moreover, *OsELP3* also affects alternative splicing and alternative polyadenylation of *EAT1* transcripts, which is possibly associated with low levels of m^6A in the 3'UTR of *EAT1* in *Oselp3* mutant. Consequently, OsELP3 likely regulates *EAT1* expression in both transcriptional and post-transcriptional mechanisms.

IBM2 has also been characterized in rice (You *et al*, 2021). *Os*IBM2 positively regulates pollen development, rice heading date, seed setting rate and miRNA abundance, partially via promoting the expression of an XRN-like exonuclease, *OsXRNL*. Like IBM2 in Arabidopsis, *Os*IBM2 also regulates alternative polyadenylation, especially for those alternative polyadenylation sites associated with high density of repressive histone marks, H3K9me2 and

H3K27me3, and downstream areas of polyadenylation sites that are enriched with high DNA cytosine methylation levels regardless of cytosine contexts. Alternative polyadenylation at *OsXRNL* is also regulated by OsIBM2, which facilitates the usage of the distal polyadenylation site, promoting expression of *OsXRNL* full length transcripts, while suppressing the usage of the promoter-proximal one, causing downregulation of the short transcripts by targeting to the intragenic heterochromatin in its largest intron. Thus, like IBM2 in Arabidopsis, *Os*IBM2 also prefers to regulate alternative polyadenylation at intragenic heterochromatin-containing genes.

Two EDM3 (aka AIPP1) homologs (*Os*AIPP1a and *Os*AIPP1b) and one EDM2-like protein (*Os*ELP2) were pulled down by *Os*IBM2 immunoprecipitation. In Arabidopsis, the interaction between IBM2 and EDM2 requires EDM3. Similarly in rice, *Os*IBM2 cannot interact with *Os*ELP2, which likely requires *Os*AIPP1 as well. However, both *Os*AIPP1a and *Os*AIPP1b interact with *Os*IBM2 and *Os*ELP2, respectively. Like *Os*IBM2, *Os*ELP2 and *Os*AIPP1 also positively regulate pollen development, seed setting rate and rice heading date (You *et al*, 2021). Lower expression levels of *Os*XRNL full length transcripts and ectopic accumulation of the shorter ones were observed in mutants of *Os*AIPP1a and *Os*ELP2 as well, suggesting that *Os*AIPP1a and *Os*ELP2 likely also regulate those developmental processes via *Os*XRNL.

References

Abramovitch RB & Martin GB (2004) Strategies used by bacterial pathogens to suppress plant defenses. *Curr Opin Plant Biol* 7: 356–364

Agius F, Kapoor A & Zhu J-K (2006) Role of the Arabidopsis DNA glycosylase/lyase ROS1 in active DNA demethylation. *Proc Natl Acad Sci U S A* 103: 11796–11801

Bartee L, Malagnac F & Bender J (2001) Arabidopsis cmt3 chromomethylase mutations block non-CG methylation and silencing of an endogenous gene. *Genes Dev* 15: 1753–1758

Bennetzen JL & Wang H (2014) The contributions of transposable elements to the structure, function, and evolution of plant genomes. *Annu Rev Plant Biol* 65: 505–530

Chen FX, Smith ER & Shilatifard A (2018) Born to run: control of transcription elongation by RNA polymerase II. *Nat Rev Mol Cell Biol* 19: 464–478

Chen X (2009) Small RNAs and their roles in plant development. *Annu Rev Cell Dev Biol* 25: 21–44

Coustham V, Vlad D, Deremetz A, Gy I, Cubillos FA, Kerdaffrec E, Loudet O & Bouché N (2014) SHOOT GROWTH1 maintains Arabidopsis epigenomes by regulating IBM1. *PLoS One* 9: e84687

Cowley M & Oakey RJ (2013) Transposable elements re-wire and fine-tune the transcriptome. *PLoS Genet* 9: e1003234

Davidson L, Muniz L & West S (2014) 3’ end formation of pre-mRNA and phosphorylation of Ser2 on the RNA polymerase II CTD are reciprocally coupled in human cells. *Genes Dev* 28: 342–356

Dodds PN & Rathjen JP (2010) Plant immunity: towards an integrated view of plant–pathogen interactions. *Nat Rev Genet* 11: 539–548

Duan C-G, Wang X, Zhang L, Xiong X, Zhang Z, Tang K, Pan L, Hsu C-C, Xu H, Tao WA, *et al* (2017) A protein complex regulates RNA processing of intronic heterochromatin-containing genes in Arabidopsis. *Proc Natl Acad Sci U S A* 114: E7377–E7384

Du J, Johnson LM, Jacobsen SE & Patel DJ (2015) DNA methylation pathways and their crosstalk with histone methylation. *Nat Rev Mol Cell Biol* 16: 519–532

Du J, Zhong X, Bernatavichute YV, Stroud H, Feng S, Caro E, Vashisht AA, Terragni J, Chin HG, Tu A, *et al* (2012) Dual binding of chromomethylase domains to H3K9me2-containing nucleosomes directs DNA methylation in plants. *Cell* 151: 167–180

Ebbs ML & Bender J (2006) Locus-specific control of DNA methylation by the Arabidopsis SUVH5 histone methyltransferase. *Plant Cell* 18: 1166–1176

Erdmann RM & Picard CL (2020) RNA-directed DNA Methylation. *PLOS Genetics* 16: e1009034 doi:10.1371/journal.pgen.1009034 [PREPRINT]

Eulgem T, Tsuchiya T, Wang X-J, Beasley B, Cuzick A, Tör M, Zhu T, McDowell JM, Holub E & Dangl JL (2007) EDM2 is required for RPP7-dependent disease resistance in Arabidopsis and affects RPP7 transcript levels. *Plant J* 49: 829–839

Flor HH (1956) The complementary genic systems in flax and flax rust. In *Advances in Genetics*, Demerec M (ed) pp 29–54. San Diego, CA: Elsevier

Flor HH (1971) Current status of the gene-for-gene concept. *Annu Rev Phytopathol* 9: 275–296

Glazebrook J, Chen W, Estes B, Chang H-S, Nawrath C, Métraux J-P, Zhu T & Katagiri F (2003) Topology of the network integrating salicylate and jasmonate signal transduction derived from global expression phenotyping. *Plant J* 34: 217–228

Henderson IR & Jacobsen SE (2008) Tandem repeats upstream of the Arabidopsis endogene SDC recruit non-CG DNA methylation and initiate siRNA spreading. *Genes Dev* 22: 1597–1606

Inagaki S, Miura-Kamio A, Nakamura Y, Lu F, Cui X, Cao X, Kimura H, Saze H & Kakutani T (2010) Autocatalytic differentiation of epigenetic modifications within the Arabidopsis genome. *EMBO J* 29: 3496–3506

Jackson JP, Lindroth AM, Cao X & Jacobsen SE (2002) Control of CpNpG DNA methylation by the KRYPTONITE histone H3 methyltransferase. *Nature* 416: 556–560

Jones JDG & Dangl JL (2006) The plant immune system. *Nature* 444: 323–329

Jones JDG, Vance RE & Dangl JL (2016) Intracellular innate immune surveillance devices in plants and animals. *Science* 354

Kankel MW, Ramsey DE, Stokes TL, Flowers SK, Haag JR, Jeddeloh JA, Riddle NC, Verbsky ML & Richards EJ (2003) Arabidopsis MET1 cytosine

methyltransferase mutants. *Genetics* 163: 1109–1122

Ko S-S, Li M-J, Sun-Ben Ku M, Ho Y-C, Lin Y-J, Chuang M-H, Hsing H-X, Lien Y-C, Yang H-T, Chang H-C, *et al* (2014) The bHLH142 Transcription Factor Coordinates with TDR1 to Modulate the Expression of EAT1 and Regulate Pollen Development in Rice. *Plant Cell* 26: 2486–2504

Lai Y, Cuzick A, Lu XM, Wang J, Katiyar N, Tsuchiya T, Le Roch K, McDowell JM, Holub E & Eulgem T (2019) The Arabidopsis RRM domain protein EDM3 mediates race-specific disease resistance by controlling H3K9me2-dependent alternative polyadenylation of RPP7 immune receptor transcripts. *Plant J* 97: 646–660

Lai Y, Lu XM, Daron J, Pan S, Wang J, Wang W, Tsuchiya T, Holub E, McDowell JM, Slotkin RK, *et al* (2020) The Arabidopsis PHD-finger protein EDM2 has multiple roles in balancing NLR immune receptor gene expression. *PLoS Genet* 16: e1008993

Lei M, La H, Lu K, Wang P, Miki D, Ren Z, Duan C-G, Wang X, Tang K, Zeng L, *et al* (2014) Arabidopsis EDM2 promotes IBM1 distal polyadenylation and regulates genome DNA methylation patterns. *Proc Natl Acad Sci U S A* 111: 527–532

Le TN, Miyazaki Y, Takuno S & Saze H (2015) Epigenetic regulation of intragenic transposable elements impacts gene transcription in Arabidopsis thaliana. *Nucleic Acids Research* 43: 3911–3921 doi:10.1093/nar/gkv258 [PREPRINT]

Lindroth AM, Cao X, Jackson JP, Zilberman D, McCallum CM, Henikoff S & Jacobsen SE (2001) Requirement of CHROMOMETHYLASE3 for maintenance of CpXpG methylation. *Science* 292: 2077–2080

Lippman Z, Gendrel A-V, Black M, Vaughn MW, Dedhia N, McCombie WR, Lavine K, Mittal V, May B, Kasschau KD, *et al* (2004) Role of transposable elements in heterochromatin and epigenetic control. *Nature* 430: 471–476

Lisch D (2013) How important are transposons for plant evolution? *Nat Rev Genet* 14: 49–61

Ma K, Han J, Zhang Z, Li H, Zhao Y, Zhu Q, Xie Y, Liu Y-G & Chen L (2021) OsEDM2L mediates m6A of EAT1 transcript for proper alternative splicing and polyadenylation regulating rice tapetal degradation. *J Integr Plant Biol* 63: 1982–1994

Maurer-Stroh S, Dickens NJ, Hughes-Davies L, Kouzarides T, Eisenhaber F & Ponting CP (2003) The Tudor domain 'Royal Family': Tudor, plant Agenet, Chromo, PWWP and MBT domains. *Trends Biochem Sci* 28: 69–74

Niu N, Liang W, Yang X, Jin W, Wilson ZA, Hu J & Zhang D (2013) EAT1 promotes tapetal cell death by regulating aspartic proteases during male reproductive development in rice. *Nat Commun* 4: 1445

Ortega-Galisteo AP, Morales-Ruiz T, Ariza RR & Roldán-Arjona T (2008) Arabidopsis DEMETER-LIKE proteins DML2 and DML3 are required for appropriate distribution of DNA methylation marks. *Plant Mol Biol* 67: 671–681

Parker MT, Knop K, Sherwood AV, Schurch NJ, Mackinnon K, Gould PD, Hall AJ, Barton GJ & Simpson GG (2020) Nanopore direct RNA sequencing maps the complexity of Arabidopsis mRNA processing and m6A modification. *Elife* 9

Penterman J, Zilberman D, Huh JH, Ballinger T, Henikoff S & Fischer RL (2007) DNA demethylation in the *Arabidopsis* genome. *Proceedings of the National Academy of Sciences* 104: 6752–6757 doi:10.1073/pnas.0701861104 [PREPRINT]

Qian S, Lv X, Scheid RN, Lu L, Yang Z, Chen W, Liu R, Boersma MD, Denu JM, Zhong X, *et al* (2018) Dual recognition of H3K4me3 and H3K27me3 by a plant histone reader SHL. *Nature Communications* 9 doi:10.1038/s41467-018-04836-y [PREPRINT]

Ramos A, Hollingworth D, Adinolfi S, Castets M, Kelly G, Frenkiel TA, Bardoni B & Pastore A (2006) The structure of the N-terminal domain of the fragile X mental retardation protein: a platform for protein-protein interaction. *Structure* 14: 21–31

Saze H, Kitayama J, Takashima K, Miura S, Harukawa Y, Ito T & Kakutani T (2013) Mechanism for full-length RNA processing of Arabidopsis genes containing intragenic heterochromatin. *Nat Commun* 4: 2301

Saze H, Shiraishi A, Miura A & Kakutani T (2008) Control of genic DNA methylation by a jmjC domain-containing protein in Arabidopsis thaliana. *Science* 319: 462–465

Segonzac C & Zipfel C (2011) Activation of plant pattern-recognition receptors by bacteria. *Curr Opin Microbiol* 14: 54–61

Stroud H, Do T, Du J, Zhong X, Feng S, Johnson L, Patel DJ & Jacobsen SE (2014) Non-CG methylation patterns shape the epigenetic landscape in Arabidopsis. *Nat Struct Mol Biol* 21: 64–72

Stroud H, Greenberg MVC, Feng S, Bernatavichute YV & Jacobsen SE (2013) Comprehensive analysis of silencing mutants reveals complex regulation of

the Arabidopsis methylome. *Cell* 152: 352–364

Tsuchiya T & Eulgem T (2010a) Co-option of EDM2 to distinct regulatory modules in Arabidopsis thaliana development. *BMC Plant Biology* 10: 203 doi:10.1186/1471-2229-10-203 [PREPRINT]

Tsuchiya T & Eulgem T (2010b) The Arabidopsis defense component EDM2 affects the floral transition in an FLC-dependent manner. *Plant J* 62: 518–528

Tsuchiya T & Eulgem T (2011) EMSY-like genes are required for full RPP7-mediated race-specific immunity and basal defense in Arabidopsis. *Mol Plant Microbe Interact* 24: 1573–1581

Tsuchiya T & Eulgem T (2013a) Mutations in EDM2 selectively affect silencing states of transposons and induce plant developmental plasticity. *Sci Rep* 3: 1701

Tsuchiya T & Eulgem T (2013b) An alternative polyadenylation mechanism coopted to the Arabidopsis RPP7 gene through intronic retrotransposon domestication. *Proc Natl Acad Sci U S A* 110: E3535–43

Tsuchiya T & Eulgem T (2014) The PHD-finger module of the Arabidopsis thaliana defense regulator EDM2 can recognize triply modified histone H3 peptides. *Plant Signal Behav* 9: e29202

Tsuda K, Sato M, Stoddard T, Glazebrook J & Katagiri F (2009) Network properties of robust immunity in plants. *PLoS Genet* 5: e1000772

Wang X, Duan C-G, Tang K, Wang B, Zhang H, Lei M, Lu K, Mangrauthia SK, Wang P, Zhu G, *et al* (2013) RNA-binding protein regulates plant DNA methylation by controlling mRNA processing at the intronic heterochromatin-containing gene IBM1. *Proc Natl Acad Sci U S A* 110: 15467–15472

You L-Y, Lin J, Xu H-W, Chen C-X, Chen J-Y, Zhang J, Zhang J, Li Y-X, Ye C, Zhang H, *et al* (2021) Intragenic heterochromatin-mediated alternative polyadenylation modulates miRNA and pollen development in rice. *New Phytol* 232: 835–852

Zipfel C (2014) Plant pattern-recognition receptors. *Trends Immunol* 35: 345–351

Chapter 2

Two Arabidopsis RRM Domain Proteins EDM3 and IBM2 Coordinate the Floral Transition and Basal Immunity

Abstract

The *Arabidopsis thaliana* (Arabidopsis) PHD finger protein EDM2 and the RRM domain proteins EDM3 and IBM2 are known to form chromatin-associated complexes controlling transcript processing. We are now reporting that interactions between EDM3 and IBM2 preferentially occur between distinct splice isoforms. These interacting isoforms control the intensity of basal immunity and, via a separate pathway, the timing of the floral transition, a developmental switch from vegetative to reproductive growth. Transcripts encoding interacting EDM3 and IBM2 isoforms strongly and gradually accumulate prior to the floral transition, while transcripts of the floral repressor gene *FLC* are down-regulated during the same period of time. The gradual reduction of *FLC* expression is dependent on the interacting EDM3 and IBM2 isoforms. Furthermore, these isoforms coordinate the timing of the floral transition with a gradual suppression of basal immunity and co-localize *in vivo* at various chromatin sites associated with basal immunity. We are providing clear evidence for a functional link between the floral transition and basal immunity in Arabidopsis. Coordination of these two biological

processes, which compete for metabolic resources, is likely critical for plant survival and reproductive success.

Introduction

Plant immune responses against pathogens are controlled by two interconnected layers of non-self-recognition mechanisms (Chisholm *et al*, 2006; Jones & Dangl, 2006). Pattern recognition receptor-mediated perception of conserved microbe associated molecular patterns (MAMPs) induces in plants pattern-triggered immunity (PTI). Host-adapted pathogens attenuate PTI by secreting effector molecules, suppressing this defense mechanism. The remaining weakened plant immune response during such compatible interactions, called basal immunity or basal defense (Glazebrook, 2001), limits the spread of virulent pathogens in their hosts, but is typically insufficient to fully prevent disease. In many cases plants have evolved disease resistance (R)-proteins, a second class of plant immune receptors besides pattern recognition receptors, that recognize effectors and activate effector-triggered immunity (ETI), a manifestation of race-specific resistance. ETI efficiently protects plants from avirulent pathogens during incompatible interactions. While pattern recognition receptors are typically plasma-membrane resident receptor-like protein kinases or receptor-like proteins (Zipfel, 2014), R-proteins are usually intracellularly localized proteins with a central nucleotide binding site and a C-terminal leucine-rich repeat (LRR) domain (Jones & Dangl, 2006). Such NLR proteins also

contain a variable N-terminal domain, such as coiled coil (CC) or toll-interleukine-1 receptor (TIR) domains.

Homeostasis of NLR activity is critical (Jacob *et al*, 2013; Li *et al*, 2015; Lai & Eulgem, 2018) and the stability of NLR proteins and their expression are strictly controlled (Lai & Eulgem, 2018). The efficiency of NLRs in sensing effectors and triggering immunity depends on their dose (Bieri *et al*, 2004; Holt *et al*, 2005), while NLR overexpression can result in autoimmunity and fitness penalties, such as reduced growth and impaired reproduction(Stokes *et al*, 2002; Li *et al*, 2007).

Regulatory pathways controlling ETI, PTI and basal immunity are highly intertwined and share numerous components, such as the defense hormone salicylic acid, as well as multiple signal transducers and transcription factors (Ngou *et al*, 2021; Lu & Tsuda, 2021; Yuan *et al*, 2021). While basal immunity seems mainly to be a weakened form of PTI, ETI has been proposed to result from boosted basal defense or PTI-associated responses (Tao *et al*, 2003; Jones & Dangl, 2006; Shen *et al*, 2007).

We previously reported on the *Arabidopsis thaliana* (Arabidopsis) defense regulator EDM2 (Eulgem *et al*, 2007), a protein with typical features of transcriptional and epigenetic regulators, including atypical PHD-finger motifs. EDM2 is nuclear localized and promotes expression of the R-protein RPP7. Both the *EDM2* and *RPP7* genes are required for race-specific resistance of Arabidopsis against the Hiks1 isolate of the pathogenic oomycete

Hyaloperonospora arabidopsidis (*Hpa*). Mutants of *EDM2* also exhibit developmental defects (Tsuchiya & Eulgem, 2010a, 2013a). Trans-generational variability and instability of such phenotypes implied roles of EDM2 in epigenetic processes (Tsuchiya & Eulgem, 2013a). Consequently, we found EDM2 to control silencing states of transposable elements (TEs) by modulating levels of di-methylated lysine 9 of histone H3 (H3K9me2), a ubiquitous epigenetic TE silencing signal in plants (Tsuchiya & Eulgem, 2013a; Lai *et al*, 2020). While at some loci EDM2 promotes high H3K9me2 levels, it mostly has a suppressive effect on this mark. The PHD finger-containing domain of EDM2 has a strong *in vitro*-binding preference for histone H3 carrying certain combinations of posttranslational modifications, but not single marks (Tsuchiya & Eulgem, 2014). Strikingly, strongly preferred by this domain are combinations between H3 marks associated with active transcription (H3K4me1, H3K4me2 or H3K4me3) and the silencing signal H3K9me2. Such combinations of histone marks are expected to occur specifically at border regions between transcriptionally silent and active chromatin. EDM2 controls alternative transcript polyadenylation at *RPP7* as well as several other direct targets, such as the histone demethylase gene *IBM1*, by forming a complex with the two RNA-Recognition Motif (RRM) domain proteins EDM3/AIPP1 (hereafter EDM3) and IBM2/ASI1 (hereafter IBM2) (Tsuchiya & Eulgem, 2013b; Lei *et al*, 2014; Duan *et al*, 2017; Lai *et al*, 2019). Upon recruitment to H3K9me2-marked chromatin sites EDM2/EDM3/IBM2 complexes suppress proximal polyadenylation and promote the synthesis of full-length

transcripts at these genes (Tsuchiya & Eulgem, 2013b; Lei *et al*, 2014; Wang *et al*, 2013; Saze *et al*, 2013; Duan *et al*, 2017; Lai *et al*, 2019).

Recent genome profiling studies uncovered numerous additional direct and indirect target genes of EDM2 including a large number of NLR genes (Lai *et al*, 2020; Zhang *et al*, 2021). EDM2 seems to have a dual role in the regulation of these immune receptors by (1) promoting expression of a small number of NLRs, like RPP7, and (2) suppressing a larger set of additional NLRs. In *edm2* mutant plants almost four-times more NLR genes are up-regulated than down-regulated, likely resulting in net-increase of NLR background activity and, as a possible consequence of this, phenotypes related to constitutive basal immunity and reduced fitness. Consequently, we also observed in *edm2* mutants enhanced basal defense against virulent strains of *Hpa* and *Pseudomonas syringae* (Pst DC3000) (Lai *et al*, 2020) as well as retarded growth of the rosette (Tsuchiya & Eulgem, 2010a) and reduced fertility/seed production (Tsuchiya & Eulgem, 2013a).

We further reported that EDM2 regulates the transition from vegetative to reproductive growth (flowering), as *edm2* mutants flower late (Tsuchiya & Eulgem, 2010b). Consistent with this we observed transcript levels of the negative flowering time regulator gene *FLC* (*Flowering Locus C*) to be substantially elevated in *edm2* mutants. The *FLC* gene proved to be epistatic over *EDM2* in this process and to act downstream from *EDM2*. In Arabidopsis, *FLC* plays a central role in the complex regulation of flowering by being

responsive to the vernalization and autonomous pathways. By regulating expression of the flowering promoting floral integrator genes *FT* (*Flowering Locus T*) and *SOC1* (*Suppressor of Overexpression of Constans1*) (Mouradov *et al*, 2002), FLC optimizes the timing of flowering. Expression of *FT* and *SOC1* is further regulated by additional *FLC*-independent pathways controlled by gibberellin and the photoperiod (Mouradov *et al*, 2002). As the flowering-related *edm2* phenotypes are independent from the photoperiod, EDM2 may formally be considered as a member of the autonomous floral promotion pathway, which controls the floral transition by suppressing *FLC* expression independent from day-length (Veley & Michaels, 2008).

Increasing evidence implies complex connections between plant-pathogen interactions and the timing of developmental transitions in plants. In some cases, pathogen infections were found to increase the expression of floral integrator genes thereby accelerating the transition from vegetative to reproductive plant growth (Korves & Bergelson, 2003). Arabidopsis was observed to flower earlier when infected by necrotrophic root pathogen *Fusarium oxysporum* (Lyons *et al,* 2015). For annual plants like Arabidopsis, accelerated production of viable seeds can be more efficient for the maintenance of its lineage than utilizing critical resources to fend off pathogens attacking it. Such stress escape strategies prioritize, under adverse conditions, the reproduction of plants before they succumb to the respective stress factor. These strategies have been described for plants in response to multiple abiotic or biotic stressors (Kazan & Lyons,

2016). While stress escape strategies prioritize use of resources for the progression of plant development and successful reproduction rather than defense, in some situations stresses delay developmental transitions, including flowering. Likely this is due to the depletion of critical plant resources consumed by stress and damage-related defense processes (Schiestl *et al*, 2014; Kazan & Lyons, 2016).

Common to the observations described above is that a stressor causally affects the normal progression of development. Reciprocally, developmental programs also dictate the extent of stress response measures in plants. For example, ETI mediated by some R-genes can follow certain developmental patterns and increase with plant age (McDowell *et al*, 2005). Likely, such age-related ETI is due to differential expression of the respective R-genes (Tan *et al*, 2007). In annuals, like Arabidopsis, the transition to flowering along with rapid growth of a florescence consumes a substantial amount of metabolic resources. Therefore, this step represents a particularly vulnerable phase in the life of plants and should require adjustments to other costly processes (Kazan & Lyons, 2016). Consistent with this view, transcript levels of some defense associated genes positively correlate with the length of flowering time in natural Arabidopsis accessions (Glander *et al*, 2018), suggesting that early flowering plants invest less in immunity than late flowering plants. Similarly, woody plants with faster growth rates were found to have lower tolerance against herbivores (Endara & Coley, 2011). In addition, Arabidopsis has been reported to exhibit age-related

resistance and to become more tolerant to virulent *Pseudomonas syringae* pv. tomato bacteria after the switch from vegetative growth to reproductive development (Rusterucci *et al*, 2005). However, the timing of this type of age-related basal immunity seems not directly controlled by the floral transition and rather reflects the overall state of maturation (Wilson *et al*, 2013). A positive correlation between the time to flowering and quantitative resistance against the root pathogen *Fusarium oxysporum* has been observed for numerous natural accessions of Arabidopsis as well as late flowering mutants of this species (Lyons *et al*, 2015). However, if there is a direct relationship of this immune mechanism to the timing of flowering has not been examined.

While numerous examples of age-related immune responses, including links between the flowering and defense reactions have been described, the underlying mechanisms connecting developmental transitions to the plant immune system remain largely elusive. Here we show that Arabidopsis plants gradually suppress basal defense against the virulent *Hyaloperonospora arabidopsidis* (*Hpa*) strain Noco2 prior to the transition to flowering. This effect is mediated by specific splice isoforms of the interacting RRM proteins IBM2 and EDM3. A long isoform of IBM2 (IBM2L), but not the shorter IBM2S isoform, can interact with either one of two EDM3 isoforms. However, its interaction with the longer EDM3 isoform (EDM3L) appears to be more pronounced and of higher biological relevance than its interactions with the shorter EDM3S variant. These interacting isoforms likely suppress basal immunity by targeting multiple defense-

associated genes. Moreover, IBM2L and EDM3L were found to promote the floral transition via down-regulating *FLC* expression. Consistent with this, we found the gradual decrease of *FLC* mRNA levels prior to flowering to be correlated with a pronounced increase of *IBM2L* and *EDM3L* mRNA levels. In *edm3* and *ibm2* mutants, the decline of *FLC* expression is delayed and IBM2L and EDM3L are able to rescue this decline, but not the shorter isoforms of these two RRM proteins. Taken together, our study shows that isoform-specific interactions between EDM3 and IBM2 coordinate the floral transition with a gradual reduction of basal immunity.

Results

Two Distinct EDM3 Isoforms Interact in Yeast With a Long Isoform of IBM2, but not a Shorter one That Lacks its RRM Domain

The Arabidopsis *EDM3* gene (AT1G05970) expresses two separate splice isoforms that only differ in the presence/absence of two adjacent codons at the 5' end of exon 2 (Lai *et al*, 2019). The longer isoform (EDM3L) contains a KQ dipeptide outside the RRM domain that may be important for the formation of a putative coiled coil structure close to the C-terminus of the protein (Fig 2.1A). Lack of the KQ dipeptide in the shorter isoform EDM3S substantially reduces the probability for the formation of this type of secondary structure (Fig 2.2). According to the TAIR 10 annotation of the Arabidopsis genome, *IBM2* (AT5G11470) also expresses two different splice isoforms. We could confirm the

existence of the respective mRNAs for one of them (IBM2.1) by RT-PCR. While we could not amplify mRNA specific for the other isoform annotated in TAIR10 (IBM2.2), we identified three additional splice isoforms (IBM2.3, IBM2.4 and IBM2.5). The longer IBM2.1, IBM2.3 and IBM2.4 isoforms share the same coding sequence, while the shorter IBM2.5 features a premature stop codon in the retained third intron that prevents the translation of an RRM domain (Fig 2.1A and 2.3). The hypothetical IBM2.2 transcript, which we were not able to confirm, is similar to IBM2.1 but encodes a slightly longer C-terminal stretch (Fig 2.3). In this paper we will jointly refer to the protein encoded by IBM2.1, IBM2.3 and IBM2.4 as IBM2L and the shorter one encoded by IBM2.5 as IBM2S.

We used IBM2S and IBM2L as baits to assess their interaction with EDM3S and EDM3L, respectively, by yeast two-hybrid experiments (Fig 2.1B). We detected only interactions of IBM2L, but not IBM2S, with either one of the EDM3 isoforms. The interactions of IBM2L with EDM3S seemed substantially weaker than those with EDM3L. Thus, interactions between both tested RRM domain proteins appeared to be isoform specific.

Our results further suggested the Bromo-adjacent homology (BAH) domain, which is common to both IBM2S and IBM2L, to be insufficient for interactions with EDM3 in yeast. However, the RRM domain of IBM2 proved to be sufficient for such interactions, as this domain even in isolated form as a bait interacted with both EDM3S and EDM3L (Fig 2.4A). It also interacted with the isolated C-terminal domain of EDM3 isoforms, but not the isolated EDM3 RRM

domain (Fig 2.4B). We further observed that both EDM3 isoforms can form homo- and heterodimers with each other in yeast (Fig 2.5). These interactions are likely mediated by their RRM domain, as this isolated EDM3 domain forms homodimers in yeast, while IBM2 RRM domain did not form homodimers (Fig 2.4B). Taken together these results suggested that only the long isoform of IBM2, containing both the BAH and RRM domains, can interact with EDM3 via its C-terminal domain and that EDM3S may be less capable of interacting with this IBM2 isoform than EDM3L, which contains the KQ peptide and may be more likely to form a stable coiled-coil structure in its C-terminal region.

Effects of EDM3 and IBM2 Isoforms on the Floral Transition

For functional complementation assays and *in vivo*-binding studies we used stably transformed Arabidopsis lines expressing epitope-tagged versions of the EDM3 or IBM2 isoforms in their respective mutant backgrounds (Fig 2.6A). We previously constructed lines separately expressing each of the two *EDM3* isoforms (*EDM3S* and *EDM3L*) in the *edm3-1* mutant, which is the Col-5 accession (Lai *et al*, 2019). We further constructed lines expressing the short (IBM2S) or long (IBM2L) isoforms in the Col-0 *IBM2* mutant *sg1-3* (*sg1-3/ibm2*; Coustham *et al*, 2014). Two lines homozygous for a single transgene insertion site for each of the four complementation constructs (*EDM3S-1, EDM3S-2, EDM3L-1, EDM3L-2*; *IBM2S-1, IBM2S-2, IBM2L-1, IBM2L-2*) were used for further experiments. The used *EDM3* and *IBM2* isoform-specific

complementation lines express their transgene-specific transcripts to similar levels (Lai *et al*, 2019; Fig 2.6B).

As we reported previously, *edm2* mutants exhibit elevated mRNA levels of the floral suppressor gene *FLC* and are delayed in their floral transition in a photoperiod independent manner (Tsuchiya & Eulgem, 2010b). Hence, we investigated the effects of *EDM3* and *IBM2* on flowering time. Based on the numbers of rosette leaves formed at the time of bolting, three *EDM3* mutants we tested (*edm3-1*, *edm3-2* and *edm3-3*) as well as *sg1-3/ibm2* flowered later than wild-type Col-0 under both short day (SD) and long day (LD) conditions (Fig 2.7A, C and 2.8). Consistent with these results, *FLC* mRNA levels were increased in *edm3-1* and *sg1-3/ibm2* compared to Col-0 (Fig 2.7B and D). Thus, EDM3 and IBM2 positively regulate the floral transition by downregulation of *FLC* transcript levels.

A construct carrying the wild type *EDM3* gene (*gEDM3*) leading to simultaneous expression of both splice isoforms (Lai *et al*, 2019) restored wild type flowering timing and low *FLC* expression in the *edm3-1* mutant (Fig 2.7A and B). The late flowering phenotype in *edm3-1* was also fully rescued by expression of *EDM3L* in both *EDM3L* complementation lines, but not by expression of *EDM3S* (Fig 2.7C). The effects on flowering time were mirrored by transcript levels of *FLC*, which were reduced to wild type levels in the *EDM3L* complementation lines and exhibited intermediate levels in *edm3-1* lines expressing *EDM3S* (Fig 2.7C and D). Expression of *IBM2L*, which was shown to

associate with both EDM3 isoforms in our yeast assays, was able to rescue the late flowering phenotype in *sg1-3/ibm2* (Fig 2.7A). Both tested *IBM2L* complementation lines also showed reduced levels of *FLC* transcripts compared to *sg1-3/ibm2* (Fig 2.7B). However, this effect was only partial in *IBM2L-2*, while expression of *IBM2S* in both tested lines was unable to provide even partial complementation regarding flowering time and *FLC* expression (Fig 2.7A and B).

As expression of *EDM3S* and *EDM3L* in the *edm3-1* complementation lines is driven by *35S Cauliflower Mosaic Virus* (*CaMV*) promoter, we generated isoform-specific complementation lines in the *edm3-2* background for *EDM3* with its native promoter ($EDM3S^{np}$ and $EDM3L^{np}$; Fig 2.9A and B) to limit possible artificial effects. This also allowed us to perform all experiments in the same accession background, Col-0. Only $EDM3L^{np}$, but not $EDM3S^{np}$, was able to rescue the late flowering phenotype and high *FLC* transcript levels of the *edm3-2* mutant (Fig 2.10A and B). Taken together, we observed with high consistency that flowering time-related effects of *ibm2* and *edm3* mutants are predominantly due to deficiencies of their respective longer splice isoforms and not the shorter ones.

We also generated *edm2-2;edm3-2*, *edm3-2;sg1-3/ibm2*, and *edm2-2;sg1-3/ibm2* double mutants. All three double mutants flowered later than Col-0, but their rosette leaf numbers at the time of bolting were similar to those of each of the respective single mutants (Fig 2.7E). The absence of additive or synergistic outcomes on flowering time delay in the tested double mutants

compared to the respective single mutants suggests that *EDM2*, *EDM3* and *IBM2* affect the floral transition via the same pathway and do not act independently.

We previously showed *FLC* to be epistatic over *EDM2* in the control of the floral transition and *FLC* expression, as an *edm2-2;flc-6* double mutant exhibited the same flowering time-related phenotypes like its parental early flowering *flc-6* line and not its *edm2-2* parent. We observed the same for the *edm3-2;flc-6* and *sg1-3*/*ibm2;flc-6* double mutants we generated (Fig 2.7F). Thus, like *EDM2*, *EDM3* and *IBM2* act upstream from *FLC* and affect the timing of the floral transition by suppressing *FLC* expression.

FLC expression is known to be gradually down-regulated during vegetative Arabidopsis development as plants approach their floral transition. We observed that the decline of *FLC* mRNA levels prior to this developmental transition is delayed in *edm2-2*, *edm3-2* and *sg1-3/ibm2* plants (Fig 2.11A). The wild type pattern of *FLC* mRNA down regulation is restored in the *EDM3L* and *IBM2L* complementation lines, but not in the *EDM3S* and *IBM2S* lines (Fig 2.11B and C). We further found transcript levels of all *EDM3* and *IBM2* isoforms to increase during the same time-span (Fig 2.11D and E). This increase is particularly pronounced for *EDM3L* and *IBM2L*-encoding transcripts. While *EDM3S*-encoding mRNAs rise to levels about 60% of those of *EDM3L*, the increase of *IBM2S*-encoding transcripts is much less than that of *IBM2L*-encoding ones.

Taken together our results support a model for EDM3 and IBM2-controlled *FLC* expression in which the gradual reduction of mRNAs of this central flowering suppressor is mediated by simultaneous accumulation of the longer isoforms of *EDM3* and *IBM2*. While the expression of the respective shorter isoforms is increasing during the same time-span, neither seems to significantly contribute to the gradual suppression of *FLC* expression.

EDM3L and IBM2L Suppress Basal Immunity and Expression of Various NLR Genes

EDM2 is known to suppress basal immunity against the Noco2 strain of *Hpa* and the bacterial pathogen *Pseudomonas syringae* (Lai *et al*, 2020). We tested if isoforms of EDM3 and IBM2 also affect basal defense by performing infection assays with *Hpa*Noco2, which is virulent on the Col-0 and Col-5 accessions of Arabidopsis. Mutants of *EDM3* and *IBM2* behaved in these experiments similar to *edm2* lines (Fig 2.12A and B). Compared to Col-0, the *edm3-2* and *sg1-3/ibm2* mutants allowed for the formation of a lesser number of *Hpa*Noco2 spores on infected seedlings indicating enhanced basal immunity. Expression of the longer isoforms of *EDM3* and *IBM2* in their respective mutant backgrounds restored basal immunity to the lower levels observed in Col-0 (Fig 2.12A and B). However, expression of *IBM2S* or *EDM3S* was unable to provide significant levels of functional complementation in *sg1-3/ibm2* or *edm3-2*, respectively. The Col-0 *pad4* mutant, which is fully deficient in basal defense

against *Hpa* and wild type plants of the Arabidopsis accession Landsberg erecta (Ler), which carry the *RPP5* immune receptor gene mediating strong protection against *Hpa*Noco2 (Glazebrook *et al*, 1996, 1997; Parker *et al*, 1993), served in this experiment as negative and positive controls, respectively. As described above, in the context of flowering time control *FLC* behaves epistatic to *EDM3* and *IBM2*. However, *FLC* seems not to have any effect on the basal immunity-related roles of *EDM3* and *IBM2*. Neither does the *flc-6* mutant show any significant difference in levels of resistance against *Hpa*Noco2 compared to Col-0, nor is the enhanced basal defense phenotype of *edm3-2* or *sg1-3/ibm2* changed in double mutants with *flc-6* (Fig 2.12C). Thus, while the effects of *EDM3* and *IBM2* on the floral transition are mediated via *FLC*, their effects on basal defense are *FLC*-independent and controlled by a separate pathway. However, as in the regulation of the floral transition, basal defense is controlled by the long isoforms of *EDM3* and *IBM2*.

Potentially associated with their roles in suppressing basal defense, we found EDM3L and IBM2L to share with EDM2 a broad role in suppressing NLR genes. Inspecting published RNA-seq data we compared the expression levels of all 165 annotated Arabidopsis NLR genes (Zhang *et al*, 2016) in mutants of *EDM2*, *EDM3* and *IBM2* (Duan *et al,* 2017; Zhang *et al*, 2020). As we had observed for the *edm2*-2 mutant previously (Lai *et al*, 2020), compared to their wild type parent a large number of NLRs are up-regulated in the *edm3* mutant *aipp1* and the *ibm2* mutant *asi1-2*, while only a small number of NLR genes are

down-regulated in them (Fig 2.13). A set of 26 NLR genes are jointly up-regulated in the *edm2-4*, *aipp1* and *asi-1* lines, while only two NLR genes (*RPP4* and *RPP7*) are jointly down-regulated in this set of mutants. For four selected NLRs, which are highly up-regulated in all three of these mutants, we confirmed the roles of EDM3L and IBM2L in their suppression by qRT-PCR. We observed elevated transcript levels for each of them in the *sg1-3/ibm2* and *edm3-2* mutant compared to Col-0. However, only in *IBM2L* but not in *IBM2S* lines the low expression levels of these genes observed in Col-0 was restored. Likewise, only in *EDM3L*^{np} but not *EDM3S*^{np} plants these gene's expression levels were fully or partially rescued to wild type levels (Fig 2.12D-K).

EDM3L and IBM2L Directly Control Defense-Regulating Genes

Inspecting previously published EDM2 and IBM2 ChIP-seq data (Zhang *et al*, 2021), we found that EDM2 and IBM2 jointly bind to numerous defense-associated genes. We further investigated roles of EDM3 and IBM2 isoforms in the regulation of three of these genes, which were also found by RNA-seq to be consistently up-regulated in mutants of *EDM2*, *EDM3* and *IBM2* compared to their parental wild type lines (Lai *et al*, 2020; Duan *et al*, 2017).

Among the tested three genes, the transcription factor gene *WRKY18* (Wang *et al,* 2006) and the phasi-RNA-generating NLR gene AT1G63750 (Cai *et al*, 2018) have been described to play a positive role in plant immunity, while the thaumatin-type pathogenesis-related (PR) protein-encoding AT4G36010 was

reported to be frequently induced after infection with various types of pathogens (Verhagen *et al*, 2004). In line with the enhanced basal defense phenotypes of *edm3* and *ibm2* lines, *WRKY18,* AT1G63750*,* and AT4G36010 are expressed at higher levels in each of these mutants (Fig 2.14A-F). Only the longer isoforms of *EDM3* and *IBM2*, but not the shorter ones, successfully complemented these effects and restored lower wild type transcript levels of these genes.

As EDM2 complexes are known to preferentially associate with heterochromatic repeat regions next to actively transcribed euchromatic regions, we examined by ChIP areas for each of these genes, regions that are close to transposable elements (TEs) or other repeats and/or carry methylation marks at cytosines or H3K9. Our results for IBM2 are consistent with previously published data (Zhang *et al*, 2021). While levels of enrichment varied substantially between individual replicates for some experiments, we observed a clear trend for IBM2L, but not IBM2S, to be physically associated with all three tested regions (Fig 2.14G-I). Both EDM3 isoforms associate with the tested region of *WRKY18*, but not with that of AT4G36010 (Fig 2.14J and K). The examined region of AT1G63750 exhibited physical association with EDM3L, but not EDM3S. Taken together our results strongly support that both EDM3L and IBM2L directly target *WRKY18* to suppress its expression. While EDM3S seems also to be able to interact with the tested *WRKY18* region in our ChIP-qPCR assays, our qRT-PCRs showed that EDM3S is insufficient to suppress expression of this transcription factor gene. The roles of *EDM3* and *IBM2* isoforms in the regulation

of *WRKY18* and AT1G63750 seem to be similar. Although both IBM2L and EDM3L suppress expression of AT4G36010, we can only detect binding of IMB2L to the tested region of this PR gene.

Coordination of Flowering Time and Basal Defense by EDM3 and IBM2 Isoforms

The fact that EDM3 and IBM2 isoforms cooperate in controlling the floral transition as well as basal defense, suggested they may coordinate both processes. We observed a marked decline of basal defense against *Hpa*Noco2 in Col-0 seedlings prior to the transition to flowering. Numbers of *Hpa*Noco2 spores produced on Col-0 seedlings infected by this pathogen more than doubled between 8 days post germination (dpg) and the initiation of bolting at 16 dpg (Fig 2.15A). In *edm2-2*, *edm3-2* and *sg1-3/ibm2* mutants we did not observe a decline of basal defense during this time span and the intensity of this immune mechanism remained constantly high. While *IBM2L* and *EDM3L* restored the wild type pattern of basal defense decline in their respective mutant backgrounds allowing for a significant increase of *Hpa*Noco2 spores in our assays, *IBM2S* and *EDM3S* were unable to do so (Fig 2.15B and C). Results we obtained with the Col-0 *EDM3* complementation lines and the Col-5 *EDM3* complementation lines were similar (Fig 2.16).

Taken together our results imply the following mechanism regarding the coordination of floral transition timing with basal defense intensity. As plants

approach the floral transition, expression of the interacting EDM3L and IBM2L isoforms exhibits a strong continuous increase. Increasing levels of these RRM protein isoforms suppress basal defense (possibly by down-regulating positive defense regulators, such as *WRKY18* and AT1G63750). At the same time, both interacting EDM3 and IBM2 isoforms gradually suppress *FLC* expression by a separate unknown pathway. As shown previously (Lee *et al*, 2000; Helliwell *et al*, 2006) decreasing levels of *FLC* result in de-repression of floral integrator genes allowing the floral transition to progress. A likely purpose of this coordinating mechanism is to limit metabolic resource expenditure for defense reactions and preserve these resources for the energetically costly transition to vegetative growth and the establishment of an inflorescence.

Discussion

While multiple examples demonstrating age-related modulation of plant immune responses have been reported, our understanding of the coordination of plant development with immunity is only vague and mechanistic details underlying these processes are largely unknown. Our results clearly link a gradual decline of basal immunity with the progression through the developmental phase immediately prior to the floral transition in Arabidopsis. Furthermore, we were able to link the coordination of both processes at the mechanistic level to isoform-specific interactions between two RRM domain proteins.

Plant immune responses are known to be costly, as they require metabolic resources otherwise needed for growth and development (Lozano-Durán *et al*, 2013; Fan *et al*, 2014; Gangappa *et al*, 2017; Guo *et al*, 2018). Like other Arabidopsis mutants with constitutively elevated levels of basal defense (Bowling *et al*, 1994; Dietrich *et al*, 1994; Petersen *et al*, 2000; Clarke *et al*, 2000; Maleck *et al*, 2002), *edm2*, *edm3* and *ibm2* lines exhibit developmental abnormalities and retardation of growth (Tsuchiya & Eulgem, 2010a, 2013a; Saze *et al*, 2013; Wang *et al*, 2013; Lei *et al*, 2014; Coustham *et al*, 2014), a phenotypic characteristic likely due to wasteful expenditure of critical resources. In Arabidopsis the transition from vegetative to reproductive development is marked by the emergence and rapid growth of the main stem, which turns into the inflorescence. Thus, suppressing basal immunity immediately prior to and during this developmental transition should free metabolic resources and be supportive of it.

We found isoform-specific interactions between the two RRM domain proteins, EDM3 and IBM2 to be of central importance for the coordination of basal immunity with the floral transition in Arabidopsis. While EDM3 (AIPP1) and IBM2 (ASI-1) have been shown before to physically associate with each other (Duan *et al*, 2017), the isoform-specific nature of their interactions has been unknown. Despite being expressed, the short IBM2 transcript isoform we cloned, and which only encodes the N-terminal BAH domain, is insufficient to fulfill any of the roles we found IBM2 to be involved in. Although the BAH domain can bind to

chromatin (Du *et al*, 2012; Zhao *et al*, 2016), we did not observe any physical association of IBM2S with a selection of defense-associated genes to which IBM2L and EDM3L co-localize *in vivo* to suppress their expression. Consistent with their suppressive effects on certain defense-associated loci and NLR receptor genes, mutants of *EDM3* and *IBM2* show increased resistance to *Hpa*Noco2. Only EDM3L and IBM2L fully rescued this effect by functional complementation.

Likewise, we observed that only EDM3L and IBM2L, and not EDM3S and IBM2S are capable of mediating proper timing of *FLC*-dependent floral transition under both short-day and long-day conditions. As we demonstrated previously for EDM2 (Tsuchiya & Eulgem, 2010b), EDM3L and IBM2L act upstream of *FLC* in this pathway in a light-period independent manner, and, thus, may be considered as components of the autonomous pathway. Intriguingly, transcripts of *IBM2L* and *EDM3L* strongly and continuously accumulate, while *FLC* transcript levels gradually decrease as plants approach the floral transition. IBM2L and EDM3L are required for this gradual suppression of *FLC* expression and mediate at the same time a gradual suppression of basal immunity against *Hpa*Noco2. Importantly, their roles in both the floral transition and basal immunity can be genetically separated, as the *flc-6* mutant shows wild type levels of basal defense against *Hpa*Noco2 and the enhanced basal defense phenotype of *edm3* or *ibm2* mutants is not affected in double mutants with *flc-6*. Thus, while the effects of

EDM3L and IBM2L on the floral transition are mediated via *FLC*, their effects on basal defense are *FLC*-independent and controlled by (a) separate pathway(s).

In some replicates of our *Hpa*Noco2 infection assays we observed a mild reduction of basal immunity in *flc-6* plants. This effect was not always reproducible and only of modest extent. We speculate that accelerated developmental progression in this mutant towards the time point of flowering may have resulted in a slightly accelerated increase of EDM3L and IBM2L expression and, thus, marginally increased suppression of basal immunity via the defense-related functions of these RRM domain proteins. However, as this effect seems to be very weak and possibly influenced by minor variations in environmental conditions, we were not able to consistently reproduce it.

Inspecting publicly available ATH1 Arabidopsis microarray data (Toufighi *et al*, 2005), we found expression of many defense-associated genes targeted by EDM2 and IBM2 to be increasingly suppressed in rosette leaves formed as plants approach the floral transition (Table 2.1). Rosette leaves 2, 4, 6, 8, 10 and 12 show progressively reduced levels of *WRKY18*, the phasi-RNA-generating NLR gene AT1G63750 or AT4G36010 transcripts, a trend that is mirrored by the gradual down-regulation of *FLC* as well as 13 out of the 26 NLR genes that are jointly suppressed by EDM2, EDM3 and IBM2 (Fig 2.17 and Table 2.2). This includes AT5G18360 and AT5G66630, the expression of which we examined by qRT-PCR. Similar trends can be seen in microarray data of Arabidopsis plants of increasing ages prior to flowering (Table 2.3 and 2.4). Some genes targeted by

EDM3L and IBM2L, such as the NLR genes AT1G58400, AT3G44670 and AT4G14370 are not represented on the ATH1 array. Collectively all these observations strongly support that increased expression of the interacting EDM3 and IBM2 isoforms aligns the timing of flowering with a gradual decrease of the plants' basal defense capacity by coordinated suppression of *FLC* on the one hand and a set of defense-associated and NLR genes on the other hand. Two defense-regulatory genes directly suppressed by EDM3L and IBM2L and down-regulated prior to flowering may indeed contribute to the decrease of basal immunity, *WRKY18*, which encodes a well characterized transcription factor that can play positive role in immunity (Chen & Chen, 2002; Wang *et al*, 2006) as well as the NLR gene AT1G63750. Expression of AT1G63750 is inversely correlated with the production of phasiRNAs at the same locus suppressing expression of a multitude of other NLR genes (Cai *et al*, 2018). Interestingly the NLR gene set putatively suppressed by these phasiRNAs shows substantial overlap with those NLRs suppressed by EDM2, EDM3 and IBM2 (Fig 2.17; Cai *et al*, 2018).

An intriguing question to address in the future will be, what causes the strong increase of EDM3L and IBM2L expression? As levels of transcripts encoding their shorter isoforms also increase during the same time span, transcriptional up-regulation of the *EDM3* and *IBM2* genes and/or attenuated turnover of the respective transcripts may be operating in concert with an alternative splicing mechanism that favors their longer isoforms. The hypothetical mechanisms leading to transcriptional up-regulation and/or attenuated transcript

turnover must be responsive to an endogenous development-related signal, while the splicing mechanism seems to be constitutive. Candidates for development-related signals indirectly responsible for the accumulation of EDM3 and IBM2 transcript may be the micro RNAs miR156 and/or miR172. The former miRNA suppresses the latter by targeting SPL (SQUAMOSA PROMOTER BINDING PROTEIN LIKE) genes that are involved in promoting expression of miR172 (Xu *et al*, 2016; Zhu & Helliwell, 2011). Since levels of miR156 decrease with plant age, levels of miR172 simultaneously increase (Wu *et al*, 2009). High levels of miR156 prevent precocious flowering and vegetative phase change while miR172 has the opposite effects (Wang *et al*, 2009; Wu *et al*, 2009; Zhu & Helliwell, 2011). As the expression pattern of miR172 is similar and that of miR156 is opposite to that of *EDM3L* and *IBM2L*, they are possibly regulators that are involved in transcriptional up-regulation of *EDM3* and *IBM2* isoforms.

The composition of EDM3L and IBM2L containing protein complexes and interactions among its components may be complex and dynamic. Our yeast two-hybrid studies suggest that the C-terminal coiled coil motif of EDM3L interacts with the RRM domain of IBM2, while the same domain of EDM3 interacts with itself, possibly promoting homodimers. Previous RNA immunoprecipitation studies have shown that EDM3 and IBM2 can physically associate with RNA *in vivo* and *in vitro*, respectively (Lai *et al*, 2019; Wang *et al*, 2013), a function that likely involves their RRM domains. It will be interesting to examine in the future if the EDM3 and IBM2 RRM domains can simultaneously

engage in interactions with proteins and RNA, or if these types of interactions are mutually exclusive, possibly allowing for a dynamic switching process. However, such studies may be challenging, as we had difficulties to detect epitope-tagged versions of EDM3 and IBM2 in our stably transformed Arabidopsis complementation lines by western blotting or Co-IP assays. We previously reported similar issues with EDM2 (Lai *et al*, 2020). Likely *in vivo* levels of these proteins are extremely low. Consistently with this, EDM2 contains a potentially destabilizing PEST motif (Rechsteiner & Rogers, 1996), while EDM3 and IBM2 have putative N-end rule pathway-targeting N terminal residues, such as alanine and glutamic acid (Gibbs *et al*, 2016), which may accelerate the turnover of these proteins. Despite these issues, our ChIP assays and functional complementation experiments unequivocally demonstrated *in vivo* association and cooperation between EDM3L and IBM2L.

While IBM2S seemed fully insufficient to functionally complement the *ibm2* mutant phenotypes examined in this study, EDM3S mediated in some experiments partial complementation. In addition, we previously reported that EDM3S can promote expression of the RPP7 immune receptor to levels sufficient for full immunity against its cognate *Hpa* isolate Hiks1 (Lai *et al*, 2019). Thus, the two amino acid deletion in its C-terminal portion may only have a moderate effect allowing this isoform to retain some functionality. This is consistent with the fact that the probability of the C-terminal region forming a coiled coil structure is only reduced, but this option not fully abolished in EDM3S.

As mutants of *EDM2* phenocopy the effects of *edm3* and *ibm2* mutants described above (Tsuchiya & Eulgem, 2010a, 2010b; Lai *et al*, 2020), the histone binding protein encoded by this gene is likely a part of complexes coordinating basal defense and flowering time. Previous studies have shown functional or physical associations of EDM2 with EDM3 and IBM2 in other biological contexts (Duan *et al*, 2017; Lai *et al*, 2020). Similarly, additional proteins which have been found to interact with EDM2, EDM3 or IBM2 may contribute to the coordination of flowering with immunity. These include WNK8, which can physically interact with EDM2 and phosphorylate it. This protein kinase modulates several functions of EDM2, such as *FLC*-mediated flowering time control (Tsuchiya & Eulgem, 2010a, 2010b). Members of the small family of EMSY-like (EML) proteins also physically interact with EDM2. These putative nucleosome remodeling factors promote basal defense and suppress the floral transition by promoting *FLC* expression (Tsuchiya & Eulgem, 2011). Furthermore, protein-protein interaction studies identified the Pol II CTD phosphatase CPL2, the plant homeodomain-containing protein AIPP2, and the BAH domain protein, AIPP3, to bind to IBM2 (ASI1) and to counter the roles of IBM2, EDM2 and EDM3 in RNA processing (Duan *et al*, 2017). Thus, most likely EDM3 and IBM2 execute their roles in coordinating basal immunity with the timing of the floral transition as components of a complex chromatin-associated protein aggregate.

How they affect expression of direct basal defense-related target genes, such as *WRKY18* and AT1G63750, remains unclear. EDM3L and IBM2L directly

bind to 5'UTR of *WRKY18*, thus possibly inhibiting *WRKY18* transcription by promoting repressive chromatin marks in this area. In contrast, we found EDM3L and IBM2L to be enriched around a transposon in the first intron of AT1G63750. According to previously published IBM2-ChIP-seq data (Zhang *et al*, 2021), IBM2 appears also to interact with the promoter area of this gene and may affect chromatin marks between the AT1G63750 promoter area and its first intron. As both EDM3 and IBM2 are RRM domain-containing proteins, it is also possible that they suppress the expression of *WRKY18* and AT1G63750 by delaying transcriptional elongation or accelerating mRNA degradation.

A likely link connecting EDM3 and IBM2 to the regulation of *FLC* is another RRM domain protein involved in polyadenylation-site choice, the autonomous pathway component FPA. This RNA binding protein promotes the floral transition by repressing *FLC* expression via proximal polyadenylation of *FLC* antisense transcripts (Hornyik *et al*, 2010). Recently mutation of *FPA* was found to suppress some *ibm2*-related effects, such as reduced expression of full-length *RPP7* and *IBM1* transcripts (Deremetz *et al*, 2019). Contrary to EDM3 and IBM2 (as well as EDM2), which suppress the use of proximal polyadenylation sites in *RPP7* and *IBM2* (Tsuchiya & Eulgem*,* 2013b*;* Saze *et al,* 2013*;* Duan *et al,* 2017*;* Lai *et al,* 2019), FPA promotes the use of them (Deremetz *et al*, 2019). Genetically *FPA* appears to be epistatic over *IBM2* in this role. The fact that FPA has also been previously implicated in basal defense related roles (Lyons *et al*, 2013, 2015) may suggest that it is functionally tightly associated with EDM3 and

IBM2. In contrast to its role in the regulation of *RPP7* and *IBM2*, which is antagonistic to that of EDM3 and IBM2, its effect on flowering time and basal defense seems co-directional with EDM3 and IBM2, as it has a promoting effect on the former and a suppressive effect on the latter process. It is unclear if FPA physically associates with EDM3 and IBM2. Besides FPA, two additional classical autonomous pathway components, FLD and FVE, were shown to negatively regulate Arabidopsis defense responses. As in the case of *edm2*, *edm3* and *ibm2* mutants, the enhanced resistance phenotypes of *fpa*, *fve*, and *fld* mutants can be uncoupled from their late flowering phenotypes in double mutants with *flc* (Lyons *et al,* 2015). Common to Arabidopsis mutants of the autonomous pathway are their late flowering and enhanced defense phenotypes, as well as effects on RNA-processing and/or the chromatin landscape. If they generally share with *edm3* and *ibm2* lines lack of coordination of the floral transition with basal defense remains to be shown.

Materials and Methods

Plant Material and Growth Conditions. The wild-type Arabidopsis lines used in this study are Col-0, Col-5 and Ler, which were obtained from the Arabidopsis Biological Resource Center (ABRC). The following mutants were used: *edm2-2* (Eulgem *et al*, 2007), *edm3-1* (Lai *et al*, 2019), *sg1-3/ibm2* (Coustham *et al*, 2014), *flc-6* (Bouveret *et al,* 2006) and *pad4* (Jirage *et al,* 1999). Transgenic

lines: *gEDM3C*, *EDM3S*, and *EDM3L* were described previously (Lai *et al*, 2019). Double mutants were produced by crossing and F2 seeds were screened by PCR-based genotyping to select homozygotes. Seeds were surface-sterilized and germinated on ½ MS medium (Research Products International Corp, M10400-50.0) or in soil under long day (16h/8h light-dark cycles) or short day (8h/16h light-dark cycles).

Gene Knockout and Generation of Transgenic Lines. The *edm3-2* mutant was produced by using Crispr/Cas9 system (Wang *et al*, 2015). HA-tagged IBM2 splicing isoforms (IBM2S or IBM2L) under its promoter were cloned into pEarleyGate 302 using Gateway cloning method (Invitrogen, USA), which were transformed into *sg1-3/ibm2* plants, respectively, by the floral dipping method (Clough & Bent, 1998). Similarly, the FLAG-tagged EDM3 splicing isoforms (EDM3S or EDM3L) driven by its promoter were cloned into pEarleyGate 302 using Gateway cloning method (Invitrogen, USA), which were transformed into *edm3-2* plants, respectively, by the same method described above.

Yeast Two-Hybrid Assays. GAL4 two-hybrid system (generously provided by Dr. Zonghua Wang) was used for yeast two-hybrid assays. Briefly, the coding sequences of EDM3 and IBM2 splicing isoforms and the isolated domains of EDM3 and IBM2 were cloned into GAL4 activation domain vector, pGADT7 or GAL4 binding domain vector, pGBKT7, respectively. The plasmid pairs were then

transformed into the yeast strain AH109 (Schiestl & Gietz, 1989). Pairs of pGBKT7-53 and pGADT7 or pGBKT7-Lam and pGADT7-T were used as positive control and negative control, respectively. Selection of positive transformants and confirmation of protein-protein interaction in yeast were done according to the manufacturer instruction (Takara Bio USA).

Flowering Time Measurement. Flowering time was measured at 22 °C under long day (16h/8h light-dark cycle) or at 18°C under short day (8h/16h light-dark cycle) by counting the rosette leaves at bolting.

RNA Extraction and qRT-PCR. Total RNA was extracted from two-week old plants using Trizol reagent (Life technologies) according to the manufacturer's instructions. 1μg of RNA was reverse transcribed into cDNA using Maxima Reverse Transcriptase (Fisher scientific) with oligo-dT18. The resulting cDNA was then used for Real-time PCR with CFX CONNETCT detection system (Bio-Rad). All primers used are listed in Table 2.5.

***Hyaloperonospora arabidopsidis* Infection**. *Hyaloperonospora* infection assays were done as described previously (McDowell *et al*, 2000). Briefly, twelve to fourteen days old plants were sprayed-inoculated with *Hpa*Noco2 spores (1-3 x 10^4 spores/ml). One week after infection, ten to twenty seedlings were collected

into 2ml of water. Spores were counted using a hemocytometer after vortexing in water to determine the degree of infection.

Chromatin Immunoprecipitation. Two-week old plants were used for ChIP assays. ChIP was performed as described previously (Tsuchiya & Eulgem, 2013b) using anti-HA (AB9110, Abcam) or anti-FLAG (F1804, Sigma)

References

Banday ZZ & Nandi AK (2015) Interconnection between flowering time control and activation of systemic acquired resistance. *Front Plant Sci* 6: 174

Bieri S, Mauch S, Shen Q-H, Peart J, Devoto A, Casais C, Ceron F, Schulze S, Steinbiss H-H, Shirasu K, *et al* (2004) RAR1 positively controls steady state levels of barley MLA resistance proteins and enables sufficient MLA6 accumulation for effective resistance. *Plant Cell* 16: 3480–3495

Bouveret R, Schönrock N, Gruissem W & Hennig L (2006) Regulation of flowering time by Arabidopsis MSI1. *Development* 133: 1693–1702

Bowling SA, Guo A, Cao H, Gordon AS, Klessig DF & Dong X (1994) A mutation in Arabidopsis that leads to constitutive expression of systemic acquired resistance. *Plant Cell* 6: 1845–1857

Cai Q, Liang C, Wang S, Hou Y, Gao L, Liu L, He W, Ma W, Mo B & Chen X (2018) The disease resistance protein SNC1 represses the biogenesis of microRNAs and phased siRNAs. *Nat Commun* 9: 1–14

Chen C & Chen Z (2002) Potentiation of developmentally regulated plant defense response by AtWRKY18, a pathogen-induced Arabidopsis transcription factor. *Plant Physiol* 129: 706–716

Chisholm ST, Coaker G, Day B & Staskawicz BJ (2006) Host-microbe interactions: shaping the evolution of the plant immune response. *Cell* 124: 803–814

Clarke JD, Volko SM, Ledford H, Ausubel FM & Dong X (2000) Roles of salicylic acid, jasmonic acid, and ethylene in cpr-induced resistance in arabidopsis. *Plant Cell* 12: 2175–2190

Clough SJ & Bent AF (1998) Floral dip: a simplified method forAgrobacterium-mediated transformation ofArabidopsis thaliana. *The Plant Journal* 16: 735–743 doi:10.1046/j.1365-313x.1998.00343.x [PREPRINT]

Coustham V, Vlad D, Deremetz A, Gy I, Cubillos FA, Kerdaffrec E, Loudet O & Bouché N (2014) SHOOT GROWTH1 maintains Arabidopsis epigenomes by regulating IBM1. *PLoS One* 9: e84687

Deremetz A, Le Roux C, Idir Y, Brousse C, Agorio A, Gy I, Parker JE & Bouché N (2019) Antagonistic Actions of FPA and IBM2 Regulate Transcript Processing from Genes Containing Heterochromatin. *Plant Physiol* 180: 392–403

Dietrich RA, Delaney TP, Uknes SJ, Ward ER, Ryals JA & Dangl JL (1994) Arabidopsis mutants simulating disease resistance response. *Cell* 77: 565–577

Duan C-G, Wang X, Zhang L, Xiong X, Zhang Z, Tang K, Pan L, Hsu C-C, Xu H, Tao WA, *et al* (2017) A protein complex regulates RNA processing of intronic heterochromatin-containing genes in Arabidopsis. *Proc Natl Acad Sci U S A* 114: E7377–E7384

Du J, Zhong X, Bernatavichute YV, Stroud H, Feng S, Caro E, Vashisht AA, Terragni J, Chin HG, Tu A, *et al* (2012) Dual binding of chromomethylase domains to H3K9me2-containing nucleosomes directs DNA methylation in plants. *Cell* 151: 167–180

Endara M-J & Coley PD (2011) The resource availability hypothesis revisited: a meta-analysis. *Functional Ecology* 25: 389–398 doi:10.1111/j.1365-2435.2010.01803.x [PREPRINT]

Eulgem T, Tsuchiya T, Wang X-J, Beasley B, Cuzick A, Tör M, Zhu T, McDowell JM, Holub E & Dangl JL (2007) EDM2 is required for RPP7-dependent disease resistance in Arabidopsis and affects RPP7 transcript levels. *Plant J* 49: 829–839

Fan M, Bai M-Y, Kim J-G, Wang T, Oh E, Chen L, Park CH, Son S-H, Kim S-K, Mudgett MB, *et al* (2014) The bHLH Transcription Factor HBI1 Mediates the Trade-Off between Growth and Pathogen-Associated Molecular Pattern–Triggered Immunity in Arabidopsis. *Plant Cell* 26: 828–841

Gangappa SN, Berriri S & Kumar SV (2017) PIF4 Coordinates Thermosensory Growth and Immunity in Arabidopsis. *Curr Biol* 27: 243–249

Gibbs DJ, Bailey M, Tedds HM & Holdsworth MJ (2016) From start to finish: amino-terminal protein modifications as degradation signals in plants. *New Phytologist* 211: 1188–1194 doi:10.1111/nph.14105 [PREPRINT]

Glander S, He F, Schmitz G, Witten A, Telschow A & de Meaux J (2018) Assortment of Flowering Time and Immunity Alleles in Natural Arabidopsis thaliana Populations Suggests Immunity and Vegetative Lifespan Strategies Coevolve. *Genome Biol Evol* 10: 2278–2291

Glazebrook J (2001) Genes controlling expression of defense responses in Arabidopsis—2001 status. *Curr Opin Plant Biol* 4: 301–308

Glazebrook J, Rogers EE & Ausubel FM (1996) Isolation of Arabidopsis mutants with enhanced disease susceptibility by direct screening. *Genetics* 143: 973–982

Glazebrook J, Zook M, Mert F, Kagan I, Rogers EE, Crute IR, Holub EB, Hammerschmidt R & Ausubel FM (1997) Phytoalexin-deficient mutants of Arabidopsis reveal that PAD4 encodes a regulatory factor and that four PAD genes contribute to downy mildew resistance. *Genetics* 146: 381–392

Guo Q, Yoshida Y, Major IT, Wang K, Sugimoto K, Kapali G, Havko NE, Benning C & Howe GA (2018) JAZ repressors of metabolic defense promote growth and reproductive fitness in Arabidopsis. *Proc Natl Acad Sci U S A* 115: E10768–E10777

Helliwell CA, Wood CC, Robertson M, James Peacock W & Dennis ES (2006) The Arabidopsis FLC protein interacts directly in vivo with SOC1 and FT chromatin and is part of a high-molecular-weight protein complex. *Plant J* 46: 183–192

Holt BF 3rd, Belkhadir Y & Dangl JL (2005) Antagonistic control of disease resistance protein stability in the plant immune system. *Science* 309: 929–932

Hornyik C, Terzi LC & Simpson GG (2010) The spen family protein FPA controls alternative cleavage and polyadenylation of RNA. *Dev Cell* 18: 203–213

Jacob F, Vernaldi S & Maekawa T (2013) Evolution and Conservation of Plant NLR Functions. *Front Immunol* 4: 297

Jirage D, Tootle TL, Reuber TL, Frost LN, Feys BJ, Parker JE, Ausubel FM & Glazebrook J (1999) Arabidopsis thaliana PAD4 encodes a lipase-like gene that is important for salicylic acid signaling. *Proc Natl Acad Sci U S A* 96: 13583–13588

Jones JDG & Dangl JL (2006) The plant immune system. *Nature* 444: 323–329

Kazan K & Lyons R (2016) The link between flowering time and stress tolerance. *J Exp Bot* 67: 47–60

Korves TM & Bergelson J (2003) A developmental response to pathogen infection in Arabidopsis. *Plant Physiol* 133: 339–347

Lai Y, Cuzick A, Lu XM, Wang J, Katiyar N, Tsuchiya T, Le Roch K, McDowell JM, Holub E & Eulgem T (2019) The Arabidopsis RRM domain protein EDM3 mediates race-specific disease resistance by controlling H3K9me2-dependent alternative polyadenylation of RPP7 immune receptor transcripts. *Plant J* 97: 646–660

Lai Y & Eulgem T (2018) Transcript-level expression control of plant NLR genes. *Mol Plant Pathol* 19: 1267–1281

Lai Y, Lu XM, Daron J, Pan S, Wang J, Wang W, Tsuchiya T, Holub E, McDowell JM, Slotkin RK, *et al* (2020) The Arabidopsis PHD-finger protein EDM2 has multiple roles in balancing NLR immune receptor gene expression. *PLoS Genet* 16: e1008993

Lee H, Suh SS, Park E, Cho E, Ahn JH, Kim SG, Lee JS, Kwon YM & Lee I (2000) The AGAMOUS-LIKE 20 MADS domain protein integrates floral inductive pathways in Arabidopsis. *Genes Dev* 14: 2366–2376

Lei M, La H, Lu K, Wang P, Miki D, Ren Z, Duan C-G, Wang X, Tang K, Zeng L, *et al* (2014) Arabidopsis EDM2 promotes IBM1 distal polyadenylation and regulates genome DNA methylation patterns. *Proc Natl Acad Sci U S A* 111: 527–532

Li X, Kapos P & Zhang Y (2015) NLRs in plants. *Curr Opin Immunol* 32: 114–121

Li Y, Yang S, Yang H & Hua J (2007) The TIR-NB-LRR gene SNC1 is regulated at the transcript level by multiple factors. *Mol Plant Microbe Interact* 20: 1449–1456

Lozano-Durán R, Macho AP, Boutrot F, Segonzac C, Somssich IE & Zipfel C (2013) The transcriptional regulator BZR1 mediates trade-off between plant innate immunity and growth. *Elife* 2: e00983

Lu Y & Tsuda K (2021) Intimate Association of PRR- and NLR-Mediated Signaling in Plant Immunity. *Mol Plant Microbe Interact* 34: 3–14

Lyons R, Iwase A, Gänsewig T, Sherstnev A, Duc C, Barton GJ, Hanada K, Higuchi-Takeuchi M, Matsui M, Sugimoto K, *et al* (2013) The RNA-binding protein FPA regulates flg22-triggered defense responses and transcription factor activity by alternative polyadenylation. *Sci Rep* 3: 2866

Lyons R, Rusu A, Stiller J, Powell J, Manners JM & Kazan K (2015) Investigating the Association between Flowering Time and Defense in the Arabidopsis thaliana-Fusarium oxysporum Interaction. *PLoS One* 10: e0127699

Maleck K, Neuenschwander U, Cade RM, Dietrich RA, Dangl JL & Ryals JA (2002) Isolation and characterization of broad-spectrum disease-resistant Arabidopsis mutants. *Genetics* 160: 1661–1671

McDowell JM, Cuzick A, Can C, Beynon J, Dangl JL & Holub EB (2000) Downy mildew (Peronospora parasitica) resistance genes in Arabidopsis vary in functional requirements for NDR1, EDS1, NPR1 and salicylic acid accumulation. *Plant J* 22: 523–529

McDowell JM, Williams SG, Funderburg NT, Eulgem T & Dangl JL (2005)

Genetic analysis of developmentally regulated resistance to downy mildew (Hyaloperonospora parasitica) in Arabidopsis thaliana. *Mol Plant Microbe Interact* 18: 1226–1234

Mouradov A, Cremer F & Coupland G (2002) Control of flowering time: interacting pathways as a basis for diversity. *Plant Cell* 14 Suppl: S111–30

Ngou BPM, Ahn H-K, Ding P & Jones JDG (2021) Mutual potentiation of plant immunity by cell-surface and intracellular receptors. *Nature* 592: 110–115

Parker JE, Szabo V, Staskawicz BJ, Lister C, Dean C, Daniels MJ & Jones JDG (1993) Phenotypic characterization and molecular mapping of the Arabidopsis thaliana locus RPP5, determining disease resistance to Peronospora parasitica. *Plant J* 4: 821–831

Petersen M, Brodersen P, Naested H, Andreasson E, Lindhart U, Johansen B, Nielsen HB, Lacy M, Austin MJ, Parker JE, *et al* (2000) Arabidopsis map kinase 4 negatively regulates systemic acquired resistance. *Cell* 103: 1111–1120

Rechsteiner M & Rogers SW (1996) PEST sequences and regulation by proteolysis. *Trends Biochem Sci* 21: 267–271

Rusterucci C, Zhao Z, Haines K, Mellersh D, Neumann M & Cameron RK (2005) Age-related resistance to Pseudomonas syringae pv. tomato is associated with the transition to flowering in Arabidopsis and is effective against Peronospora parasitica. *Physiol Mol Plant Pathol* 66: 222–231

Saze H, Kitayama J, Takashima K, Miura S, Harukawa Y, Ito T & Kakutani T (2013) Mechanism for full-length RNA processing of Arabidopsis genes containing intragenic heterochromatin. *Nat Commun* 4: 2301

Schiestl FP, Kirk H, Bigler L, Cozzolino S & Desurmont GA (2014) Herbivory and floral signaling: phenotypic plasticity and tradeoffs between reproduction and indirect defense. *New Phytol* 203: 257–266

Schiestl RH & Gietz RD (1989) High efficiency transformation of intact yeast cells using single stranded nucleic acids as a carrier. *Curr Genet* 16: 339–346

Shen Q-H, Saijo Y, Mauch S, Biskup C, Bieri S, Keller B, Seki H, Ulker B, Somssich IE & Schulze-Lefert P (2007) Nuclear activity of MLA immune receptors links isolate-specific and basal disease-resistance responses. *Science* 315: 1098–1103

Stokes TL, Kunkel BN & Richards EJ (2002) Epigenetic variation in Arabidopsis disease resistance. *Genes Dev* 16: 171–182

Tan X, Meyers BC, Kozik A, West MAL, Morgante M, St Clair DA, Bent AF & Michelmore RW (2007) Global expression analysis of nucleotide binding site-leucine rich repeat-encoding and related genes in Arabidopsis. *BMC Plant Biol* 7: 56

Tao Y, Xie Z, Chen W, Glazebrook J, Chang H-S, Han B, Zhu T, Zou G & Katagiri F (2003) Quantitative nature of Arabidopsis responses during compatible and incompatible interactions with the bacterial pathogen Pseudomonas syringae. *Plant Cell* 15: 317–330

Toufighi K, Brady SM, Austin R, Ly E & Provart NJ (2005) The Botany Array Resource: e-Northerns, Expression Angling, and promoter analyses. *Plant J* 43: 153–163

Tsuchiya T & Eulgem T (2010a) Co-option of EDM2 to distinct regulatory modules in Arabidopsis thaliana development. *BMC Plant Biology* 10: 203 doi:10.1186/1471-2229-10-203 [PREPRINT]

Tsuchiya T & Eulgem T (2010b) The Arabidopsis defense component EDM2 affects the floral transition in an FLC-dependent manner. *Plant J* 62: 518–528

Tsuchiya T & Eulgem T (2011) EMSY-like genes are required for full RPP7-mediated race-specific immunity and basal defense in Arabidopsis. *Mol Plant Microbe Interact* 24: 1573–1581

Tsuchiya T & Eulgem T (2013a) Mutations in EDM2 selectively affect silencing states of transposons and induce plant developmental plasticity. *Sci Rep* 3: 1701

Tsuchiya T & Eulgem T (2013b) An alternative polyadenylation mechanism coopted to the Arabidopsis RPP7 gene through intronic retrotransposon domestication. *Proc Natl Acad Sci U S A* 110: E3535–43

Tsuchiya T & Eulgem T (2014) The PHD-finger module of the Arabidopsis thaliana defense regulator EDM2 can recognize triply modified histone H3 peptides. *Plant Signal Behav* 9: e29202

Veley KM & Michaels SD (2008) Functional redundancy and new roles for genes of the autonomous floral-promotion pathway. *Plant Physiol* 147: 682–695

Verhagen BWM, Glazebrook J, Zhu T, Chang H-S, van Loon LC & Pieterse CMJ (2004) The transcriptome of rhizobacteria-induced systemic resistance in arabidopsis. *Mol Plant Microbe Interact* 17: 895–908

Wang D, Amornsiripanitch N & Dong X (2006) A genomic approach to identify

regulatory nodes in the transcriptional network of systemic acquired resistance in plants. *PLoS Pathog* 2: e123

Wang J-W, Czech B & Weigel D (2009) miR156-regulated SPL transcription factors define an endogenous flowering pathway in Arabidopsis thaliana. *Cell* 138: 738–749

Wang X, Duan C-G, Tang K, Wang B, Zhang H, Lei M, Lu K, Mangrauthia SK, Wang P, Zhu G, *et al* (2013) RNA-binding protein regulates plant DNA methylation by controlling mRNA processing at the intronic heterochromatin-containing gene IBM1. *Proc Natl Acad Sci U S A* 110: 15467–15472

Wang Z-P, Xing H-L, Dong L, Zhang H-Y, Han C-Y, Wang X-C & Chen Q-J (2015) Egg cell-specific promoter-controlled CRISPR/Cas9 efficiently generates homozygous mutants for multiple target genes in Arabidopsis in a single generation. *Genome Biol* 16: 144

Wilson DC, Carella P, Isaacs M & Cameron RK (2013) The floral transition is not the developmental switch that confers competence for the Arabidopsis age-related resistance response to Pseudomonas syringae pv. tomato. *Plant Mol Biol* 83: 235–246

Wu G, Park MY, Conway SR, Wang J-W, Weigel D & Poethig RS (2009) The sequential action of miR156 and miR172 regulates developmental timing in Arabidopsis. *Cell* 138: 750–759

Xu M, Hu T, Zhao J, Park M-Y, Earley KW, Wu G, Yang L & Poethig RS (2016) Developmental Functions of miR156-Regulated SQUAMOSA PROMOTER BINDING PROTEIN-LIKE (SPL) Genes in Arabidopsis thaliana. *PLoS Genet* 12: e1006263

Yuan M, Ngou BPM, Ding P & Xin X-F (2021) PTI-ETI crosstalk: an integrative view of plant immunity. *Curr Opin Plant Biol* 62: 102030

Zhang Y, Xia R, Kuang H & Meyers BC (2016) The Diversification of Plant NBS-LRR Defense Genes Directs the Evolution of MicroRNAs That Target Them. *Mol Biol Evol* 33: 2692–2705

Zhang Y-Z, Lin J, Ren Z, Chen C-X, Miki D, Xie S-S, Zhang J, Chang Y-N, Jiang J, Yan J, *et al* (2021) Genome-wide distribution and functions of the AAE complex in epigenetic regulation in Arabidopsis. *J Integr Plant Biol* 63: 707–722

Zhao D, Zhang X, Guan H, Xiong X, Shi X, Deng H & Li H (2016) The BAH domain of BAHD1 is a histone H3K27me3 reader. *Protein Cell* 7: 222–226

Zhu Q-H & Helliwell CA (2011) Regulation of flowering time and floral patterning by miR172. *J Exp Bot* 62: 487–495

Zipfel C (2014) Plant pattern-recognition receptors. *Trends Immunol* 35: 345–351

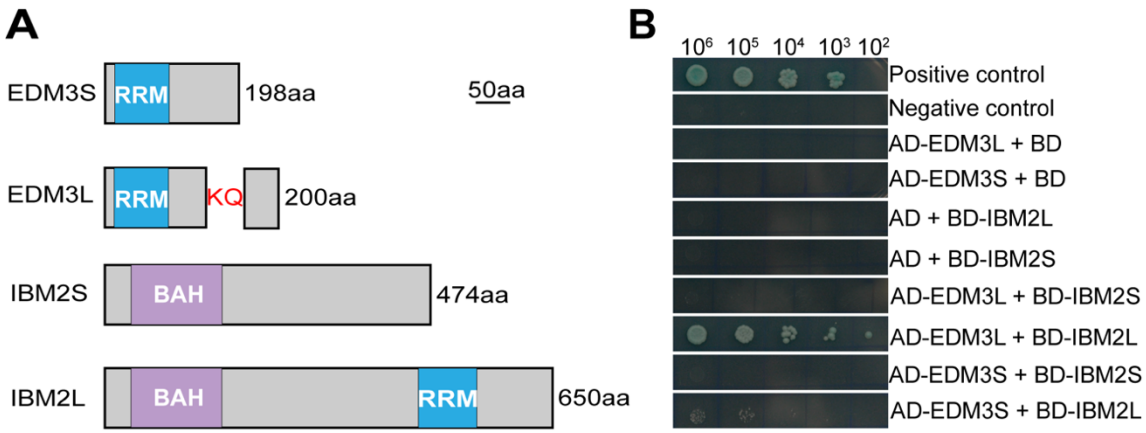

Figure 2.1. EDM3S and EDM3L interact with IBM2L but not IBM2S in yeast.
A. Predicted protein isoforms of EDM3 and IBM2 produced by alternative transcript splicing. Both EDM3 isoforms contain an RRM domain, while EDM3L has an additional KQ dipeptide near its C-terminus. Both IBM2 isoforms contain a BAH (Bromo adjacent homology) domain, while only IBM2L has an RRM domain at the C-terminus.
B. Yeast two-hybrid interactions tests with different EDM3 and IBM2 isoforms. *EDM3S* and *EDM3L* were cloned into the prey expression construct, pGADT7, while *IBM2S* and *IBM2L* were cloned into the bait expression construct, pGBKT7. The indicated pairs of constructs were transformed into yeast cells and assayed for growth after serial dilution on synthetic defined (SD) media depleted of adenine, leucine, tryptophan and histidine. Only yeast cells containing each of the two expression constructs, that are equipped with leucine and tryptophan biosynthetic marker genes, can grow on this medium if the *ADE2* and *HIS3* reporter genes are expressed due to physical interactions between the respective bait and prey proteins.

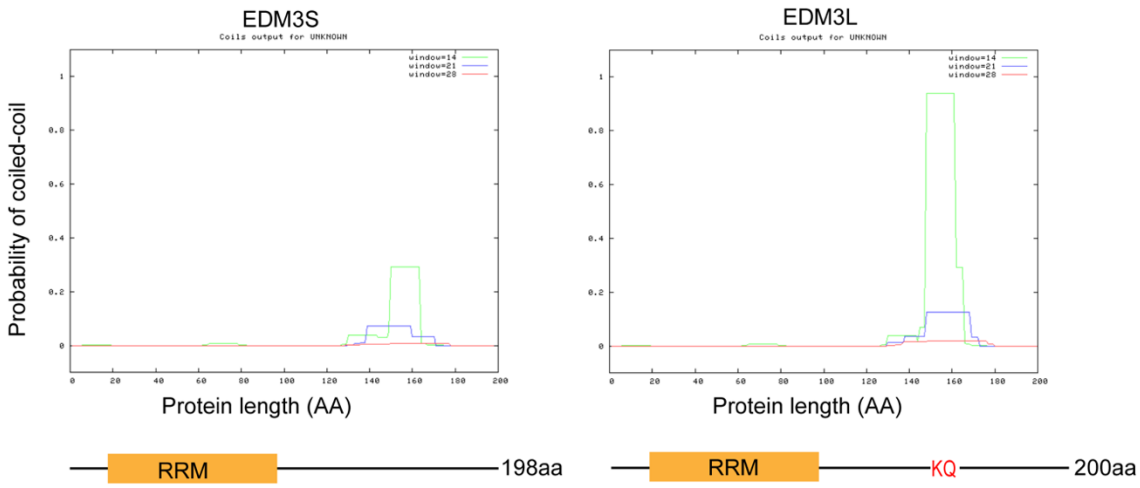

Figure 2.2. EDM3L is more likely to form a C-terminal coiled coil structure than EDM3S. Probabilities of forming coiled-coil structures for EDM3S and EDM3L determined by "COILS" (Lupas *et al*, 1991).

IBM2.1 (AT5G11470.2 CDS, IBM2L, 1953bp)

ATGGAAGAATCTGTAGCATCTGAAGGCTTAGAATTTAAGTGGGGTAAAAAGAAAGGTGTTGGTGGGAAAAAGAAAGATGTCCAGTTCTA
TGAATCTTTCACCTATGATGGCGATGAATACCGTCTTTATGACTGTGTCTTAGTTGGCAATGCCAGTGAACCAGACTCTACTGAACCCT
TCATTGGCATGATCATAAAAATTTGGGAACACGCTAATAAGCATATCCCAAAGAAAGTCAAGCTTCTCTGGTTCTTTAAACCTTCTGAG
ATTGCGCCATATCTTGAAGGAGTCCCGAATGTACTTGCCAATGAAGTGTTTTTAGCATCGGGTGAAGGTCTTGGCCTTGCTAATACCAA
CCAATTGGAAGCAATCGGTGGAAAATGCTCTGTTCTATGCATTTCAAAAGACAAAAGAAATCCACAACCCTCGGATGAAAAATTCAACT
CAGCGGACTTCGTGTTTTGCCGAGCATTTGATGTTGGAAGTTGCAAAGTTGTGGATACGATTGATGATAAGATTGCTGGAGTTGACGTT
AAATTTATCTTTAACAGAGCGTGCTCTGAGAAAGAAGCAACTGCGGTGCAGAATATTGAAGCAGACGTAAATGGGAAGTCAGATAGTTT
GAAACCAAATGGTCCTTTAGCTAGGGGAGCTAGTGGTTCAGTTAGGAAAATCGAAGACAGCGCTTTTGAATCTTCTGACTGTAAAGAAA
ACAGTAATGGTTGCAAAGAAGAGAAAGAAAAAGGTCACTACCAACTCGCTATAAAAAAATCTACACTTGCAGAAGAAAGGTCTAACAAG
GATTCTGGCTCTAGGGGAAATCATTATAATGGCAAAGATCAAGAAAGTGAAGTTAAAAAACAGTTAACTAAACAAAAATCTATGCCTGG
CGAAGAAAGATATAGTAACTCTTTTGAAGCTTCTGGCTCCAGGACAATTCATTCCATTTCAAAGAAAGCTCAAGAAAATGATGTTAAAA
AGCAGTTGACTAAACAAAAATCTATGCCCGCTGGAGAAAGATATAGTCAAGAGTCGAGTGGATTGGATGACAGGCCTCTGAAGAAACAG
AAACTTGATGGTTCTGTTACAGTACGAGATGGATGGGATACAACCATTTTGCAGAACATTACTTCTGATGGTAAAAAGGATACAGGATC
TTTTAAGAGACCTAGAGACAAAGTGACTATAGAGGAAGTCCCTCCCGAAAAGCGCAGCTTTGTTAAGAACCGAGATCTTGTAGTGTCAG
TATCTGAAGGAAAAACTACAAAAACTGTAACTGAAAAAGGTATATCCAAGAAGCCCAGCTTTGGACGTGCTGAGGACAAGATGTCGGCA
GATGATAATGAAAGAAACTATCAAGTAACTGAAGTGTGCCGAAGGCCGGATGCTGGAAAAAGTAAATGGTTCCGGAGTCTTCCTTGGGA
AGAAAGTATGAGGGAAGCAGAAAAAAAAGGGACTGTGGTACTTCTTCAAAACTTGGATCCTACTTATACATCTGATGAAGTGGAGGATA
TAGTCTATTCTGCTTTGAACCAGCAATGCGAAGCGAGGATGATAGAGCGTACATCAGTCACTATTCCTCATATTGGTGAAGCTTTGGTC
ATTTTCAAAACAAGAGAAGTTGCAGAAAGGGTGATTAGAAGACTAGATGAGGGATGCTTGTTGCTATCAAGTGGGAGGCCCCTTGTTGC
TTCTTTCGCTAAGATTACTCCACCAGGGAAGCCGTCATTATTCTCAGGCCATATCAAACTACACAAAACTCAAACGCGACGGGAGATGA
GAGATGCCGTGGCTACATCACATTCTTCTCAGCCTAACAACCTTGAATTTGACATGGCCATGGAATGGTGTTTGCACCAAGCCAGACAC
GAGCAGGCGTCTGAAAGTGTATCTAAGCGGCAATTGGAGGAGATGAAGTCGCTGCGGATTAACTTCAAGCTGAAACTTCCTTAG

IBM2.2 (AT5G11470.1 CDS, 2136bp, one of two isoforms that are annotated in TAIR10 cannot be cloned in this article)

ATGGAAGAATCTGTAGCATCTGAAGGCTTAGAATTTAAGTGGGGTAAAAAGAAAGGTGTTGGTGGGAAAAAGAAAGATGTCCAGTTCTA
TGAATCTTTCACCTATGATGGCGATGAATACCGTCTTTATGACTGTGTCTTAGTTGGCAATGCCAGTGAACCAGACTCTACTGAACCCT
TCATTGGCATGATCATAAAAATTTGGGAACACGCTAATAAGCATATCCCAAAGAAAGTCAAGCTTCTCTGGTTCTTTAAACCTTCTGAG
ATTGCGCCATATCTTGAAGGAGTCCCGAATGTACTTGCCAATGAAGTGTTTTTAGCATCGGGTGAAGGTCTTGGCCTTGCTAATACCAA
CCAATTGGAAGCAATCGGTGGAAAATGCTCTGTTCTATGCATTTCAAAAGACAAAAGAAATCCACAACCCTCGGATGAAAAATTCAACT
CAGCGGACTTCGTGTTTTGCCGAGCATTTGATGTTGGAAGTTGCAAAGTTGTGGATACGATTGATGATAAGATTGCTGGAGTTGACGTT
AAATTTATCTTTAACAGAGCGTGCTCTGAGAAAGAAGCAACTGCGGTGCAGAATATTGAAGCAGACGTAAATGGGAAGTCAGATAGTTT
GAAACCAAATGGTCCTTTAGCTAGGGGAGCTAGTGGTTCAGTTAGGAAAATCGAAGACAGCGCTTTTGAATCTTCTGACTGTAAAGAAA
ACAGTAATGGTTGCAAAGAAGAGAAAGAAAAAGGTCACTACCAACTCGCTATAAAAAAATCTACACTTGCAGAAGAAAGGTCTAACAAG
GATTCTGGCTCTAGGGGAAATCATTATAATGGCAAAGATCAAGAAAGTGAAGTTAAAAAACAGTTAACTAAACAAAAATCTATGCCTGG
CGAAGAAAGATATAGTAACTCTTTTGAAGCTTCTGGCTCCAGGACAATTCATTCCATTTCAAAGAAAGCTCAAGAAAATGATGTTAAAA
AGCAGTTGACTAAACAAAAATCTATGCCCGCTGGAGAAAGATATAGTCAAGAGTCGAGTGGATTGGATGACAGGCCTCTGAAGAAACAG
AAACTTGATGGTTCTGTTACAGTACGAGATGGATGGGATACAACCATTTTGCAGAACATTACTTCTGATGGTAAAAAGGATACAGGATC
TTTTAAGAGACCTAGAGACAAAGTGACTATAGAGGAAGTCCCTCCCGAAAAGCGCAGCTTTGTTAAGAACCGAGATCTTGTAGTGTCAG
TATCTGAAGGAAAAACTACAAAAACTGTAACTGAAAAAGGTATATCCAAGAAGCCCAGCTTTGGACGTGCTGAGGACAAGATGTCGGCA
GATGATAATGAAAGAAACTATCAAGTAACTGAAGTGTGCCGAAGGCCGGATGCTGGAAAAAGTAAATGGTTCCGGAGTCTTCCTTGGGA
AGAAAGTATGAGGGAAGCAGAAAAAAAAGGGACTGTGGTACTTCTTCAAAACTTGGATCCTACTTATACATCTGATGAAGTGGAGGATA
TAGTCTATTCTGCTTTGAACCAGCAATGCGAAGCGAGGATGATAGAGCGTACATCAGTCACTATTCCTCATATTGGTGAAGCTTTGGTC
ATTTTCAAAACAAGAGAAGTTGCAGAAAGGGTGATTAGAAGACTAGATGAGGGATGCTTGTTGCTATCAAGTGGGAGGCCCCTTGTTGC
TTCTTTCGCTAAGATTACTCCACCAGGGAAGCCGTCATTATTCTCAGGCCATATCAAACTACACAAAACTCAAACGCGACGGGAGATGA
GAGATGCCGTGGCTACATCACATTCTTCTCAGCCTAACAACCTTGAATTTGACATGGCCATGGAATGGTGTTTGCACCAAGCCAGACAC
GAGCAGGCGTCTGAAAGTGTATCTAAGCGGCAATTGGAGGAGATGAAGTCGCTGCGGATTAACTTCAAGCTGAAACTTCCTTATGAGAC
TCAAGAATTTTGGTTTCATGCCATCCAGTCCCCCAACTTTGACTCGGAGGAATATACTGATGCGGCTTCTGGTCTCAAATCGGACGACC
CTTTTGTAGTTACATATTTTTTTGTAAGGGTCAGTTTCACTAGTGAAGTGCTAAACTTTTGTGTGGATCAGGAAAGGTCAAGAGAGTAA

IBM2.3 (IBM2L CDS,1953bp, cloned in this article)

ATGGAAGAATCTGTAGCATCTGAAGGCTTAGAATTTAAGTGGGGTAAAAAGAAAGGTGTTGGTGGGAAAAAGAAAGATGTCCAGTTCTA
TGAATCTTTCACCTATGATGGCGATGAATACCGTCTTTATGACTGTGTCTTAGTTGGCAATGCCAGTGAACCAGACTCTACTGAACCCT
TCATTGGCATGATCATAAAAATTTGGGAACACGCTAATAAGCATATCCCAAAGAAAGTCAAGCTTCTCTGGTTCTTTAAACCTTCTGAG
ATTGCGCCATATCTTGAAGGAGTCCCGAATGTACTTGCCAATGAAGTGTTTTTAGCATCGGGTGAAGGTCTTGGCCTTGCTAATACCAA
CCAATTGGAAGCAATCGGTGGAAAATGCTCTGTTCTATGCATTTCAAAAGACAAAAGAAATCCACAACCCTCGGATGAAAAATTCAACT
CAGCGGACTTCGTGTTTTGCCGAGCATTTGATGTTGGAAGTTGCAAAGTTGTGGATACGATTGATGATAAGATTGCTGGAGTTGACGTT
AAATTTATCTTTAACAGAGCGTGCTCTGAGAAAGAAGCAACTGCGGTGCAGAATATTGAAGCAGACGTAAATGGGAAGTCAGATAGTTT
GAAACCAAATGGTCCTTTAGCTAGGGGAGCTAGTGGTTCAGTTAGGAAAATCGAAGACAGCGCTTTTGAATCTTCTGACTGTAAAGAAA
ACAGTAATGGTTGCAAAGAAGAGAAAGAAAAAGGTCACTACCAACTCGCTATAAAAAAATCTACACTTGCAGAAGAAAGGTCTAACAAG
GATTCTGGCTCTAGGGGAAATCATTATAATGGCAAAGATCAAGAAAGTGAAGTTAAAAAACAGTTAACTAAACAAAAATCTATGCCTGG
CGAAGAAAGATATAGTAACTCTTTTGAAGCTTCTGGCTCCAGGACAATTCATTCCATTTCAAAGAAAGCTCAAGAAAATGATGTTAAAA
AGCAGTTGACTAAACAAAAATCTATGCCCGCTGGAGAAAGATATAGTCAAGAGTCGAGTGGATTGGATGACAGGCCTCTGAAGAAACAG
AAACTTGATGGTTCTGTTACAGTACGAGATGGATGGGATACAACCATTTTGCAGAACATTACTTCTGATGGTAAAAAGGATACAGGATC
TTTTAAGAGACCTAGAGACAAAGTGACTATAGAGGAAGTCCCTCCCGAAAAGCGCAGCTTTGTTAAGAACCGAGATCTTGTAGTGTCAG

TATCTGAAGGAAAAACTACAAAAACTGTAACTGAAAAAGGTATATCCAAGAAGCCCAGCTTTGGACGTGCTGAGGACAAGATGTCGGCA
GATGATAATGAAAGAAACTATCAAGTAACTGAAGTGTGCCGAAGGCCGGATGCTGGAAAAAGTAAATGGTTCCGGAGTCTTCCTTGGGA
AGAAAGTATGAGGGAAGCAGAAAAAAAAGGGACTGTGGTACTTCTTCAAAACTTGGATCCTACTTATACATCTGATGAAGTGGAGGATA
TAGTCTATTCTGCTTTGAACCAGCAATGCGAAGCGAGGATGATAGAGCGTACATCAGTCACTATTCCTCATATTGGTGAAGCTTTGGTC
ATTTTCAAAACAAGAGAAGTTGCAGAAAGGGTGATTAGAAGACTAGATGAGGGATGCTTGTTGCTATCAAGTGGGAGGCCCCTTGTTGC
TTCTTTCGCTAAGATTACTCCACCAGGGAAGCCGTCATTATTCTCAGGCCATATCAAACTACACAAAACTCAAACGCGACGGGAGATGA
GAGATGCCGTGGCTACATCACATTCTTCTCAGCCTAACAACCTTGAATTTGACATGGCCATGGAATGGTGTTTGCACCAAGCCAGACAC
GAGCAGGCGTCTGAAAGTGTATCTAAGCGGCAATTGGAGGAGATGAAGTCGCTGCGGATTAACTTCAAGCTGAAACTTCCTTAGtttca
gaatcatcttgtcactctcgtgtaagtattagctcttatctacatgtctatcatctaaacgaaccaaatgatcacttacttttctttgct
tcagacagaaatatcaccaactgtagattagaaggaaaaacacaaggtctcttttagcctctaaagacagTGAGACTCAAGAATTTTGG
TTTCATGCCATCCAGTCCCCCAACTTTGACTCGGAGGAATATACTGATGCGGCTTCTGGTCTCAAATCGGACGACCCTTTTGTAGTTAC
ATATTTTTTTGTAAGGGTCAGTTTCACTAGTGAAGTGCTAAACTTTTGTGTGGATCAGGAAAGGTCAAGAGAGTAA

IBM2.4 (IBM2L CDS, 1953bp, cloned in this article)

ATGGAAGAATCTGTAGCATCTGAAGGCTTAGAATTTAAGTGGGGTAAAAAGAAAGGTGTTGGTGGGAAAAAGAAAGATGTCCAGTTCTA
TGAATCTTTCACCTATGATGGCGATGAATACCGTCTTTATGACTGTGTCTTAGTTGGCAATGCCAGTGAACCAGACTCTACTGAACCCT
TCATTGGCATGATCATAAAAATTTGGGAACACGCTAATAAGCATATCCCAAAGAAAGTCAAGCTTCTCTGGTTCTTTAAACCTTCTGAG
ATTGCGCCATATCTTGAAGGAGTCCCGAATGTACTTGCCAATGAAGTGTTTTTAGCATCGGGTGAAGGTCTTGGCCTTGCTAATACCAA
CCAATTGGAAGCAATCGGTGGAAAATGCTCTGTTCTATGCATTTCAAAAGACAAAAGAAATCCACAACCCTCGGATGAAAAATTCAACT
CAGCGGACTTCGTGTTTTGCCGAGCATTTGATGTTGGAAGTTGCAAAGTTGTGGATACGATTGATGATAAGATTGCTGGAGTTGACGTT
AAATTTATCTTTAACAGAGCGTGCTCTGAGAAAGAAGCAACTGCGGTGCAGAATATTGAAGCAGACGTAAATGGGAAGTCAGATAGTTT
GAAACCAAATGGTCCTTTAGCTAGGGGAGCTAGTGGTTCAGTTAGGAAAATCGAAGACAGCGCTTTTGAATCTTCTGACTGTAAAGAAA
ACAGTAATGGTTGCAAAGAAGAGAAAGAAAAAGGTCACTACCAACTCGCTATAAAAAAATCTACACTTGCAGAAGAAAGGTCTAACAAG
GATTCTGGCTCTAGGGGAAATCATTATAATGGCAAAGATCAAGAAAGTGAAGTTAAAAAACAGTTAACTAAACAAAAATCTATGCCTGG
CGAAGAAAGATATAGTAACTCTTTTGAAGCTTCTGGCTCCAGGACAATTCATTCCATTTCAAAGAAAGCTCAAGAAAATGATGTTAAAA
AGCAGTTGACTAAACAAAAATCTATGCCCGCTGGAGAAAGATATAGTCAAGAGTCGAGTGGATTGGATGACAGGCCTCTGAAGAAACAG
AAACTTGATGGTTCTGTTACAGTACGAGATGGATGGGATACAACCATTTTGCAGAACATTACTTCTGATGGTAAAAAGGATACAGGATC
TTTTAAGAGACCTAGAGACAAAGTGACTATAGAGGAAGTCCCTCCCGAAAAGCGCAGCTTTGTTAAGAACCGAGATCTTGTAGTGTCAG
TATCTGAAGGAAAAACTACAAAAACTGTAACTGAAAAAGGTATATCCAAGAAGCCCAGCTTTGGACGTGCTGAGGACAAGATGTCGGCA
GATGATAATGAAAGAAACTATCAAGTAACTGAAGTGTGCCGAAGGCCGGATGCTgtaagtttatacttactatatgtttcctgcaatat
gatttagtttacattggtttggaactggctgtttcatgagatttcagagcgtgttgtaaaatctttagATGCAAGGATGTGGTTTTGCA
AGAACACAATTCTAAAAGGAGCAGTTTTGTTTTACAGTCCTTCACACTgtatgttgtatagttgtagtgatgttctgtcattcttctca
tcttattatgttaccacaatgcttggtaacattgaggtttatctaacagatttttgtttccttatttatttcagGGAAAAAGTAAATGG
TTCCGGAGTCTTCCTTGGGAAGAAAGTATGAGGGAAGCAGAAAAAAAAGGGACTGTGGTACTTCTTCAAAACTTGGATCCTACTTATAC
ATCTGATGAAGTGGAGGATATAGTCTATTCTGCTTTGAACCAGCAATGCGAAGCGAGGATGATAGAGCGTACATCAGTCACTATTCCTC
ATATTGGTGAAGCTTTGGTCATTTTCAAAACAAGAGAAGTTGCAGAAAGGGTGATTAGAAGACTAGATGAGGGATGCTTGTTGCTATCA
AGTGGGAGGCCCCTTGTTGCTTCTTTCGCTAAGATTACTCCACCAGGGAAGCCGTCATTATTCTCAGGCCATATCAAACTACACAAAAC
TCAAACGCGACGGGAGATGAGAGATGCCGTGGCTACATCACATTCTTCTCAGCCTAACAACCTTGAATTTGACATGGCCATGGAATGGT

GTTTGCACCAAGCCAGACACGAGCAGGCGTCTGAAAGTGTATCTAAGCGGCAATTGGAGGAGATGAAGTCGCTGCGGATTAACTTCAAG
CTGAAACTTCCTTAgtttcagaatcatcttgtcactctcgtgtaagtattagctcttatctacatgtctatcatctaaacgaaccaaat
gatcacttactttctttgcttcagacagaaatatcaccaactgtagattagaaggaaaaacacaaggtctcttttagcctctaaagaca
gTGAGACTCAAGAATTTTGGTTTCATGCCATCCAGTCCCCCAACTTTGACTCGGAGGAATATACTGATGCGGCTTCTGGTCTCAAATCG
GACGACCCTTTTGTAGTTACATATTTTTTTGTAAGGGTCAGTTTCACTAGTGAAGTGCTAAACTTTTGTGTGGATCAGGAAAGGTCAAG
AGAGTAA

EDM3S (AT1G05970.1 CDS, 597bp)

ATGGCGACTCCGGAAGAAGTAGCGTATGAGAAGTTCCTAGAGAGAGTTCGTCGTACTGTCTACGTAGACGAACTCACGCCTCTTGCCAC
AGCTCCTGTTATTTCATCTGCTTTCAATCAGTTTGGGACTGTCAAGAAAGTCAGCTTCATACCTAACTACTTGGGTCCAAAGGAGCTTC
CTATGGGTGTTCTTGTTGAGATGGAGAATGAAGAGATGACACAGGCTGTTATCTCTACTGTCTCACAGTTACCTTTCATGGTTGCTGGT
ATGCCAAGGCCTGTGAGAGCTTGTGCTGCTGAGCCTAATATGTTTGTTGATAAACCGAAGAAGCCTGGTAGAACGGTCCGTTTTCGCTG
GATTAAGCCTAACGATCCTGATTTCGACAAGGCCAGGAGAGTCAAGCGGCTTGCTCGTAAGCATAGTGCTGAAAATTCGTTCATGCTCA
AGCTTGAGGAGGCAGAGAAGCTGTCGAAACAGCAAGCTGAGACGGCGGTAACACATCACAAGAAGTTTGAGATGATGGATAAACTCCTC
TACGATGGTGTTGCTCAGAAACTGGCTGGCCGTTACGACCTGAAAGGTTTTCCTTATCGGTAG

EDM3L (AT1G05970.2 CDS, 603bp)

ATGGCGACTCCGGAAGAAGTAGCGTATGAGAAGTTCCTAGAGAGAGTTCGTCGTACTGTCTACGTAGACGAACTCACGCCTCTTGCCAC
AGCTCCTGTTATTTCATCTGCTTTCAATCAGTTTGGGACTGTCAAGAAAGTCAGCTTCATACCTAACTACTTGGGTCCAAAGGAGCTTC
CTATGGGTGTTCTTGTTGAGATGGAGAATGAAGAGATGACACAGGCTGTTATCTCTACTGTCTCACAGTTACCTTTCATGGTTGCTGGT
ATGCCAAGGCCTGTGAGAGCTTGTGCTGCTGAGCCTAATATGTTTGTTGATAAACCGAAGAAGCCTGGTAGAACGGTCCGTTTTCGCTG
GATTAAGCCTAACGATCCTGATTTCGACAAGGCCAGGAGAGTCAAGCGGCTTGCTCGTAAGCATAGTGCTGAAAATTCGTTCATGCTCA
AGAAACAGCTTGAGGAGGCAGAGAAGCTGTCGAAACAGCAAGCTGAGACGGCGGTAACACATCACAAGAAGTTTGAGATGATGGATAAA
CTCCTCTACGATGGTGTTGCTCAGAAACTGGCTGGCCGTTACGACCTGAAAGGTTTTCCTTATCGGTAG

EDM3S (protein sequence, 198aa)

MATPEEVAYEKFLERVRRTVYVDELTPLATAPVISSAFNQFGTVKKVSFIPNYLGPKELPMGVLVEMENEEMTQAVISTVSQLPFMVAG
MPRPVRACAAEPNMFVDKPKKPGRTVRFRWIKPNDPDFDKARRVKRLARKHSAENSFMLKLEEAEKLSKQQAETAVTHHKKFEMMDKLL
YDGVAQKLAGRYDLKGFPYR

EDM3L (protein sequence, 200aa)

MATPEEVAYEKFLERVRRTVYVDELTPLATAPVISSAFNQFGTVKKVSFIPNYLGPKELPMGVLVEMENEEMTQAVISTVSQLPFMVAG
MPRPVRACAAEPNMFVDKPKKPGRTVRFRWIKPNDPDFDKARRVKRLARKHSAENSFMLK**KQ**LEEAEKLSKQQAETAVTHHKKFEMMDK
LLYDGVAQKLAGRYDLKGFPYR

IBM2S (protein sequence, 474aa)

MEESVASEGLEFKWGKKKGVGGKKKDVQFYESFTYDGDEYRLYDCVLVGNASEPDSTEPFIGMIIKIWEHANKHIPKKVKLLWFFKPSE
IAPYLEGVPNVLANEVFLASGEGLGLANTNQLEAIGGKCSVLCISKDKRNPQPSDEKFNSADFVFCRAFDVGSCKVVDTIDDKIAGVDV
KFIFNRACSEKEATAVQNIEADVNGKSDSLKPNGPLARGASGSVRKIEDSAFESSDCKENSNGCKEEKEKGHYQLAIKKSTLAEERSNK
DSGSRGNHYNGKDQESEVKKQLTKQKSMPGEERYSNSFEASGSRTIHSISKKAQENDVKKQLTKQKSMPAGERYSQESSGLDDRPLKKQ
KLDGSVTVRDGWDTTILQNITSDGKKDTGSFKRPRDKVTIEEVPPEKRSFVKNRDLVVSVSEGKTTKTVTEKGISKKPSFGRAEDKMSA
DDNERNYQVTEVCRRPDAMQGCGFARTQF

IBM2L (protein sequence, 650aa)

MEESVASEGLEFKWGKKKGVGGKKKDVQFYESFTYDGDEYRLYDCVLVGNASEPDSTEPFIGMIIKIWEHANKHIPKKVKLLWFFKPSE
IAPYLEGVPNVLANEVFLASGEGLGLANTNQLEAIGGKCSVLCISKDKRNPQPSDEKFNSADFVFCRAFDVGSCKVVDTIDDKIAGVDV
KFIFNRACSEKEATAVQNIEADVNGKSDSLKPNGPLARGASGSVRKIEDSAFESSDCKENSNGCKEEKEKGHYQLAIKKSTLAEERSNK
DSGSRGNHYNGKDQESEVKKQLTKQKSMPGEERYSNSFEASGSRTIHSISKKAQENDVKKQLTKQKSMPAGERYSQESSGLDDRPLKKQ
KLDGSVTVRDGWDTTILQNITSDGKKDTGSFKRPRDKVTIEEVPPEKRSFVKNRDLVVSVSEGKTTKTVTEKGISKKPSFGRAEDKMSA
DDNERNYQVTEVCRRPDAGKSKWFRSLPWEESMREAEKKGTVVLLQNLDPTYTSDEVEDIVYSALNQQCEARMIERTSVTIPHIGEALV
IFKTREVAERVIRRLDEGCLLLSSGRPLVASFAKITPPGKPSLFSGHIKLHKTQTRREMRDAVATSHSSQPNNLEFDMAMEWCLHQARH
EQASESVSKRQLEEMKSLRINFKLKLP

Figure 2.3. **Nucleic acid and amino acid sequences of IBM2 and EDM3 splice isoforms.** IBM2 contains five alternative splicing isoforms, among which IBM2.2 is not able to be cloned in this study. IBM2.1, IBM2.3 and IBM2.4 share the same coding sequence, while IBM2.5 has a premature stop codon in the third intron, which prevents the translation of RRM domain. IBM2.2 has a slightly longer C-terminus (highlighted in gray) compared to IBM2.1, IBM2.3 and IBM2.4. DNA sequence that is highlighted in green indicates that sequence is retained after alternative splicing, while sequence that is crossed out means sequence is spliced out. Protein sequence that is highlighted in blue represents coding sequence that encodes RRM domain, while protein sequence that is highlighted in purple indicates sequence that encodes BAH domain.

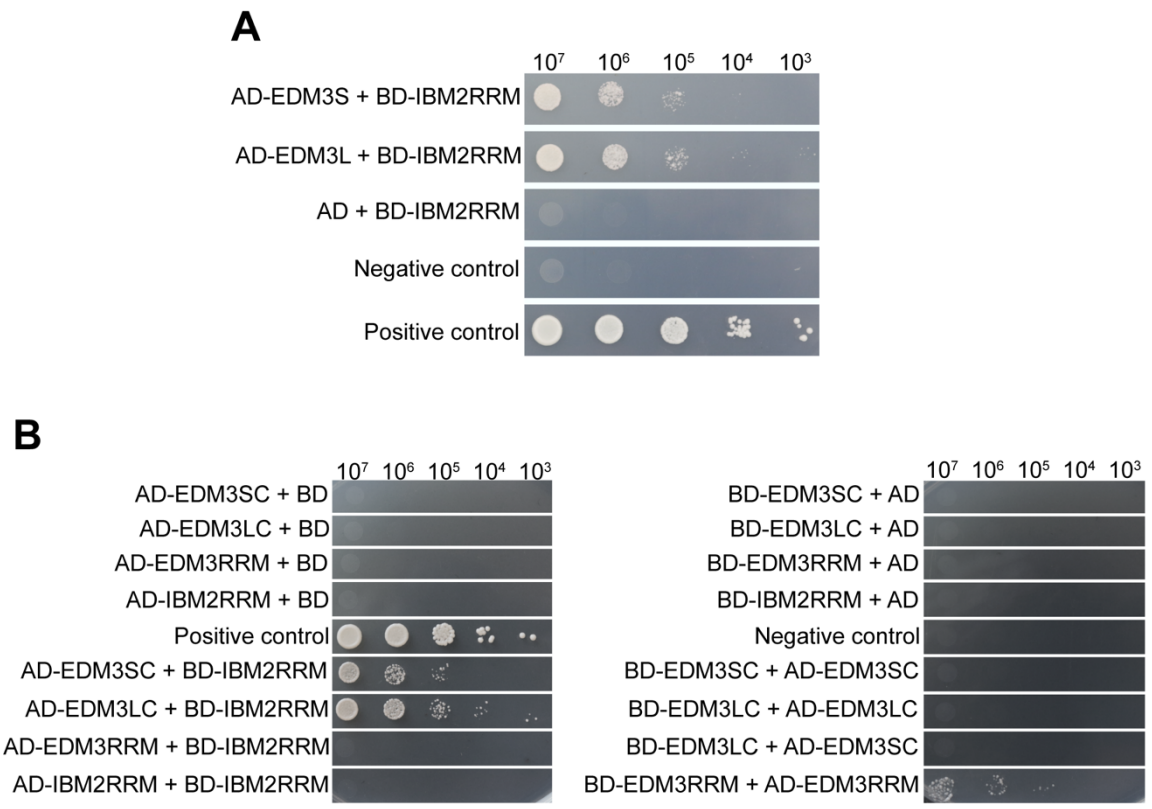

Figure 2.4. Likely roles of individual domains in EDM3-IBM2 interactions.
A. The RRM domain of IBM2 is sufficient for interactions with EDM3 isoforms in yeast.
B. The IBM2 RRM domain interacts with the C-terminal domain of EDM3, while the EDM3 RRM domain can mediate the formation of EDM3 homo- or hetero-dimers in yeast. EDM3 C-terminus (EDM3SC and EDM3LC), RRM domain and IBM2 RRM domain were cloned into prey construct, pGADT7 and bait construct, pGBKT7, respectively. Serial dilution of the yeast cells transformed with the indicated construct pairs were assayed for growth on the synthetic defined (SD) media depleted of adenine, leucine, tryptophan, and histidine.

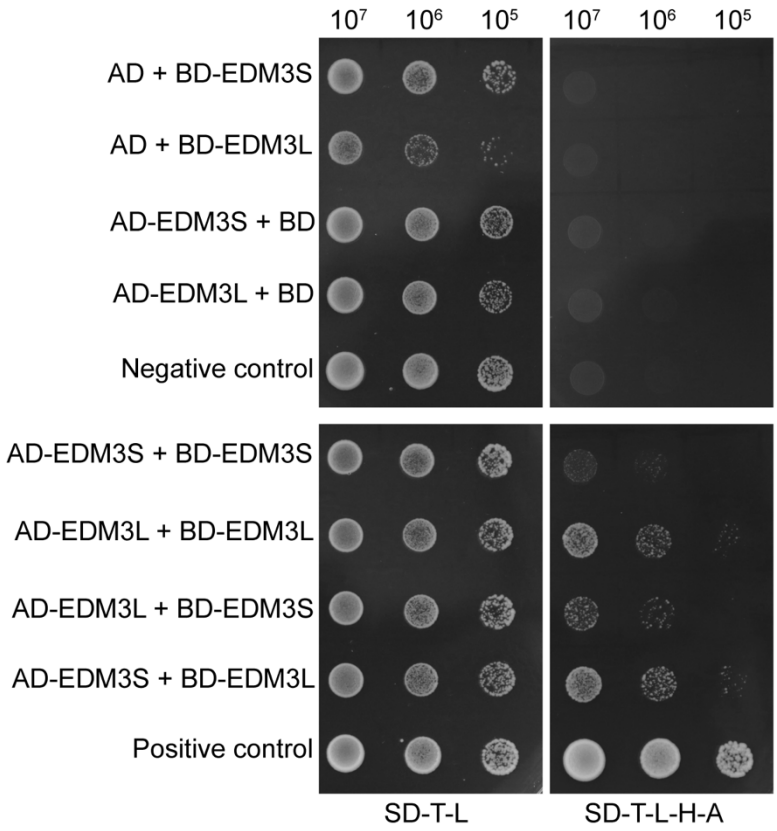

Figure 2.5. Self-association of EDM3 isoforms in yeast.
EDM3S and EDM3L were cloned into prey construct, pGADT7 and bait construct, pGBKT7, respectively. Serial dilution of yeast cells transformed with the indicated construct pairs were assayed for growth on synthetic defined (SD) media depleted of adenine, leucine, tryptophan, and histidine.

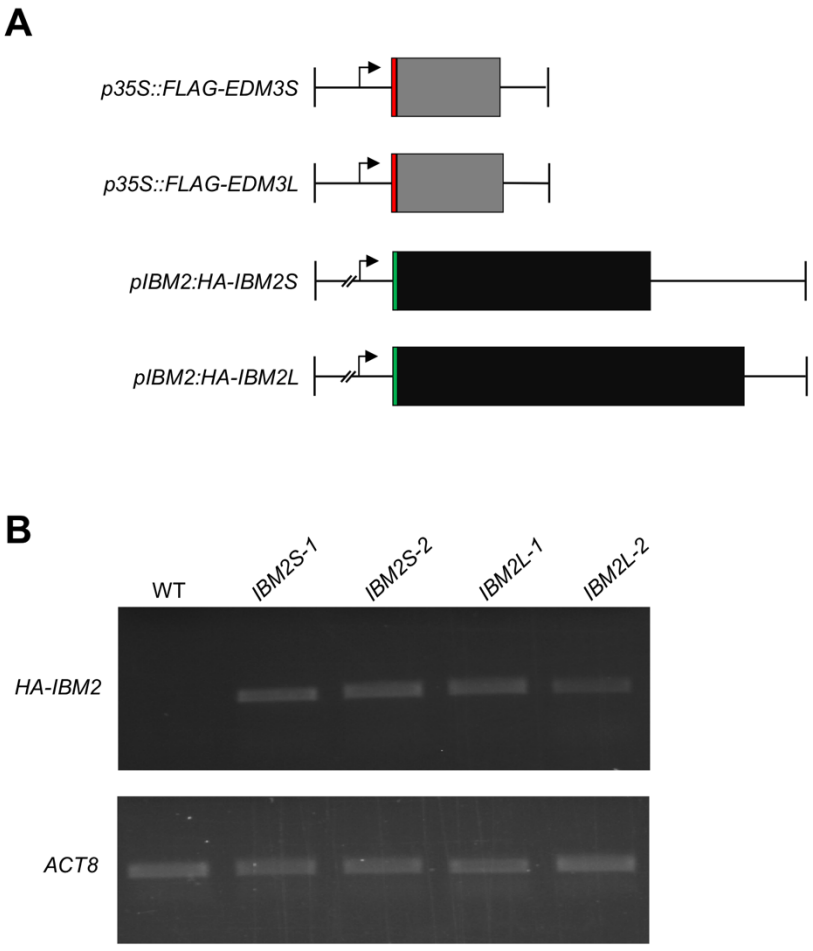

Figure 2.6. Isoform specific complementation lines used in this study.
A. Construct diagrams for complementation lines used in this study. The arrows represent transcription start sites. The red boxes represent FLAG-tag coding sequences, while the green boxes represent HA-tag coding sequences.
B. Semi-quantitative RT-PCR of *IBM2* transgene-specific transcript levels.

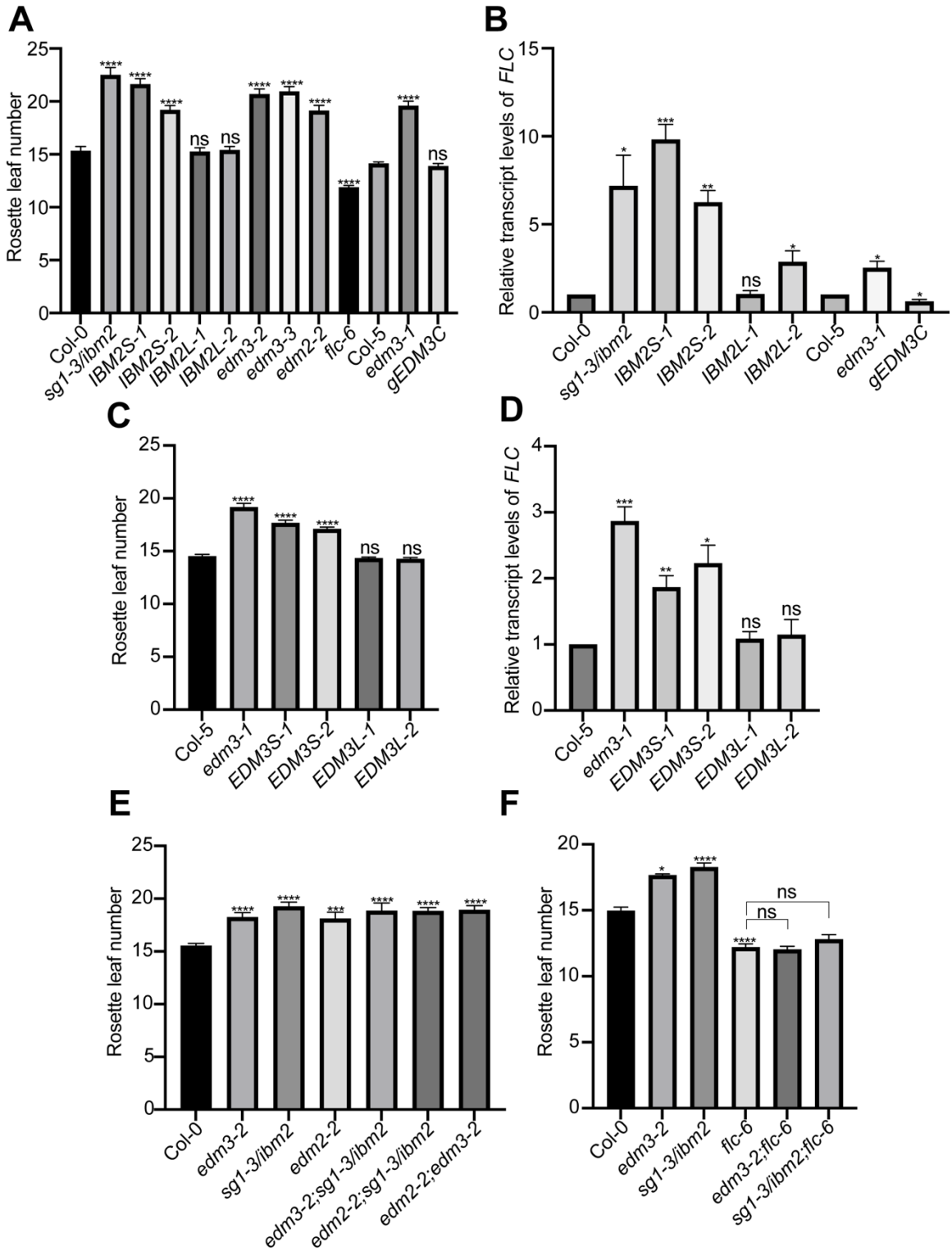
A
Rosette leaf number
Col-0
sg1-3/ibm2
IBM2S-1
IBM2S-2
IBM2L-1
IBM2L-2
edm3-2
edm3-3
edm2-2
flc-6
Col-5
edm3-1
gEDM3C
B
Relative transcript levels of FLC
C
Rosette leaf number
Col-5
edm3-1
EDM3S-1
EDM3S-2
EDM3L-1
EDM3L-2
D
Relative transcript levels of FLC
E
Rosette leaf number
Col-0
edm3-2
sg1-3/ibm2
edm2-2
edm3-2;sg1-3/ibm2
edm2-2;sg1-3/ibm2
edm2-2;edm3-2
F
Rosette leaf number
flc-6
edm3-2;flc-6
sg1-3/ibm2;flc-6

Figure 2.7. Flowering time-related effects of *EDM3* and *IBM2*.
A, C, E, F. Flowering time assays under long day conditions in lines of Col-0 **(A, E, F)** or Col-5 **(C)** backgrounds. At least 16 plants per genotype were used for each flowering time measurement. The *edm3-2* and *edm3-3* lines are deletion mutants in the Col-0 background generated by CRISPR-Cas9. *gEDM3C* represents a genomic *EDM3* complementation line (Lai *et al*, 2019).
B, D. *FLC* transcript levels in lines of Col-0 **(B)** or Col-5 **(D)** backgrounds.
Data information: Data are shown as mean ± SEM. Asterisks indicate significant difference analyzed by student's t-test **(A, B, C, D, E)** or one-way ANOVA **(F)**. (*, $p<0.05$; **, $p<0.01$; ***, $p<0.001$; ****, $p<0.0001$).

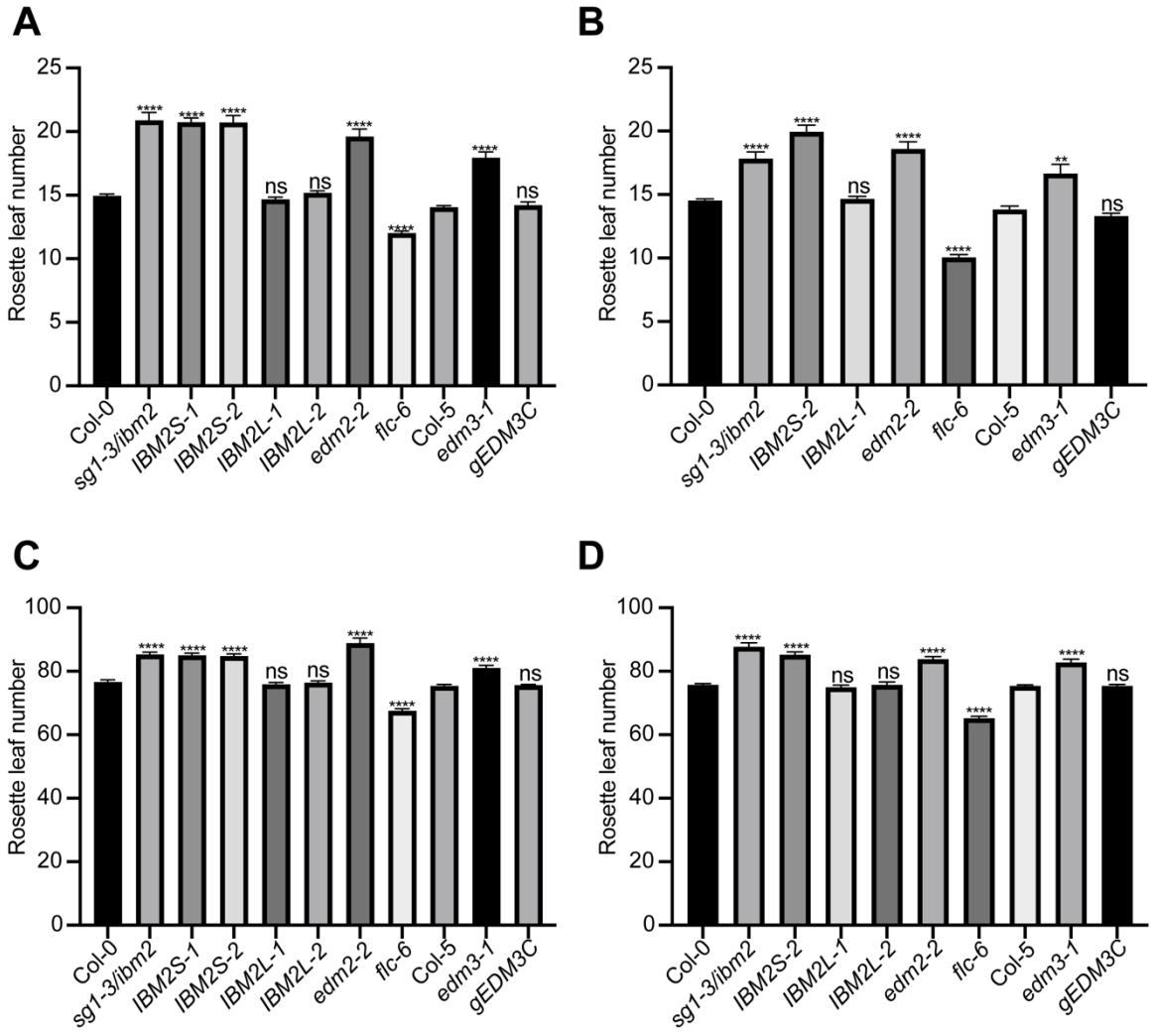

Figure 2.8. Flowering time-related effects of *EDM3* and *IBM2* under long and short-day conditions.

A, B. Two additional replicates of flowering time assays under long day conditions.

C, D. Two replicates of flowering time assays under short day conditions. *edm2-2* was used as late flowering control, while *flc-6* was used as early flowering control.

Data information: At least 16 plants were used for flowering time measurement. Error bars represent standard errors. **, p<0.01; ****, p<0.0001, student's t-test.

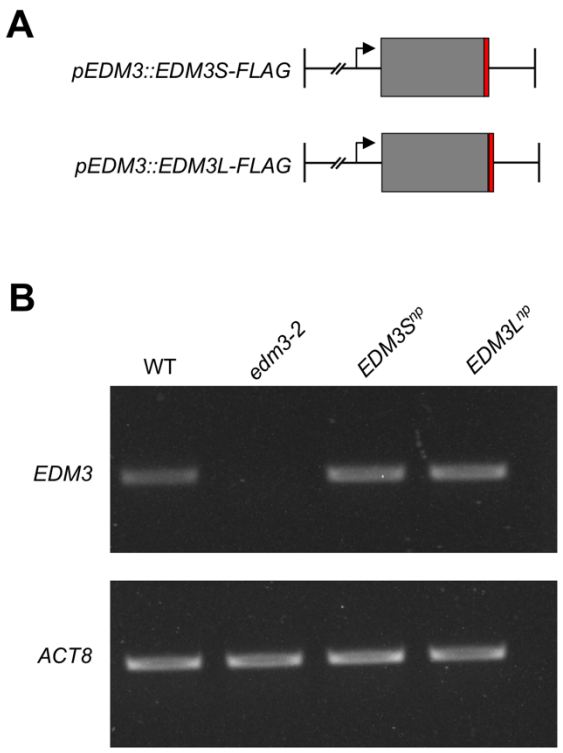

Figure 2.9. Complementation lines expressing EDM3 isoforms controlled by the native *EDM3* promoter.
A. Construct diagrams. Arrows represent transcription start sites. The red boxes represent FLAG-tag coding sequences.
B. Semi-quantitative RT-PCR of *EDM3* transgene-specific transcript levels.

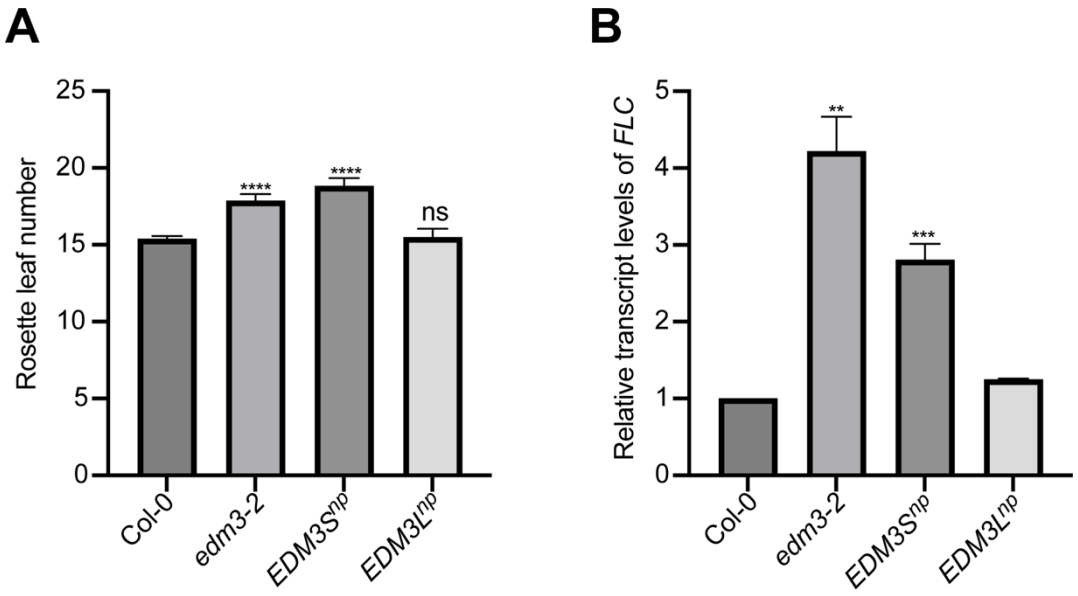

Figure 2.10. Late flowering phenotype in *edm3-2* is restored only by expression of *EDM3L*.
A. Rosette leaf number were counted at bolting under long days. At least 12 plants were used for flowering time measurement.
B. *FLC* mRNA levels in *EDM3* complementation lines under its native promoter were measured by qRT-PCR.
Data information: Data are shown as mean ± SEM. Asterisks indicate significant difference analyzed by student's t-test. (**, p<0.01; ***, p<0.001; ****, p<0.0001).

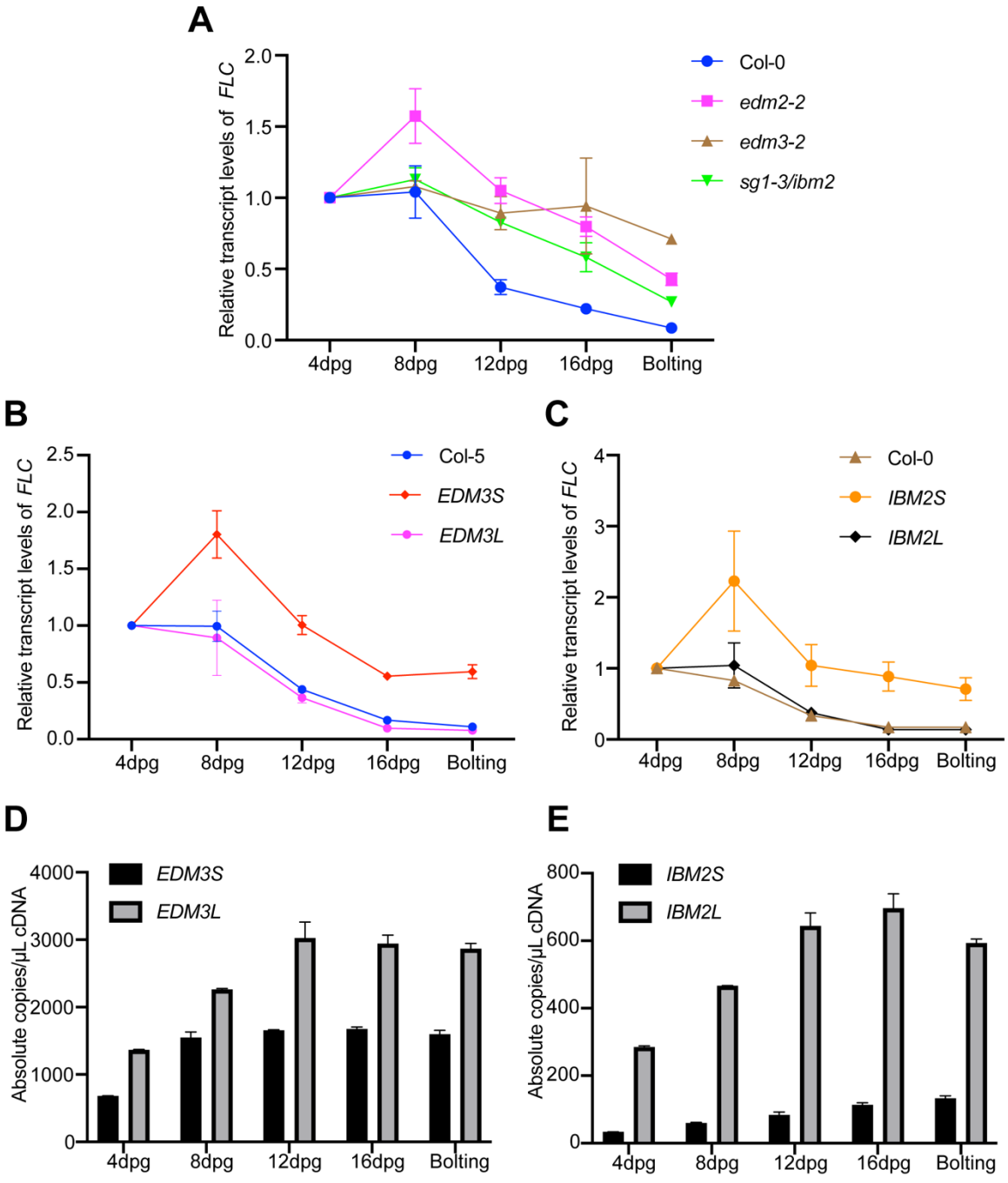
A
Relative transcript levels of FLC
2.0
1.5
1.0
0.5
0.0
4dpg
8dpg
12dpg
16dpg
Bolting
Col-0
edm2-2
edm3-2
sg1-3/ibm2
B
Relative transcript levels of FLC
2.5
2.0
1.5
1.0
0.5
0.0
Col-5
EDM3S
EDM3L
C
Relative transcript levels of FLC
4
3
2
1
0
Col-0
IBM2S
IBM2L
D
Absolute copies/μL cDNA
4000
3000
2000
1000
0
EDM3S
EDM3L
E
Absolute copies/μL cDNA
800
600
400
200
0
IBM2S
IBM2L

Figure 2.11. Decline of *FLC* transcript levels as plants approach flowering.
A-C. *FLC* transcript levels from 4 days post germination (dpg) until bolting in Col-0, *edm3-2* and *sg1-3/ibm2* **(A)**, and their corresponding complementation lines **(B&C)** were measured by qRT-PCR. All time points were normalized to 4dpg. Error bars represent standard errors from three independent experiments.
D, E. Transcript levels of *EDM3* and *IBM2* isoforms from 4dpg to bolting determined by absolute quantification PCR. Experiments were repeated three times. Results from one representative replicate are shown. Error bars represent standard errors. Bolting times: Col-0 (~22dpg), *edm2-2*, *edm3-2* and *sg1-3/ibm2* (~26dpg), *EDM3S* (~25dpg), *IBM2S* (~27dpg), *EDM3L* and *IBM2L* (~22dpg).

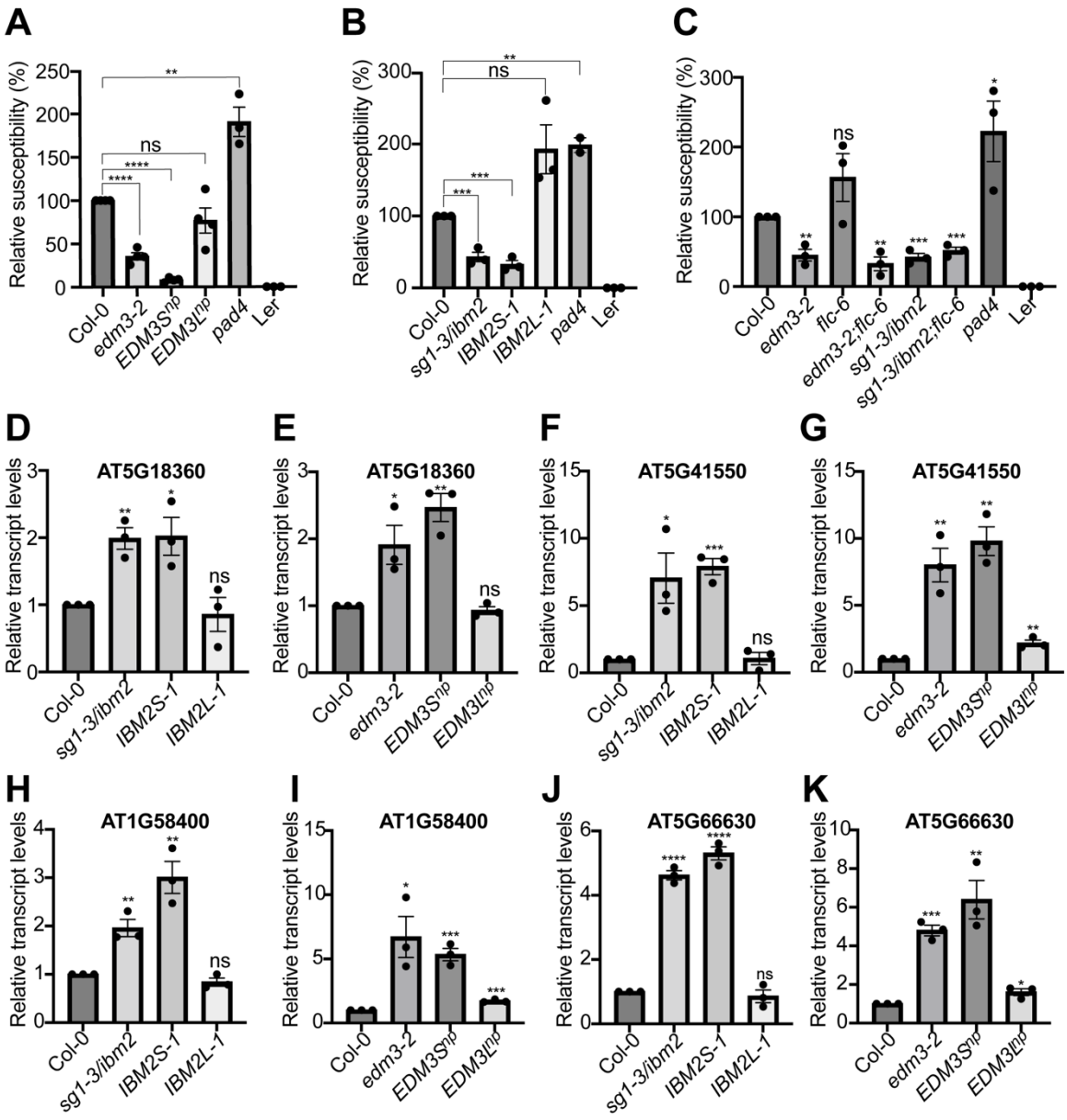
A
Relative susceptibility (%)
Col-0
edm3-2
EDM3S^np
EDM3L^np
pad4
Ler
B
Relative susceptibility (%)
Col-0
sg1-3/ibm2
IBM2S-1
IBM2L-1
pad4
Ler
C
Relative susceptibility (%)
Col-0
edm3-2
flc-6
edm3-2;flc-6
sg1-3/ibm2
sg1-3/ibm2;flc-6
pad4
Ler
D
AT5G18360
Relative transcript levels
Col-0
sg1-3/ibm2
IBM2S-1
IBM2L-1
E
AT5G18360
Relative transcript levels
Col-0
edm3-2
EDM3S^np
EDM3L^np
F
AT5G41550
Relative transcript levels
Col-0
sg1-3/ibm2
IBM2S-1
IBM2L-1
G
AT5G41550
Relative transcript levels
Col-0
edm3-2
EDM3S^np
EDM3L^np
H
AT1G58400
Relative transcript levels
Col-0
sg1-3/ibm2
IBM2S-1
IBM2L-1
I
AT1G58400
Relative transcript levels
Col-0
edm3-2
EDM3S^np
EDM3L^np
J
AT5G66630
Relative transcript levels
Col-0
sg1-3/ibm2
IBM2S-1
IBM2L-1
K
AT5G66630
Relative transcript levels
Col-0
edm3-2
EDM3S^np
EDM3L^np

Figure 2.12. Basal defense assays with *Hpa*Noco2.
A-C. Two-week old (A&B) or twelve-day old (C) plants were spray-inoculated with *Hpa*Noco2 spores (1 x 10^4/ml). Spores developed on plants were counted one-week post-infection and divided by fresh weight of the respective plants (spores/g) followed by normalization to average spores/g observed for Col-0.
D-K. Transcript levels of four selected NLR genes in *edm3* or *ibm2* mutants and complementation lines.
Data information: Error bars represent standard errors from at least three independent experiments. Asterisks indicate significant difference analyzed by student's t-test. (*, $p<0.05$; **, $p<0.01$; ***, $p<0.001$; ****, $p<0.0001$).

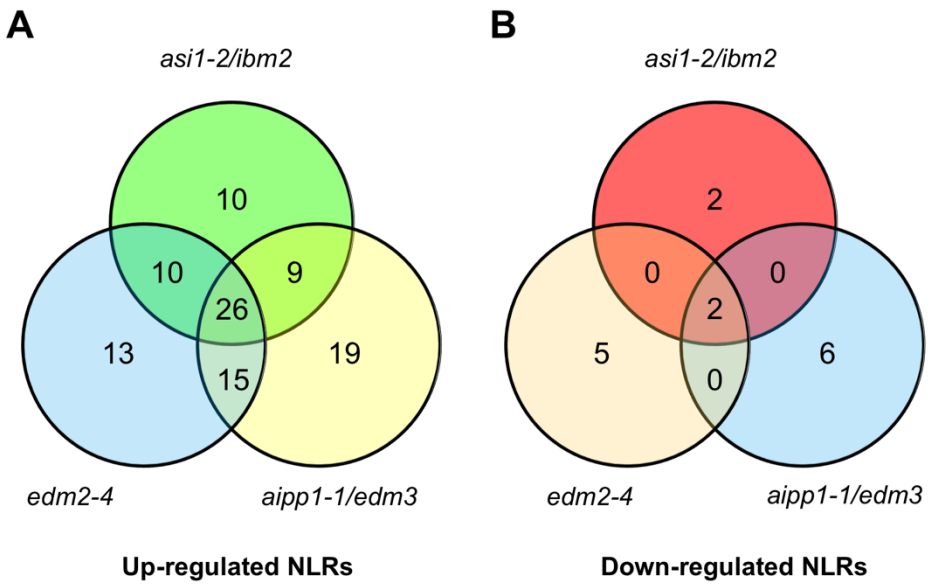

Figure 2.13. **Venn diagrams showing up-regulated and down-regulated NLRs in *edm2*, *edm3* and *ibm2* mutants.**
The data are shown as venn diagrams dependent on FPKM (Fragments Per Kilobase of transcript per Million mapped reads) (http://ipf.sustech.edu.cn/pub/athrna/). Genes are considered as differentially expressed when P < 0.05 or Fold change (FC) of two replicates > 1.4. Significant difference was analyzed by student's t-test.

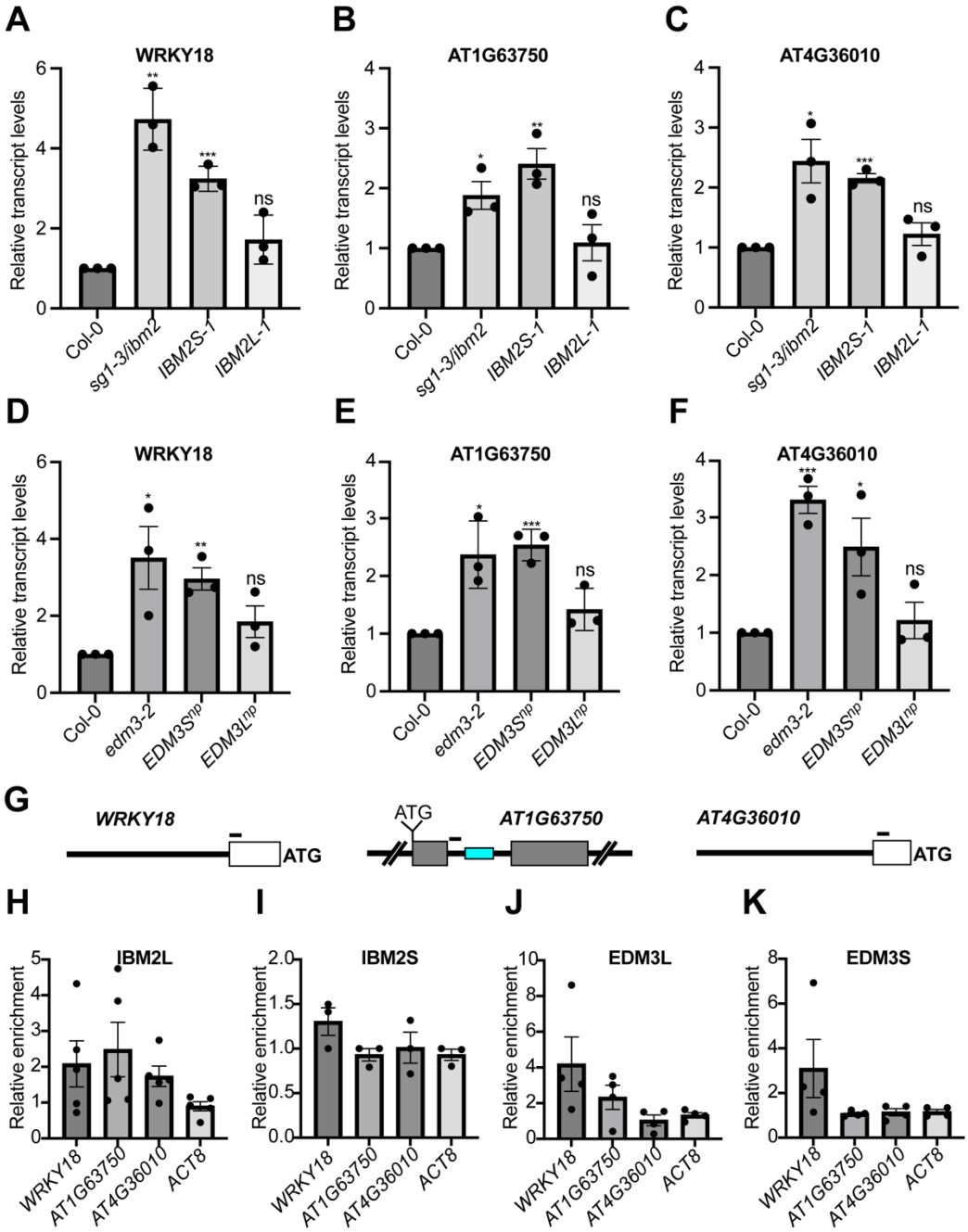
A
WRKY18
Relative transcript levels
Col-0
sg1-3/ibm2
IBM2S-1
IBM2L-1
B
AT1G63750
C
AT4G36010
D
WRKY18
edm3-2
EDM3S^np
EDM3L^np
E
AT1G63750
F
AT4G36010
G
WRKY18
ATG
AT1G63750
AT4G36010
H
IBM2L
Relative enrichment
WRKY18
AT1G63750
AT4G36010
ACT8
I
IBM2S
J
EDM3L
K
EDM3S

Figure 2.14. Association of EDM3 and IBM2 isoforms with selected defense genes.
A-F. The expression levels of IBM2 and EDM2-targeted genes are up-regulated in mutants of *IBM2* and *EDM3* and rescued to wild-type levels by their longer isoforms but not the shorter ones.
G. Schematic representation of three IBM2 and EDM2-targeted defense-associated genes. Positions of primer pairs used for ChIP-qPCR are marked. The white rectangular represents a 5'UTR, the gray rectangular indicates exons, while the blue one represents a transposable element.
H-K. EDM3L and IBM2L but not EDM3S and IBM2S physically associate with at least two of the selected defense genes as determined by by ChIP-qPCR. A region of the *Actin 8* gene, which was used as a negative control, exhibits no association with any of the tested isoforms.
Data information: Data are shown as mean ± SEM from at least three independent replicates. Asterisks indicate significant difference analyzed by student's t-test. (*, $p<0.05$; **, $p<0.01$; ***, $p<0.001$).

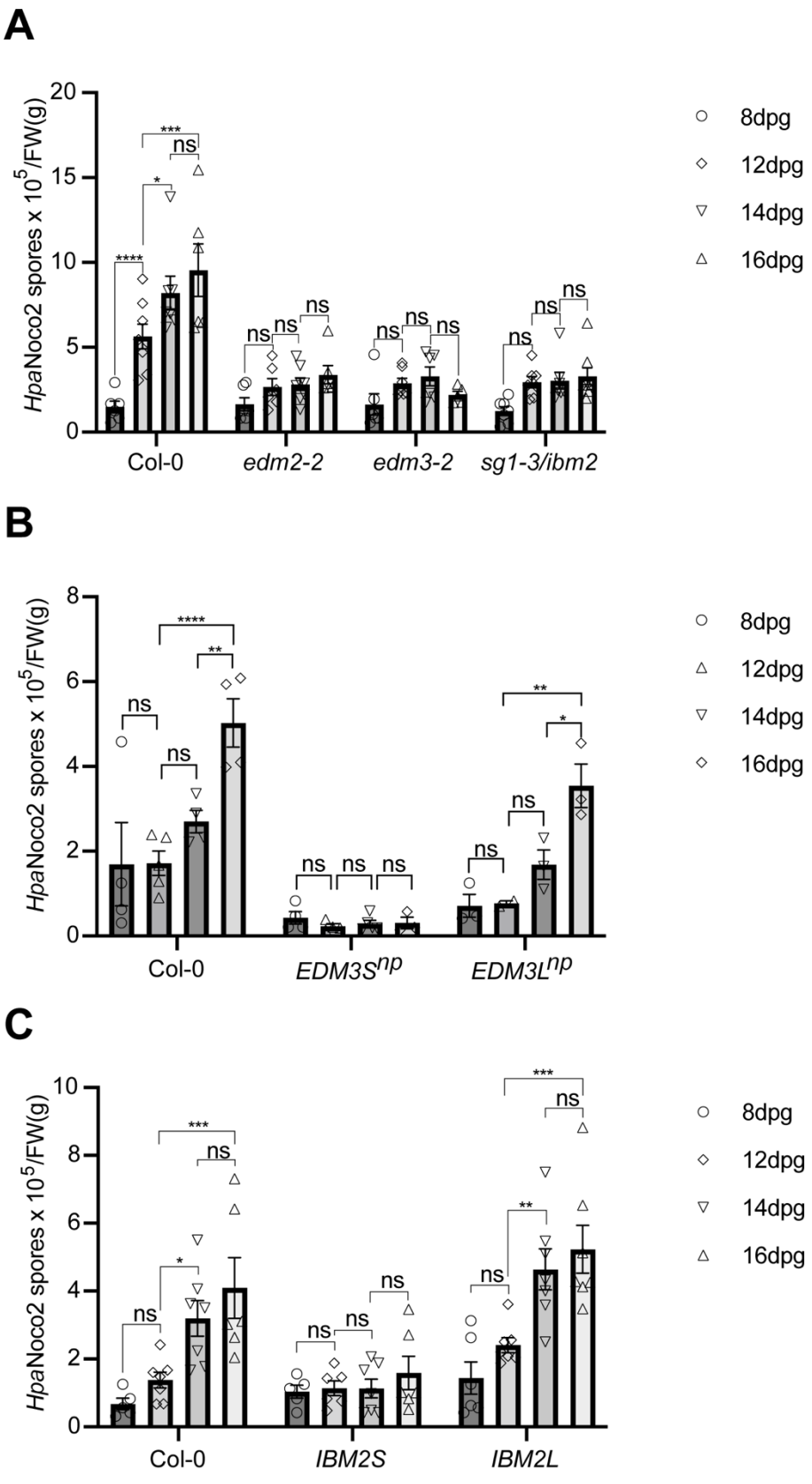
A
HpaNoco2 spores x 10^5/FW(g)
20
15
10
5
0
***
ns
*
****
ns
ns
ns
ns
ns
ns
ns
ns
ns
ns
Col-0
edm2-2
edm3-2
sg1-3/ibm2
8dpg
12dpg
14dpg
16dpg
B
HpaNoco2 spores x 10^5/FW(g)
8
6
4
2
0
****
**
ns
ns
ns
ns
ns
ns
**
*
ns
Col-0
EDM3S^np
EDM3L^np
8dpg
12dpg
14dpg
16dpg
C
HpaNoco2 spores x 10^5/FW(g)
10
8
6
4
2
0
***
ns
*
ns
ns
ns
ns
***
ns
**
ns
Col-0
IBM2S
IBM2L
8dpg
12dpg
14dpg
16dpg

Figure 2.15. EDM3L and IBM2L restore a gradual decline of basal immunity in their respective Col-0 mutants.
A-C. Seedlings of the indicated genotypes above at different ages (8dpg to 16dpg) were sprayed-inoculated with *Hpa*Noco2 spores (1 x 10^4/ml). Spores were counted after 7 days post infection, which were normalized to fresh weight (spores/g).
Data information: Data are shown as mean ± SEM. Asterisks indicate significant difference analyzed by two-way ANOVA. (*, $p<0.05$; **, $p<0.01$; ***, $p<0.001$; ****, $p<0.0001$). All the technical data points of at least three independent experiments are shown.

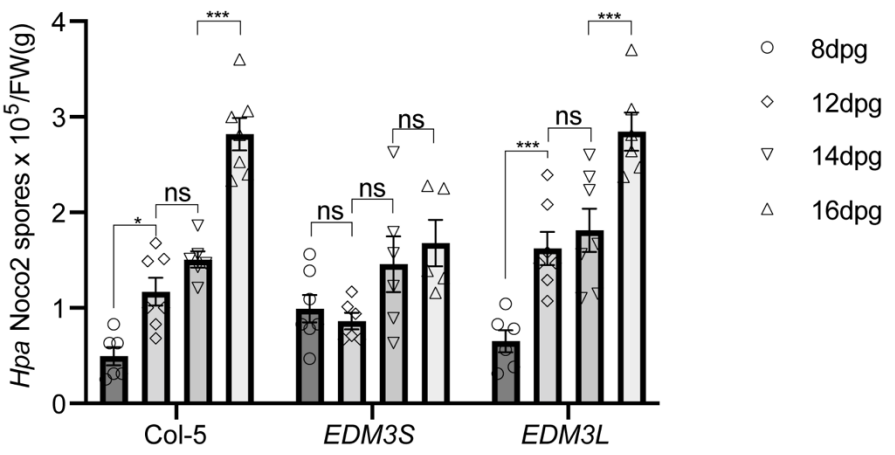

Figure 2.16. EDM3L but not EDM3S restore a gradual decline of basal immunity in the Col-5 allele *edm3-1*.

Seedlings of the indicated genotypes above at different ages (8dpg to 16dpg) were sprayed-inoculated with *Hpa*Noco2 spores (1 x 10^4/ml). Spores were counted 7 days after infection, which were normalized to fresh weight (spores/g).

Data information: Data are shown as mean ± SEM. Asterisks indicate significant difference analyzed by two-way ANOVA. (*, $p<0.05$; ***, $p<0.001$). All the technical data points of at least three independent experiments are shown.

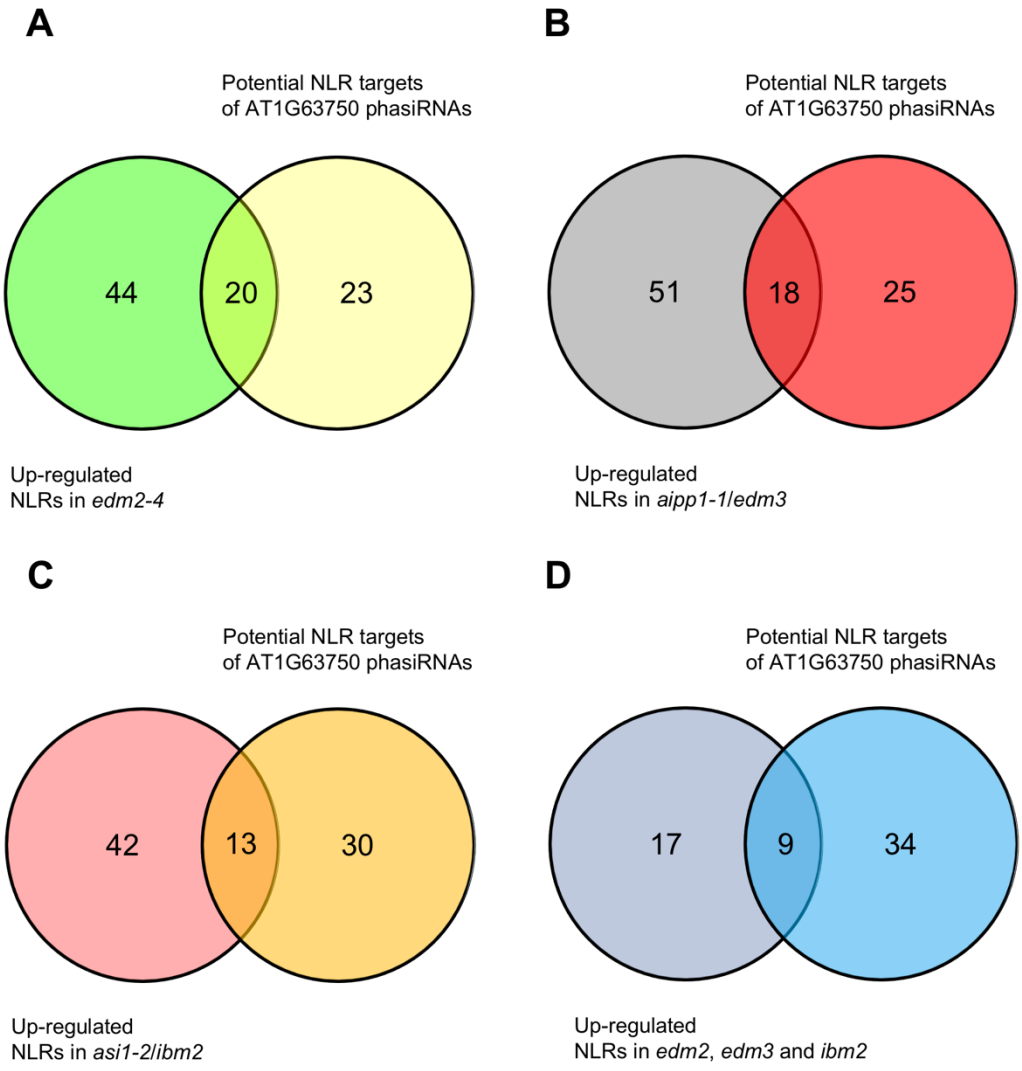

Figure 2.17. **Venn diagrams showing overlapping NLRs that are up-regulated in *edm2*, *edm3* or *ibm2* and potentially targeted by AT1G63750 producing phasiRNAs.**
A. Venn diagram showing NLR genes that are up-regulated in *edm2-4* and potentially targeted by AT1G63750-produced phasiRNAs.
B. Venn diagram showing NLR genes that are up-regulated in *aipp1-1*/*edm3* and potentially targeted by AT1G63750-produced phasiRNAs.
C. Venn diagram showing NLR genes that are up-regulated in *asi1-2*/*ibm2* and potentially targeted by AT1G63750-produced phasiRNAs.

Table 2.1. The levels of EDM2 and IBM2-targeting defense associated genes decrease in rosette leaves with plant approaching flowering

	RosLf #2	RosLf #4	RosLf #6	RosLf #8	RosLf #10	RosLf #12	
At1g63750	33.8	26.3	18.5	16	10.4	8.5	Disease resistance protein (TIR-NBS-LRR class) family
At5g24660	14.4	5.8	3.8	2.4	2	2.6	LSU2__response to low sulfur 2
At5g42650	12.9	10.1	7.3	6.7	4.2	2.1	AOS_CYP74A_DDE2__allene oxide synthase
At5g26920	12	8.1	8.2	7.1	5.7	6	CBP60G__Cam-binding protein 60-like G|
At1g06160	11.5	7.4	3.3	3.5	5.4	5.2	ERF59_ORA59__octadecanoid-responsive Arabidopsis AP2/ERF 59
At1g70890	11.1	14.9	12.3	8.9	4.2	2.2	MLP43_MLP43__MLP-like protein 43
At4g31800	9.2	5.6	5.4	5.2	3.8	2.7	ATWRKY18_WRKY18__WRKY DNA-binding protein 18
At3g04720	7.9	8.1	3.9	2.1	1.1	0.3	AtPR4_HEL_PR-4_PR4__pathogenesis-related 4
At4g08870	6.3	3.7	2.4	1.5	1	0.9	ARGAH2__Arginase/deacetylase superfamily protein
At2g34600	6.1	4.5	3.6	3	1.5	0.8	JAZ7_TIFY5B__jasmonate-zim-domain protein 7
At3g50260	5	5.8	4	3.2	2.1	1	ATERF#011_CEJ1_DEAR1__cooperatively regulated by ethylene and jasmonate 1
At3g26450	4.8	3.6	3.8	4	3.1	2.1	Polyketide cyclase/dehydrase and lipid transport superfamily protein
At5g54380	4.4	3.5	3.4	2.7	2.3	1.7	THE1__protein kinase family protein|
At5g47220	3.7	2.9	3.1	2.9	3.2	2.3	ATERF-2_ATERF2_ERF2__ethylene responsive element binding factor 2
At1g72450	3.5	2.3	1.7	1.4	0.9	0.6	JAZ6_TIFY11B__jasmonate-zim-domain protein 6|
At2g22330	3.4	4.7	2.9	1.9	1.4	0.9	CYP79B3__cytochrome P450, family 79, subfamily B, polypeptide 3
At4g08920	3.2	2.2	1.8	1.5	1.2	1.1	ATCRY1_BLU1_CRY1_HY4_OOP2__cryptochrome 1
At5g05600	3	2.3	1.7	1.4	1.1	0.3	JAO2_JOX2__2-oxoglutarate (2OG) and Fe(II)-dependent oxygenase superfamily

							protein
At3g05200	2.9	2.3	2	1.6	1.2	0.9	ATL6__RING/U-box superfamily protein
At5g67300	2.5	2.4	1.9	1.5	1	0.7	ATMYB44_ATMYBR1_MYB44_MYBR1__myb domain protein r1
At3g57330	2.2	1.8	1.7	1.5	1.5	1.3	ACA11__autoinhibited Ca2+-ATPase 11
At4g02380	2.2	1.7	1.9	1.6	1.4	0.7	AtLEA5_LEA38_SAG21__senescence-associated gene 21
At5g56980	2.2	2.5	2.4	2.2	1.5	0.9	Pathogen-associated molecular pattern-induced gene
At5g24530	2.1	3	2.4	1.9	1.7	0.8	AtDMR6_DMR6__2-oxoglutarate (2OG) and Fe(II)-dependent oxygenase superfamily protein
At1g19180	2.1	1.2	1.3	1	0.8	0.6	AtJAZ1_JAZ1_TIFY10A__jasmonate-zim-domain protein 1
At5g47910	2.1	2.2	2.2	2	1.5	1.2	ATRBOHD_RBOHD__respiratory burst oxidase homologue D
At4g36010	2	1.5	1.4	1.1	0.6	0.6	Pathogenesis-related thaumatin superfamily protein
At3g19380	2	2.2	2	1.5	1.4	0.8	PUB25__plant U-box 25
At4g30440	2	2	1.9	1.9	1.5	1.2	GAE1__UDP-D-glucuronate 4-epimerase 1|
At1g44350	1.9	1.5	1.2	0.9	0.6	0.3	ILL6__IAA-leucine resistant (ILR)-like gene 6
At3g11410	1.8	1.6	1.1	0.8	0.7	0.5	AHG3_ATPP2CA_PP2CA__protein phosphatase 2CA
At3g51550	1.7	1.5	1.2	1.2	1	0.8	FER__Malectin/receptor-like protein kinase family protein
At1g70700	1.6	1.4	1.2	1	0.9	0.8	JAZ9_TIFY7__TIFY domain/Divergent CCT motif family protein
At5g10140	1.1	1	1.1	0.8	1	0.5	AGL25_FLC_FLF_RSB6__K-box region and MADS-box transcription factor family protein

Notes: Highlighted in yellow is FLC. All others are defense associated genes that are targeted by IBM2 and EDM2 (Zhang et al., 2021). Highlighted in blue are three defense-associated genes that are tested in this study. All the data are from the Botany Array Resource, http://bar.utoronto.ca/affydb/cgi-bin/affy_db_exprss_browser_in.cgi.

Table 2.2. The levels of Up-regulated NLRs in mutants of *EDM2*, *EDM3* and *IBM2* decrease in rosette leaves as plant approaching flowering

	RosL f#2	RosL f#4	RosL f#6	RosL f#8	RosL f#10	RosL f#12	
At1g63750	33.8	26.3	18.5	16	10.4	8.5	260296_at| Disease resistance protein (TIR-NBS-LRR class) family|
At5g58120	11	13.2	13.6	14.1	9.5	4.5	247848_at| Disease resistance protein (TIR-NBS-LRR class) family|
At1g56510	8.1	7.6	7.4	6.2	4.1	2.2	259629_at| ADR2_WRR4__Disease resistance protein (TIR-NBS-LRR class)|
At5g41740	6.7	6.8	8.3	6	3.6	2.4	249264_s_at| Disease resistance protein (TIR-NBS-LRR class) family
At5g41750	6.7	6.8	8.3	6	3.6	2.4	249264_s_at| Disease resistance protein (TIR-NBS-LRR class) family|
At1g63880	5.1	4.1	3.9	3.8	3	2.3	260312_at| Disease resistance protein (TIR-NBS-LRR class) family|
At1g31540	3.4	2.9	3.7	2.5	2.9	1.5	256487_at| Disease resistance protein (TIR-NBS-LRR class) family|
At1g15890	3.3	3.8	3.2	2.9	2.8	1.6	259495_at| Disease resistance protein (CC-NBS-LRR class) family|
At4g16960	2.2	2.2	2.4	2	1.4	0.9	245457_s_at| SIKIC3__Disease resistance protein (TIR-NBS-LRR class) family|
At5g66630	2.2	1.7	1	1.1	0.2	0.2	DAR5__DA1-related protein 5
At5g18360	2.1	2.5	2.7	1.9	1.4	1	Disease resistance protein (TIR-NBS-LRR class) family
At5g22690	1.8	2.5	2.4	1.8	1.4	1.1	249903_at| Disease resistance protein (TIR-NBS-LRR class) family|
At1g33560	1.4	1	1.1	0.8	1	1	256425_at| ADR1__Disease resistance protein (CC-NBS-LRR class) family|
At5g45260	1.2	1.2	1.1	0.9	0.8	0.8	248995_at| ATWRKY52_RRS1_RRS1-R_SLH1__Disease resistance protein (TIR-NBS-LRR class)|
At3g25510	1.1	0.7	1.3	0.7	1.3	0.4	257958_at| disease resistance protein (TIR-

							NBS-LRR class), putative|
At5g41550	0.9	0.8	1.3	1.4	1.2	1.1	Disease resistance protein (TIR-NBS-LRR class) family|

Notes: AT1G63750, AT5G66630, AT5G18360 and AT5G41550 are NLRs that are tested in this study. AT1G58400 (tested in this study), AT3G44670 and AT4G14370, are not represented on the ATH1 array. All the data are from the Botany Array Resource, http://bar.utoronto.ca/affydb/cgi-bin/affy_db_exprss_browser_in.cgi.

Table 2.3. The levels of EDM2 and IBM2-targeting defense associated genes decrease in entire rosette leaves as plant approaching flowering

	21 days	22 days	23 days	
At1g63750	17	4.8	4.6	Disease resistance protein (TIR-NBS-LRR class)
At3g04210	13.8	8.5	11.7	TN13__Disease resistance protein (TIR-NBS class)|
At5g26920	12	4.1	5.7	CBP60G__Cam-binding protein 60-like G|
At4g19530	10.8	8.6	7.3	disease resistance protein (TIR-NBS-LRR class) family|
At5g42650	6	3.1	2.9	AOS_CYP74A_DDE2__allene oxide synthase|
At3g50260	5.3	0.6	0.8	CEJ1_DEAR1__cooperatively regulated by ethylene and jasmonate 1|
At4g16860	3.7	2.2	2.7	RPP4__Disease resistance protein (TIR-NBS-LRR class) family|
At5g47220	3.4	1.2	1.9	ATERF2_ERF2__ethylene responsive element binding factor 2|
At2g34600	3.1	0	0	JAZ7_TIFY5B__jasmonate-zim-domain protein 7|
At4g31800	3.1	0.3	0.4	ATWRKY18_WRKY18__WRKY DNA-binding protein
At2g22330	2.4	2	1.6	CYP79B3__cytochrome P450, family 79, subfamily B, polypeptide 3|
At5g47910	2.4	0.8	0.9	ATRBOHD_RBOHD__respiratory burst oxidase
At2g15890	2	1.1	1.2	CBP1_MEE14__maternal effect embryo arrest 14|
At5g61600	1.9	0.3	0.4	ERF104__ethylene response factor 104|
At5g56980	1.9	0.4	0.2	Pathogen-associated molecular pattern-induced gene
At3g19380	1.8	1.2	1	PUB25__plant U-box 25|
At3g61190	1.8	0.3	0.4	BAP1__BON association protein 1|
At3g44260	1.8	0.3	0.4	AtCAF1a_CAF1a__Polynucleotidyl transferase,
At2g03760	1.7	1.2	1.1	AtSOT1_AtSOT12_ATST1_AtSULT202A1_RAR047_SOT12_ST
At2g23810	1.6	0.4	0.5	TET8__tetraspanin8|
At3g05200	1.5	0.6	0.8	ATL6__RING/U-box superfamily protein|
At4g36010	1.5	0.4	0.4	Pathogenesis-related thaumatin superfamily protein|
At1g32640	1.4	0.4	0.4	ATMYC2_JAI1_JIN1_MYC2_RD22BP1_ZBF1__
At5g67300	1.4	0.4	0.4	ATMYB44_ATMYBR1_MYB44_MYBR1__myb domain protein
At1g19180	1.3	0.1	0.1	AtJAZ1_JAZ1_TIFY10A__jasmonate-zim-domain protein 1|
At2g40140	1.3	0.3	0.4	CZF1_SZF2_TZF10_ZFAR1__zinc finger (CCCH-type) family protein|
At4g03110	1.3	0.9	0.9	AtRBP-DR1_BRN1_RBP-DR1__RNA-binding protein-defense related 1|
At1g72450	1.3	0.5	0.6	JAZ6_TIFY11B__jasmonate-zim-domain protein 6|
At4g30440	1.3	0.7	0.7	GAE1__UDP-D-glucuronate 4-epimerase 1|
At1g74930	1.2	0.2	0.3	ORA47__Integrase-type DNA-binding superfamily protein|
At3g15210	1.2	0.3	0.4	ATERF4_ERF4_RAP2.5__ethylene responsive element binding factor 4|
At4g31550	1.2	0.6	0.6	ATWRKY11_WRKY11__WRKY DNA-binding protein 11|
At3g44720	1.2	0.8	0.6	ADT4__arogenate dehydratase 4|
At5g05600	1.1	0.2	0.2	JOX2__2-oxoglutarate (2OG) and Fe(II)-dependent oxygenase

At1g70700	1	0.5	0.4	AZ9_TIFY7__TIFY domain/Divergent CCT motif family
At1g02660	0.9	0.2	0.2	PLIP2__alpha/beta-Hydrolases superfamily protein|
At5g10140	0.9	0.8	0.6	FLC_MADS-box transcription factor family protein|
At1g44350	0.8	0.4	0.3	ILL6__IAA-leucine resistant (ILR)-like gene 6|
At5g22630	0.8	0.4	0.4	ADT5__arogenate dehydratase 5|
At3g23170	0.8	0.4	0.5	PRP|
At3g30775	0.4	0.1	0.1	POX_ATPDH_ATPOX_ERD5_PDH1_PRO1_PRODH_

Notes: Highlighted in yellow is FLC. All other genes are targeted by IBM2 and EDM2. Highlighted in blue are three defense associated genes that are tested in this study. All the data are from the Botany Array Resource, http://bar.utoronto.ca/affydb/cgi-bin/affy_db_exprss_browser_in.cgi.

Table 2.4. The levels of Up-regulated NLRs in mutants of *EDM2*, *EDM3* and *IBM2* decrease in entire rosette leaves as plant approaching flowering

	21 days	22 days	23 days	
At1g63750	17	4.8	4.6	260296_at| Disease resistance protein (TIR-NBS-LRR class) family|
At5g58120	11.3	3.2	3.3	247848_at| Disease resistance protein (TIR-NBS-LRR class) family|
At1g56520	9.9	1.4	3.7	259602_at| Disease resistance protein (TIR-NBS-LRR class) family|
At5g41740	7.7	1.2	1.7	249264_s_at| Disease resistance protein (TIR-NBS-LRR class) family
At5g41750	7.7	1.2	1.7	249264_s_at| Disease resistance protein (TIR-NBS-LRR class) family|
At1g56510	5.9	1.8	1.9	259629_at| ADR2_WRR4__Disease resistance protein (TIR-NBS-LRR class)|
At3g50950	4.9	2.2	2.7	252126_at| ZAR1__HOPZ-ACTIVATED RESISTANCE 1|
At5g46260	3.5	2.4	2.5	248851_s_at| disease resistance protein (TIR-NBS-LRR class) family|
At4g19520	3	2.5	1	254587_at| disease resistance protein (TIR-NBS-LRR class) family|
At1g15890	3	1.7	1.7	259495_at| Disease resistance protein (CC-NBS-LRR class) family|
At5g46510	2	1	1	248847_at| VICTL__Disease resistance protein (TIR-NBS-LRR class) family|
At5g22690	1.9	0.7	0.8	249903_at| Disease resistance protein (TIR-NBS-LRR class) family|
At4g08450	1.3	0.8	0.5	255146_at| Disease resistance protein (TIR-NBS-LRR class) family|
At5g18360	2	1.3	1.4	250038_at| Disease resistance protein (TIR-NBS-LRR class) family|
At5g66630	1.4	0.3	1.3	247105_at| DAR5__DA1-related protein 5|
At5g41550	0.9	0.4	0.5	249312_at| Disease

				resistance protein (TIR-NBS-LRR class) family|

Notes: Highlighted in yellow are four NLR genes that are tested in this study. AT1G58400 (tested in this study), AT3G44670 and AT4G14370 are not represented on the ATH1 array. All the data are from the Botany Array Resource, http://bar.utoronto.ca/affydb/cgi-bin/affy_db_exprss_browser_in.cgi.

Table 2.5. Primers used in this study

Primer name	Sequence (5'-3')	Notes
EDM3_Y2H_F	CCGGAATTCATGGCGACTCCGGAAGAAGTAGC	
EDM3_Y2H_R	AAAACTGCAGCTACCGATAAGGAAAACCTTTCAG	
EDM3C_Y2H_F	CCGGAATTCAATATGTTTGTTGATAAA	
EDM3C_Y2H_R	CGCGGATCCCTACCGATAAGGAAAACC	
EDM3RRM_Y2H_F	CCGGAATTCCGTCGTACTGTCTACGTA	
EDM3RRM_Y2H_R	CGCGGATCCCTAAGGCTCAGCAGCACA	
IBM2_Y2H_F	CCGGAATTCATGGAAGAATCTGTAGCATCTGAAG	
IBM2_Y2H_R	AAAACTGCAGTTACTCTCTTGACCTTTCCTGATCC	
IBM2RRM_S_Y2H_F	GGAATTCCATATGGGAAAAAGTAAATGGTTCC	
IBM2RRM_S_Y2H_R	CCGGAATTCCTATGGTGGAGTAATCTTAGCGAA	
HA-IBM2_F	TCCCTATGATGTGCCAGACT	
HA-IBM2_R	ACTGAACCACTAGCTCCCCT	
ACT8_RT_F	ATGAAGATTAAGGTCGTGGCAC	Tsuchiya & Eulgem, 2010
ACT8_RT_R	GTTTTTATCCGAGTTTGAAGAGGC	Tsuchiya & Eulgem, 2010
ACT8_qRT_F	CAG TGT CTG GAT TGG TGG TTC TAT C	Tsuchiya & Eulgem, 2013
ACT8_qRT_R	ATC CCG TCA TGG AAA CGA TGT	Tsuchiya & Eulgem, 2013
FLC_qRT_F	AACTGGAGGAACACCTTGAGACTG	Tsuchiya & Eulgem, 2010
FLC_qRT_R	GGAAGATTGTCGGAGATTTGTCC	Tsuchiya & Eulgem, 2010
EDM3_RT_F	AGAATGAAGAGATGACACAGGCT	
EDM3_RT_R	ATGTGTTACCGCCGTCTCAG	
EDM3S_qRT_F	AGCCTAACGATCCTGATTTCG	
EDM3S_qRT_R	CTC TGC CTC CTC AAG CTTG	
EDM3L_qRT_F	AGCCTAACGATCCTGATTTCG	
EDM3L_qRT_R	GCC TCC TCA AGC TGT TTC T	
IBM2S_qRT_F	GAACCGAGATCTTGTAGTG	
IBM2S_qRT_R	ACCACATCCTTGCATAGC	
IBM2L_qRT_F	TTTGGACGTGCTGAGGACAA	
IBM2L_qRT_R	ACCATTTACTTTTTCCAGCATCCG	
AT5G18360_qRT_F	GGGAAGGAACACAACCTCTT	
AT5G18360_qRT_R	CTGAGACAGAGTTCCTCGATATTT	
AT5G41550_qRT_F	AGGAATCCAGCCCCTTCCTA	
AT5G41550_qRT_R	GCTTTTCGCACCCTGACATC	
AT1G58400_qRT_F	CAAAGTCCAACACATTCCTTCTG	

AT1G58400_qRT_R	GTGAGCCGCCTGGAATATAG	
AT5G66630_qRT_F	CCAAGGACGGGTCAGAACAA	
AT5G66630_qRT_R	CCTGTTAGCAATCTAGGAAGTCCA	
WRKY18_qRT_F	CGACATACGAAGGGACGCAT	
WRKY18_qRT_R	AAGTCACTGTGCTTGACCCA	
AT1G63750_qRT_F	TCAAGGCAAGGGGATAAC	
AT1G63750_qRT_R	GCCTTTTTGCGCTTCATG	
AT4G36010_qRT_F	TCCTGCTCAGCTGAAAGTGG	
AT4G36010_qRT_R	ACTGTGAGTACTCGCTTGGC	
WRKY18_ChIP_F	CAAAGTCTTTAATGTCTTCTGGACT	
WRKY18_ChIP_R	GGAAGGAAAGTCGTTCGAAAGTG	
AT1G63750_ChIP_F	AAAGCTTTGACTGATGTGAGCA	
AT1G63750_ChIP_R	AGTTGATCGATTGAACACAAACC	
AT4G36010_ChIP_F	CATGAACGACACATTGGCCG	
AT4G36010_ChIP_R	GAGTGCAAATGTGAAGGCGT	
ACT8_ChIP_F	CTAAAGAGACATCGTTTCCATGACGG	

Chapter 3

Two Arabidopsis RRM Domain Proteins EDM3 and IBM2 Control RPP7 Immune Receptor Expression

Abstract

In a separate study, we showed interactions of specific splice isoforms of the *Arabidopsis thaliana* (Arabidopsis) RRM domain proteins EDM3 and IBM2 to coordinate the floral transition with innate basal immunity. Of two IBM2 isoforms expressed in Arabidopsis only the longer BAH and RRM domain-containing IBM2L, but not the shorter IBM2S isoform lacking the RRM domain, can interact with EDM3. In the context of basal defense and flowering time regulation only the longer of both expressed EDM3 isoforms EDM3L can efficiently interact with IBM2L. Here we show that isoform specific interactions between IBM2 and EDM3 also govern proper expression of *RPP7* and race-specific immunity against the Hiks1 isolate of the pathogenic oomycete *Hyaloperonospora arabidopsidis* (*Hpa*) mediated by this immune receptor. However, in the context of this pathway, the shorter EDM3 isoform EDM3S seems partly functional and capable to sufficiently interact with IBM2L in mediating *RPP7* expression levels sufficient for full immunity against *Hpa*Hiks1.

Introduction

Plant immune responses against pathogens are controlled by two interconnected layers of non-self-recognition mechanisms (Chisholm *et al*, 2006; Jones & Dangl, 2006). Pattern recognition receptor-mediated perception of conserved microbe associated molecular patterns (MAMPs) induces in plants pattern-triggered immunity (PTI). Host-adapted pathogens attenuate PTI by secreting effector molecules, suppressing this defense mechanism. The remaining weakened plant immune response during such compatible interactions, called basal immunity or basal defense (Glazebrook, 2001), limits the spread of virulent pathogens in their hosts, but is typically insufficient to fully prevent disease. In many cases plants have evolved disease resistance (R)-proteins, a second class of plant immune receptors besides PRRs that recognize effectors and activate effector-triggered immunity (ETI), a manifestation of race-specific resistance. ETI efficiently protects plants from avirulent pathogens during incompatible interactions. While Pattern recognition receptors are often plasma-membrane-resident receptor-like protein kinases with extracellular leucine-rich repeat (LRR) domains, R proteins typically are intracellularly localized proteins termed NLRs. They contain a central nucleotide binding site (NB), C-terminal LRRs and a variable C-terminal domain. Regulatory pathways controlling ETI, PTI and basal immunity are highly intertwined and share numerous components, such as the defense hormones salicylic acid, ethylene and jasmonic acid, as well as multiple signal transducers and transcription factors (Ngou *et al*, 2021; Lu &

Tsuda, 2021; Yuan *et al*, 2021). While basal immunity seems mainly to be a weakened form of PTI, ETI has been proposed to result from boosted basal defense or PTI-associated responses (Tao *et al*, 2003; Jones & Dangl, 2006; Shen *et al*, 2007).

We previously reported on the *Arabidopsis thaliana* (Arabidopsis) defense regulator EDM2, a protein with typical features of transcriptional and epigenetic regulators (Eulgem *et al*, 2007). Besides atypical PHD-finger motifs and a G gamma subunit-like protein-protein interaction domain, it contains an N6-adenine methyltransferase-like domain (Eulgem *et al*, 2007). EDM2 is nuclear localized and known to promote expression of the NLR-type R protein *RPP7*. Both *EDM2* and *RPP7* genes are required for race-specific immunity of Arabidopsis against the Hiks1 isolate of the pathogenic oomycete *Hyaloperonospora arabidopsidis (Hpa)*. Mutants of *EDM2* also exhibit developmental defects and are stunted (Tsuchiya & Eulgem, 2010a, 2013a). Developmental roles of *EDM2* include promotion of the floral transition, as *edm2* mutants flower late. Trans-generational variability and instability of such phenotypes implied roles of EDM2 in epigenetic processes (Tsuchiya & Eulgem, 2013a). Consequently, we found EDM2 to control silencing states of transposable elements (TEs) by modulating levels of di-methylated lysine 9 of histone H3 (H3K9me2), a ubiquitous epigenetic TE silencing signal in plants (Tsuchiya & Eulgem, 2013a; Lai *et al*, 2020). While at some loci EDM2 promotes high H3K9me2 levels, it mostly has a suppressive effect on this mark. The PHD finger-containing domain of EDM2 has a strong *in*

vitro-binding preference for histone H3 carrying certain combinations of posttranslational modifications, but not single marks (Tsuchiya & Eulgem, 2014). Strikingly, strongly preferred by this domain are combinations between H3 marks associated with active transcription (H3K4me1, H3K4me2 or H3K4me3) and the silencing signal H3K9me2. Such combinations of histone marks are expected to occur specifically at border regions between transcriptionally silent and active chromatin. EDM2 controls alternative transcript polyadenylation at *RPP7* as well as several other direct targets, such as the histone demethylase gene *IBM1*, by forming a complex with the two RNA Recognition Motif (RRM) domain proteins EDM3/AIPP1 (hereafter EDM3) and IBM2/ASI1 (hereafter IBM2) (Tsuchiya & Eulgem, 2013b; Lei *et al*, 2014; Duan *et al*, 2017; Lai *et al*, 2019). Upon recruitment to H3K9me2-marked chromatin sites EDM2/EDM3/IBM2 complexes suppress proximal polyadenylation and promote the synthesis of full-length transcripts at these genes (Tsuchiya & Eulgem, 2013b; Lei *et al*, 2014; Wang *et al*, 2013; Saze *et al*, 2013; Duan *et al*, 2017) . Recent genome profiling studies uncovered numerous additional direct target genes of EDM2, and IBM2 (Lai *et al*, 2020; Zhang *et al*, 2021). Among those is the NLR type immune receptor gene *RPP4*, which is regulated by EDM2 in a complex manner that includes alternative polyadenylation control (Lai *et al*, 2020; Deremetz *et al*, 2019).

By RNA-seq analysis of *edm2-2* and its wild type parent Col-0 (Lai *et al*, 2020), we found that *EDM2* significantly affects transcript levels of a large number of NLR genes (51 of all 165 NLR genes annotated in Col (Zhang *et al*,

2016)). The sets of all genes that are significantly up- or downregulated in *edm2-2* compared to Col-0 are nearly equally large with 56% up- and 44% downregulated. This also applies to most functional categories of genes differentially expressed in *edm2-2*. However, the role of EDM2 is significantly shifted towards a broad function in suppressing NLR gene expression, as the majority of differentially expressed NLR genes (78%, 40 of 51 NLRs) are up-regulated, while only 22% (11 NLRs including *RPP7* & *RPP4*) are down-regulated in *edm2-2* compared to Col-0. A similar, but less pronounced, significant shift is observed for general defense genes, including markers of immune responses controlled by the defense hormone salicylic acid, suggesting constitutively increased basal defense. Thus, EDM2 has a dual role in NLR regulation by (1) promoting expression of a small number of NLRs, including *RPP7* and *RPP4*, and (2) suppressing a larger set of additional NLR genes. In *edm2* plants almost four-times more NLRs are up-regulated than down-regulated likely resulting in net-increase of NLR background activity and, as a possible consequence of this, phenotypes related to constitutive basal immunity and reduced fitness. Consistent with this, we also observed in *edm2* mutants enhanced basal defense against virulent strains of *Hpa* (Tsuchiya & Eulgem, 2010b) and *Pseudomonas syringae* (*Pst* DC3000) as well as retarded growth of the rosette (Tsuchiya & Eulgem, 2010a) and reduced fertility/seed production (Tsuchiya & Eulgem, 2013a). Based on this we speculated that the dual role of EDM2 in NLR expression control reflects the need to compensate for fitness

penalties caused by high expression of *RPP7* (and possibly additional NLRs) by suppression of others limiting their expression to levels that are less detrimental for proper plant development and fitness. The *EDM3* mutant *aipp1*, for which transcriptomic data are available, exhibits very similar effects on NLR genes (Duan *et al*, 2017) . While largely equal numbers of all genes are up- or downregulated in this mutant, its ratio between up- and down-regulated NLR genes is even more strongly shifted towards up-regulated NLRs than in *edm2-2*. At least 27 of all 40 NLRs significantly upregulated in *edm2-2* are also significantly upregulated in *edm3*/*aipp1*. Typically entire transcriptional units of these genes are upregulated in *edm2* and *edm3* mutants, implying that rates of transcript synthesis are affected and not, as in the case of the established EDM2 and EDM3 targets *RPP7*, *RPP4* or *IBM1*, local alternative polyadenylation processes. Consistent with the upregulation of numerous NLR genes in *aipp1*, we found *edm3* mutants also to exhibit elevated basal immunity against virulent *Hpa* (Chapter 2) as well as mutants of the EDM3 interaction partner IBM2.

We further reported that, besides the suppression of basal immunity, EDM2, EDM3 and IBM2 share a role in promotion of the floral transition (chapter 2). These functions are executed by long splice-isoforms of the EDM3 and IBM2 proteins (EDM3L and IBM2L), which can physically interact with each other, but not by shorter isoforms (EDM3S and IBM2S). While EDM3S lacks only two amino acids compared to EDM3L, IBM2S lacks the entire RRM domain present in IBM2L.

IBM2L and EDM3L promote the floral transition by gradually down-regulating expression of the negative flowering time regulator gene *FLC* prior to the transition to flowering. At the same time EDM3L and IBM2L gradually suppress basal immunity against the virulent *Hpa* strain Noco2 by a separate mechanism, which likely involves direct suppression of a variety of defense-associated genes.

Here we demonstrate that isoform specific interactions between IBM2 and EDM3 also control expression of the RPP7 immune receptor and gene-for-gene resistance against its cognate pathogen *Hpa*Hiks1. While only IBM2L and not IBM2S are involved in this process, we previously showed that both EDM3 isoforms, EDM3L and EDM3S, can mediate sufficient levels of RPP7 expression for strong immunity against *Hpa*Hiks1 (Lai *et al*, 2019).

Results

Functional Complementation of *RPP7*-Mediated Immunity by IBM2 Isoforms

We previously constructed and described lines separately expressing FLAG epitope-tagged versions of each of the two EDM3 isoforms (*EDM3S* and *EDM3L*) in the *edm3-1* mutant, which is the Col-5 accession (Lai *et al*, 2019). For these *EDM3* complementation lines the *35S Cauliflower Mosaic Virus (CaMV 35S)* promoter was used. For the functional complementation assays and *in vivo*-binding studies described below we also used stably transformed Arabidopsis lines expressing HA epitope-tagged versions of IBM2 isoforms driven by the

native *IBM2* promoter in the *sg1-3/ibm2* mutant (Coustham *et al*, 2014), which is in the Col-0 accession background (Chapter 2). Up to two lines homozygous for a single transgene insertion site for each of the four complementation constructs (*EDM3S-1, EDM3S-2, EDM3L-1, EDM3L-2*; *IBM2S-1, IBM2S-2, IBM2L-1, IBM2L-2*) were used for further experiments. The used *EDM3* and *IBM2* isoform-specific complementation lines express their transgene-specific transcripts to similar levels (Lai *et al*, 2019; Chapter 2).

Like *EDM2*, the *EDM3* and *IBM2* genes are required for immunity mediated by the NLR-type receptor protein RPP7, which confers molecular recognition of the *Hyaloperonospora arabidopsidis* (*Hpa*) isolate Hiks1 (Eulgem *et al*, 2007; Lai *et al*, 2019; Derememetz *et al*, 2019). By measuring the number of sporangiophores (asexual *Hpa* propagation structures) per cotyledon of two-week old Arabidopsis seedlings at 7 days post infection (dpi) with spores of *Hpa*Hiks1 we found IBM2L, but not IBM2S, to mediate full resistance to *Hpa*Hiks1 in the *IBM2 mutant sg1-3* and to completely suppress sporangiophore development (Fig 3.1A). IBM2S failed in both tested *IBM2S* lines to even partially restore loss of *HpaHiks1* resistance. The *edm3-2*, *edm3-3* and *rpp7-15* mutants (like the tested *IBM2* lines in the Col-0 background) served as susceptible controls. Like *sg1-3/ibm2* plants they permitted the emergence of 14 to 17 sporangiophores per cotyledon. Wild type Col-0, which carries intact alleles of *RPP7*, *EDM2*, *EDM3* and *IBM2* behaved fully resistant, not allowing for the formation of any sporangiophores.

Treatment of cotyledons of the tested seedlings with trypan blue, a dye that stains *Hpa* structures and dead plant cells dark blue, confirmed these observations (Fig 3.1B). While cotyledons of wild type Col-0 seedlings exhibited discrete sites of hypersensitive responsive (HR) cell death (local programmed plant cell death indicative of strong immunity prohibiting further growth of germinated *Hpa*Hiks1 spores), the *IBM2* mutant *sg1-3/ibm2* along with the *edm3-2* and *rpp7-17* mutants showed unhindered growth of a *Hpa* hyphal network, the emergence of sporangiophores and/or the formation of sexual oospores, all of which indicate that *Hpa*Hiks1 can successfully complete its life cycle in Arabidopsis tissue. HR sites were absent in the tested mutants of *IBM2*, *EDM3* and *RPP7*. IBM2L, but not IBM2S, restored in the *sg1-3/ibm2* background the ability to respond to *Hpa*Hiks1 with HR and suppressed the development of *Hpa* hyphae, oospores and sporangiophores. We previously demonstrated that both EDM3 isoforms, EDM3S and EDM3L, can fully restore resistance to HpaHiks1 in the *edm3-1* mutant background (Lai *et al*, 2019).

Only IBM2L, but not IBM2S, can Suppress Polyadenylation at a Critical Proximal Polyadenylation Site of *RPP7*

A characteristic feature of *EDM2*, *EDM3* and *IBM2* mutants is that levels of full-length RPP7 coding transcripts are drastically reduced, while levels of the shortened non-coding ECL (Exon1-containing 5'LTR) transcripts are strongly elevated (Tsuchiya & Eulgem, 2013b; Lai *et al*, 2019; Deremetz *et al*, 2019). The

latter transcripts are generated by proximal polyadenylation at the insertion of the *COPIA-R7* retrotransposon in the first *RPP7* intron. We found that IBM2L, but not IBM2S, is able to rescue levels of full-length RPP7-coding transcripts and ECL transcripts in the *sg1-3/ibm2* mutant to those of wild wild-type plants (Fig 3.2A and B). For EDM3S and EDM3L, we showed previously that both isoforms can restore wild type levels of full length RPP7 mRNAs and ECL transcripts in the *edm3-1* mutant.

Only Interacting EDM3 and IBM2 Isoforms Co-localize *in vivo* to Regulatory Chromatin Sites of Known EDM2 Target Genes

We performed chromatin-immune precipitation (ChIP) assays using chromatin from isoform-specific EDM3 and IBM2 complementation lines to test *in-vivo* associations of EDM3 and IBM2 isoforms with two adjacent regions at the *COPIA-R7* retrotransposon insertion site in *RPP7* (RPP7 V and RPP7 VI, (Tsuchiya & Eulgem, 2013b; Lai *et al*, 2019). This area serves as a critical proximal polyadenylation site required for the synthesis of non-coding ECL transcripts. The usage of this polyadenylation site is suppressed in wild type Col-0, while it is used strongly in *edm2*, *edm3* and *ibm2* mutants (Tsuchiya & Eulgem, 2013b; Lai *et al*, 2019; Deremetz *et al*, 2019). We consistently observed clear physical association of HA-tagged IBM2L, but not HA-tagged IBM2S, with these regions (Fig 3.3A). While both EDM3S and EDM3L can be enriched at them, binding of the longer EDM3 isoform seems more pronounced (Fig 3.3B).

Discussion

We previously reported on splice-isoform specific IBM2-EDM3 interactions in the context of basal immunity and flowering time control of Arabidopsis. The longer IBM2L and EDM3L isoforms, but not the shorter IBM2S and EDM3S isoforms, coordinate a gradual decrease of basal defense against the Col-0 virulent *Hpa* isolate Noco2 with the developmental progression towards the floral transition. The strict isoform specific function of IBM2L does also apply to alternative polyadenylation control of *RPP7* as well as *Hpa*Hiks1 resistance mediated by this immune receptor. However, for EDM3 we previously observed that both isoforms can fulfill these roles.

The two EDM3 isoforms differ in the presence/absence of a KQ dipeptide outside their RRM domain. The coiled-coil structure prediction program “COILS” (Lupas *et al*, 1991) indicated this dipeptide to be important for the formation of a coiled-coil structure close to the C-terminus of the protein (Chapter 2). The longer EDM3 isoform is predicted to form this coiled-coil structure with a very high probability. Absence of the KQ dipeptide in EDM3S does not eliminate the possibility of a coiled-coil in this region, but drastically reduces its likelihood. More importantly, the coiled-coil-containing C-terminal region of EDM3 proved to be critical in our yeast-two hybrid experiments for interactions with IBM2 (Chapter 2). Based on our results on *RPP7* regulation, the shorter EDM3 isoform seems to have retained some functionality and is able to physically associate with the proximal polyadenylation site close to *COPIA-R7*. Although association of

EDM3S with this site is weaker than that of EDM3L, the shorter isoform seems to be able to prevent proximal transcript polyadenylation to an extent, sufficient for full expression of RPP7 and tight immunity against *Hpa*Hiks1. However, functionality of EDM3S appears to be insufficient for the roles of EDM3 in the coordination of the floral transition with basal defense.

Future studies may address if and to what extent EDM3L and EDM3S are capable of forming a C-terminal coiled coil structure and if this structure is indeed involved in physical interactions with IBM2, as suggested by our yeast-two hybrid results. However, as already discussed in the previous chapter (Chapter 2) *in vivo* protein biochemical work with EDM3 and IBM2 is challenging due to possible instability of these proteins. We had difficulties to detect epitope-tagged versions of EDM3 and IBM2 in our stably transformed Arabidopsis complementation lines by western blotting or Co-Immuno-precipitation assays. We previously reported similar issues with EDM2 (Lai *et al*, 2020). Likely *in vivo* levels of these proteins are extremely low. EDM3 and IBM2 have putative N-end rule pathway-targeting N terminal residues, such as alanine and glutamic acid (Gibbs *et al*, 2016), which may accelerate the turnover of these proteins. Despite these issues, our ChIP assays and functional complementation experiments unequivocally demonstrated *in vivo* association and cooperation between EDM3L and IBM2L.

Together with the previous chapter, results described in this chapter clearly show that the RRM domain of IBM2L, which is lacking in IBM2S is

absolutely critical for the various biological roles of IBM2. The bromo-adjacent homology (BAH) domain that both tested IBM2 isoforms are equipped with is insufficient for the roles of IBM2 in the coordination of basal defense with the timing of the floral transition as well as *RPP7*-mediated gene for gene resistance. As this domain can serve as a chromatin-binding domain, it seems surprising that IBM2S cannot physically associate with the tested regulatory chromatin sites, each of which is clearly targeted by IBM2L. Likely protein/protein or protein/RNA interactions mediated by its RNA-binding RRM domain are required for successful recruitment of IBM2L to these sites. It will be interesting in this respect to examine if recruitment of IBM2L to chromatin requires EDM3. This can be addressed by crossing the transgene encoding HA-tagged IBM2L from one of the complementation lines we generated into an *edm3* mutant background. The resulting *edm3;HA-IBM2L* line that expresses HA-IBM2L in the absence of EDM3 could then be tested by ChIP for physical association of HA-IBM2L with its regulatory target sites, such as the proximal polyadenylation site in *RPP7*. We already have unpublished data from similar experiments using the *suvh4/5/6; edm2-2; pE2:HA-EDM2* line, which is deficient in all three Arabidopsis H3K9 methyltransferases as well as *EDM2* and which expresses an HA-tagged EDM2 version. ChIP with this line showed that HA-EDM2 requires H3K9me2 marks at the proximal *RPP7* polyadenylation site in order to be recruited there (Wang & Eulgem unpublished). Use of an *edm3-1; pE2:HA-EDM2* line that expresses HA-EDM2 in the absence of EDM3 further showed that HA-EDM2 also requires

EDM3 for binding to this site (Yan Lai & TE, unpublished). Based on these data it seems possible that recruitment of EDM2, EDM3 isoforms and IBM2L to H3K9me2-marked chromatin sites is strongly interdependent on each of these proteins including H3K9me2.

Besides these mechanistic details, an important question to address will be why regulation of *RPP7* expression is so sophisticated? EDM2, EDM3 and IBM2-dependent alternative polyadenylation control is a dynamic mechanism leading to a transient increase of RPP7 coding transcripts followed by a decline and return to its ground state (Tsuchiya & Eulgem, 2013b). In addition, the rate of *RPP7* transcription seems to be up-regulated by a transposon-derived promoter element (Wei & Eulgem, unpublished) after defense induction. Extensive forward genetics screens of Arabidopsis Col mutants for loss of *Hpa*Hiks1 resistance led, besides numerous mutant alleles for *RPP7* itself (Alaine Cuzick, John McDowell, Eric Holub and Jeff Dangl, unpublished) only to mutants affecting *RPP7* expression (*edm2*; *edm3*; (Eulgem *et al*, 2007; Lai *et al*, 2019) or RPP7 protein stability (*sgt1b*; (Tör *et al*, 2002). No mutants of defense signaling components were found to strongly affect *RPP7*-mediated immunity. This highlights the importance of regulatory mechanisms controlling *RPP7* expression and activity. Homeostasis of NLR activity is known to be critical (Li *et al*, 2015; Jacob *et al*, 2013; Lai & Eulgem, 2018) and the stability of NLR proteins and expression of their genes is strictly controlled (Lai & Eulgem, 2018). The efficiency of NLRs in sensing effectors and triggering immunity depends on their dose (Bieri *et al*,

2004; Holt *et al*, 2005), while NLR overexpression can result in autoimmunity and fitness penalties, such as reduced growth and impaired reproduction (Stokes *et al*, 2002; Li *et al*, 2007). Compared to other NLRs recognizing *Hpa* isolates, immunity mediated by *RPP7* is particularly strong, typically completely suppressing *Hpa* growth in host tissues. Interestingly, *RPP7*-triggered immunity only weakly depends on known Arabidopsis defense signaling components like EDS1, NDR1, PAD4 or NPR1 (McDowell *et al*, 2000; Eulgem *et al*, 2007). Only higher-order mutants combining deficiencies in some of these signal transducers exhibit a partial reduction of *Hpa*Hiks1 resistance (McDowell *et al*, 2000). The strength and genetic robustness of *RPP7*-mediated immunity suggests that this NLR generates strong defense signaling input and does only weakly depend on signal amplification loops consisting of canonical defense components (Tao *et al*, 2003; Katagiri, 2004). Consistent with this, certain alleles of the *RPP7* paralog *RPP7b*, which is structurally closely related to *RPP7*, can trigger strong hybrid necrosis in intraspecific *dangerous mix* combinations (Barragan *et al*, 2019a, 2019b; Li & Weigel, 2021). Hybrid necrosis is a cell death-related phenomenon observed in crosses between different natural plant accessions, leading to premature death and developmental defects, likely due to the constitutive activation of immune responses. Preliminary unpublished data from our lab recently revealed that *RPP7* expression results in a substantial reduction of growth in wild type plants (Lai & Eulgem, unpublished). Mutation of *RPP7* leads to increased growth, vigor, and seed yield in the respective mutants. Thus,

expression of *RPP7* appears to require a very fine balance and is stringently controlled by sophisticated mechanisms to enable the immune receptor encoded by this gene to provide sufficient protection against its cognate pathogen race, while limiting its negative impact on plant growth, fitness, and reproductive success.

Materials and Methods

Plant Material and Growth Conditions. The Arabidopsis accessions, Col-0 and Col-5 are used as wild type. All other mutants and transgenic lines used in this study are: *sg1-3/ibm2* (Coustham *et al*, 2014); *edm3-2* and *edm3-3* (Chapter 2), *IBM2S-1*, *IBM2S-2*, *IBM2L-1* and *IBM2L-2* (Chapter 2); *EDM3S-1* and *EDM3L-1* (Lai *et al*., 2019). All the plants were grown under long day (16h-light/8h-dark).

RNA Extraction and qRT-PCR. Trizol reagent (Life technologies) was used to extract RNA from 2 weeks old plants according to the instructions of the manufacturer. Maxima Reverse Transcriptase (Fisher scientific) was used to reverse transcribe 1mg of RNA using oligo-dT18. qRT-PCR was performed by using CFX CONNETCT detection system (Bio-Rad). All primers used are listed in Table 3.1.

***Hyaloperonospora arabidopsidis* Infection and Trypan Blue Staining**. The infection assay was performed as described previously (McDowell *et al*, 2000). In

short, two weeks old plants were sprayed inoculated with *Hpa*Hiks1 spores (5 x 10^4/ml). Sporangiophores on cotyledons were counted seven days after infection. Trypan blue staining was done as described previously (McDowell *et al*, 2000).

Chromatin Immunoprecipitation. ChIP was performed as previously described (Tsuchiya & Eulgem, 2013b) using anti-HA (AB9110, Abcam) or anti-FLAG (F1804, Sigma). Two weeks old plants were used for the assay.

References

Barragan CA, Wu R, Kim S-T, Xi W, Habring A, Hagmann J, Van de Weyer A-L, Zaidem M, Ho WWH, Wang G, *et al* (2019a) RPW8/HR repeats control NLR activation in Arabidopsis thaliana. *PLoS Genet* 15: e1008313

Barragan CA, Wu R, Kim S, Xi W & Habring A (2019b) RPW8/HR Repeats Predict NLR-dependent Hybrid Performance.

Bieri S, Mauch S, Shen Q-H, Peart J, Devoto A, Casais C, Ceron F, Schulze S, Steinbiss H-H, Shirasu K, *et al* (2004) RAR1 positively controls steady state levels of barley MLA resistance proteins and enables sufficient MLA6 accumulation for effective resistance. *Plant Cell* 16: 3480–3495

Chisholm ST, Coaker G, Day B & Staskawicz BJ (2006) Host-microbe interactions: shaping the evolution of the plant immune response. *Cell* 124: 803–814

Coustham V, Vlad D, Deremetz A, Gy I, Cubillos FA, Kerdaffrec E, Loudet O & Bouché N (2014) SHOOT GROWTH1 maintains Arabidopsis epigenomes by regulating IBM1. *PLoS One* 9: e84687

Deremetz A, Le Roux C, Idir Y, Brousse C, Agorio A, Gy I, Parker JE & Bouché N (2019) Antagonistic Actions of FPA and IBM2 Regulate Transcript Processing from Genes Containing Heterochromatin. *Plant Physiol* 180: 392–403

Duan C-G, Wang X, Zhang L, Xiong X, Zhang Z, Tang K, Pan L, Hsu C-C, Xu H, Tao WA, *et al* (2017) A protein complex regulates RNA processing of intronic heterochromatin-containing genes in Arabidopsis. *Proc Natl Acad Sci U S A* 114: E7377–E7384

Eulgem T, Tsuchiya T, Wang X-J, Beasley B, Cuzick A, Tör M, Zhu T, McDowell JM, Holub E & Dangl JL (2007) EDM2 is required for RPP7-dependent disease resistance in Arabidopsis and affects RPP7 transcript levels. *Plant J* 49: 829–839

Gibbs DJ, Bailey M, Tedds HM & Holdsworth MJ (2016) From start to finish: amino-terminal protein modifications as degradation signals in plants. *New Phytologist* 211: 1188–1194 doi:10.1111/nph.14105 [PREPRINT]

Glazebrook J (2001) Genes controlling expression of defense responses in Arabidopsis—2001 status. *Curr Opin Plant Biol* 4: 301–308

Holt BF 3rd, Belkhadir Y & Dangl JL (2005) Antagonistic control of disease resistance protein stability in the plant immune system. *Science* 309: 929–

932

Jacob F, Vernaldi S & Maekawa T (2013) Evolution and Conservation of Plant NLR Functions. *Front Immunol* 4: 297

Jones JDG & Dangl JL (2006) The plant immune system. *Nature* 444: 323–329

Katagiri F (2004) A global view of defense gene expression regulation--a highly interconnected signaling network. *Curr Opin Plant Biol* 7: 506–511

Lai Y, Cuzick A, Lu XM, Wang J, Katiyar N, Tsuchiya T, Le Roch K, McDowell JM, Holub E & Eulgem T (2019) The Arabidopsis RRM domain protein EDM3 mediates race-specific disease resistance by controlling H3K9me2-dependent alternative polyadenylation of RPP7 immune receptor transcripts. *Plant J* 97: 646–660

Lai Y & Eulgem T (2018) Transcript-level expression control of plant NLR genes. *Mol Plant Pathol* 19: 1267–1281

Lai Y, Lu XM, Daron J, Pan S, Wang J, Wang W, Tsuchiya T, Holub E, McDowell JM, Slotkin RK, *et al* (2020) The Arabidopsis PHD-finger protein EDM2 has multiple roles in balancing NLR immune receptor gene expression. *PLoS Genet* 16: e1008993

Lei M, La H, Lu K, Wang P, Miki D, Ren Z, Duan C-G, Wang X, Tang K, Zeng L, *et al* (2014) Arabidopsis EDM2 promotes IBM1 distal polyadenylation and regulates genome DNA methylation patterns. *Proc Natl Acad Sci U S A* 111: 527–532

Li L & Weigel D (2021) One Hundred Years of Hybrid Necrosis: Hybrid Autoimmunity as a Window into the Mechanisms and Evolution of Plant–Pathogen Interactions. *Annual Review of Phytopathology* 59: 213–237 doi:10.1146/annurev-phyto-020620-114826 [PREPRINT]

Li X, Kapos P & Zhang Y (2015) NLRs in plants. *Curr Opin Immunol* 32: 114–121

Li Y, Yang S, Yang H & Hua J (2007) The TIR-NB-LRR gene SNC1 is regulated at the transcript level by multiple factors. *Mol Plant Microbe Interact* 20: 1449–1456

Lupas A, Van Dyke M & Stock J (1991) Predicting coiled coils from protein sequences. *Science* 252: 1162–1164

Lu Y & Tsuda K (2021) Intimate Association of PRR- and NLR-Mediated Signaling in Plant Immunity. *Mol Plant Microbe Interact* 34: 3–14

McDowell JM, Cuzick A, Can C, Beynon J, Dangl JL & Holub EB (2000) Downy mildew (Peronospora parasitica) resistance genes in Arabidopsis vary in functional requirements for NDR1, EDS1, NPR1 and salicylic acid accumulation. *Plant J* 22: 523–529

Ngou BPM, Ahn H-K, Ding P & Jones JDG (2021) Mutual potentiation of plant immunity by cell-surface and intracellular receptors. *Nature* 592: 110–115

Saze H, Kitayama J, Takashima K, Miura S, Harukawa Y, Ito T & Kakutani T (2013) Mechanism for full-length RNA processing of Arabidopsis genes containing intragenic heterochromatin. *Nat Commun* 4: 2301

Shen Q-H, Saijo Y, Mauch S, Biskup C, Bieri S, Keller B, Seki H, Ulker B, Somssich IE & Schulze-Lefert P (2007) Nuclear activity of MLA immune receptors links isolate-specific and basal disease-resistance responses. *Science* 315: 1098–1103

Stokes TL, Kunkel BN & Richards EJ (2002) Epigenetic variation in Arabidopsis disease resistance. *Genes Dev* 16: 171–182

Tao Y, Xie Z, Chen W, Glazebrook J, Chang H-S, Han B, Zhu T, Zou G & Katagiri F (2003) Quantitative nature of Arabidopsis responses during compatible and incompatible interactions with the bacterial pathogen Pseudomonas syringae. *Plant Cell* 15: 317–330

Tör M, Gordon P, Cuzick A, Eulgem T, Sinapidou E, Mert-Türk F, Can C, Dangl JL & Holub EB (2002) Arabidopsis SGT1b is required for defense signaling conferred by several downy mildew resistance genes. *Plant Cell* 14: 993–1003

Tsuchiya T & Eulgem T (2010a) Co-option of EDM2 to distinct regulatory modules in Arabidopsis thaliana development. *BMC Plant Biology* 10: 203 doi:10.1186/1471-2229-10-203 [PREPRINT]

Tsuchiya T & Eulgem T (2010b) The Arabidopsis defense component EDM2 affects the floral transition in an FLC-dependent manner. *Plant J* 62: 518–528

Tsuchiya T & Eulgem T (2013a) Mutations in EDM2 selectively affect silencing states of transposons and induce plant developmental plasticity. *Sci Rep* 3: 1701

Tsuchiya T & Eulgem T (2013b) An alternative polyadenylation mechanism coopted to the *Arabidopsis RPP7* gene through intronic retrotransposon domestication. *Proceedings of the National Academy of Sciences* 110 doi:10.1073/pnas.1312545110 [PREPRINT]

Tsuchiya T & Eulgem T (2014) The PHD-finger module of the Arabidopsis thaliana defense regulator EDM2 can recognize triply modified histone H3 peptides. *Plant Signal Behav* 9: e29202

Wang X, Duan C-G, Tang K, Wang B, Zhang H, Lei M, Lu K, Mangrauthia SK, Wang P, Zhu G, *et al* (2013) RNA-binding protein regulates plant DNA methylation by controlling mRNA processing at the intronic heterochromatin-containing gene IBM1. *Proc Natl Acad Sci U S A* 110: 15467–15472

Yuan M, Ngou BPM, Ding P & Xin X-F (2021) PTI-ETI crosstalk: an integrative view of plant immunity. *Curr Opin Plant Biol* 62: 102030

Zhang Y, Xia R, Kuang H & Meyers BC (2016) The Diversification of Plant NBS-LRR Defense Genes Directs the Evolution of MicroRNAs That Target Them. *Mol Biol Evol* 33: 2692–2705

Zhang Y-Z, Lin J, Ren Z, Chen C-X, Miki D, Xie S-S, Zhang J, Chang Y-N, Jiang J, Yan J, *et al* (2021) Genome-wide distribution and functions of the AAE complex in epigenetic regulation in Arabidopsis. *J Integr Plant Biol* 63: 707–722

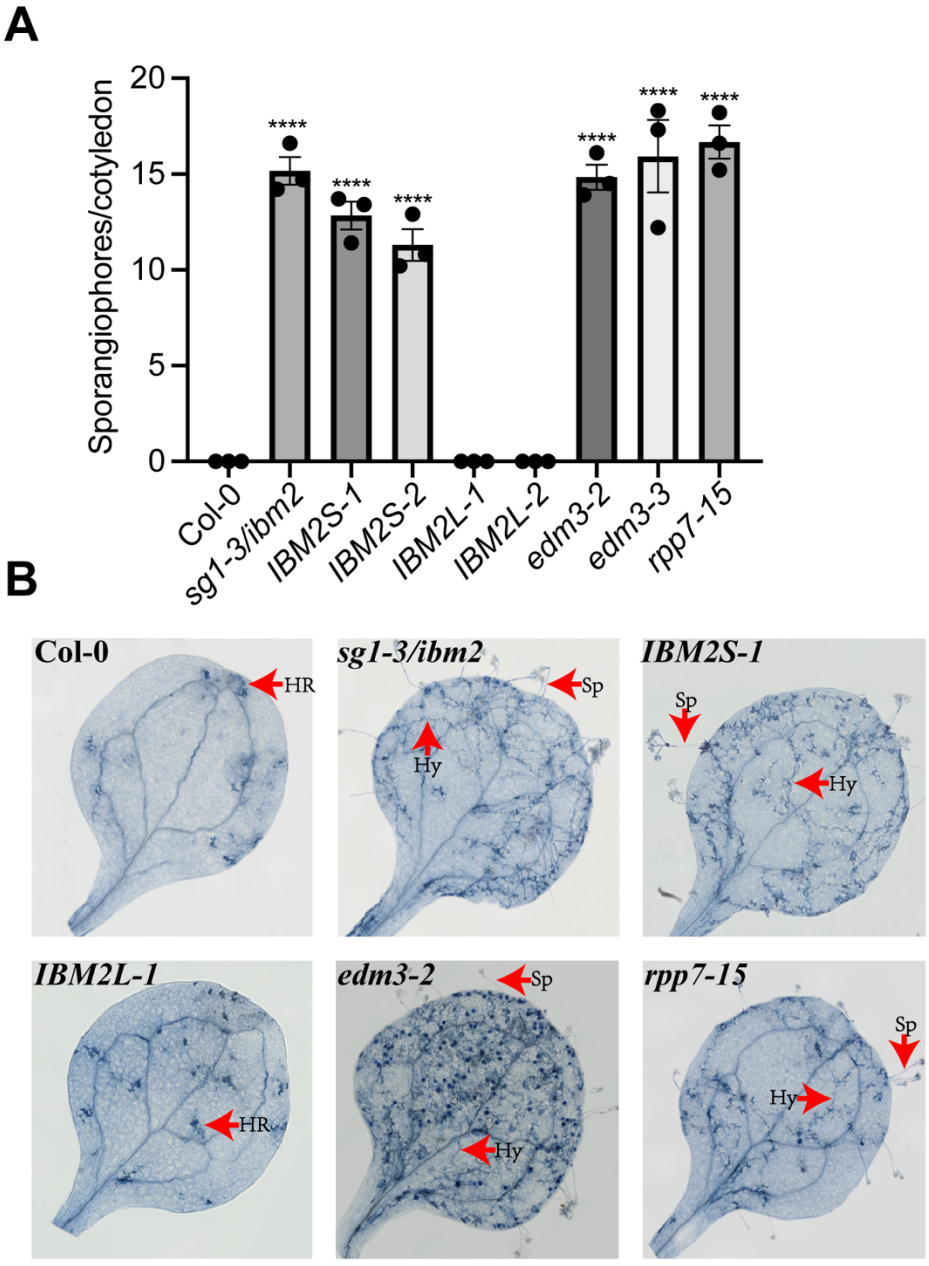
A
Sporangiophores/cotyledon
20
15
10
5
0
****
****
****
****
****
****
Col-0
sg1-3/ibm2
IBM2S-1
IBM2S-2
IBM2L-1
IBM2L-2
edm3-2
edm3-3
rpp7-15
B
Col-0
HR
sg1-3/ibm2
Sp
Hy
IBM2S-1
Sp
Hy
IBM2L-1
HR
edm3-2
Sp
Hy
rpp7-15
Sp
Hy

Figure 3.1. Loss of *Hpa*Hiks1 resistance in *sg1-3/ibm2* can only be rescued by IBM2L but not IBM2S.

A. The number of sporangiophores on cotyledons of the indicated genotypes. Two-week old plants were sprayed-inoculated with *Hpa*Hiks1 spores (5 x 10^4/ml). Sporangiophores on cotyledons were counted one-week post-infection.

B. Representative pictures of trypan blue stained cotyledons after *Hpa*Hiks1 infection. Hypersensitive response (HR), Sporangiophore (Sp) and Hyphae (Hy) are pointed by red arrows.

Data information: Error bars represent standard errors from three independent experiments. Asterisks indicate significant difference analyzed by student's t-test. (****, $p<0.0001$).

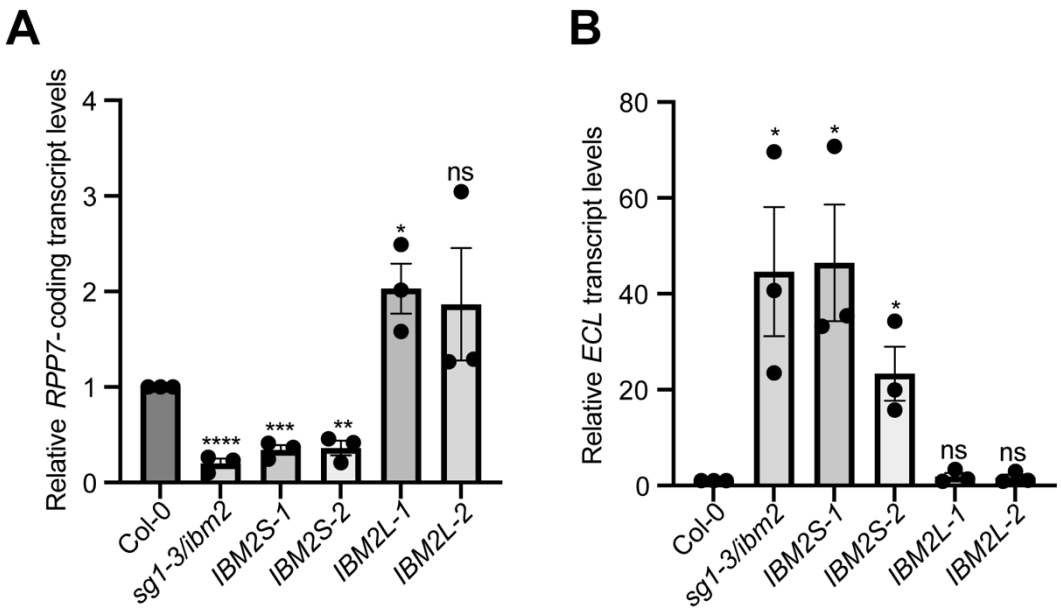

Figure 3.2. RPP7-coding transcripts in *sg1-3/ibm2* are rescued by *IBM2L* but not *IBM2S*.
A. The expression levels of *RPP7*-coding transcripts were measured by qRT-PCR in the indicated genotypes.
B. The expression levels of ECL transcripts were measured by qRT-PCR in the indicated genotypes.
Data information: Error bars represent standard errors from three independent experiments. Asterisks indicate significant difference analyzed by student's t-test. (*, $p<0.05$; **, $p<0.01$; ***, $p<0.001$; ****, $p<0.0001$).

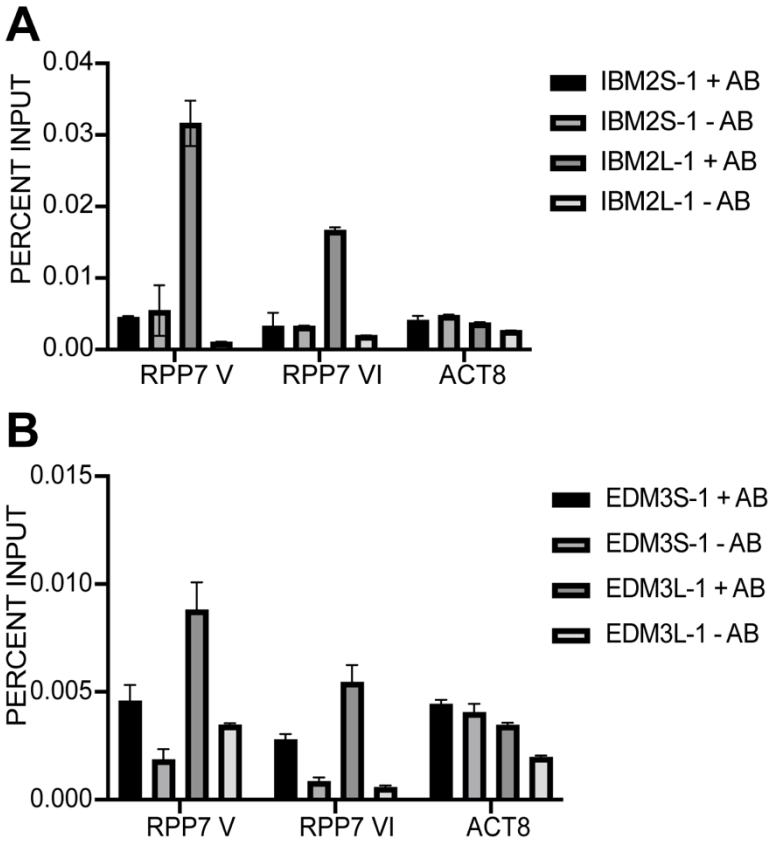

Figure 3.3. IBM2 and EDM3 isoform-specific enrichment at *RPP7* chromatin.
A. ChIP-qPCR shows that IBM2L but not IBM2S binds *RPP7* chromatin.
B. ChIP-qPCR shows that both EDM3 isoforms bind *RPP7* chromatin.
Data information: One representative replicate is shown. Error bars represent standard deviation.
Actin 8 gene is served as negative control.

Table 3.1. Primers used in this study.

Primer names	Sequence (5'-3')	Notes
RPP7_F	ACGTGAACTATATCAATTGTTGGAA	Tsuchiya & Eulgem, 2013
RPP7_R	TTTGTAGGCGCAACGATACTCT	Tsuchiya & Eulgem, 2013
ECL_F	CATATGTGTGATTCTTCCCTAAGAGG	Tsuchiya & Eulgem, 2013
ECL_R	AAATCTTGCACAGAGGTCCTGA	Tsuchiya & Eulgem, 2013
RPP7_V_F	AATAGTGTGATTAGCTTCTCCGTT	Tsuchiya & Eulgem, 2013
RPP7_V_R	CCTACAAACACTGGTTATATCTGGC	Tsuchiya & Eulgem, 2013
RPP7_VI_F	CCCAAGAAGCAGAGGCAACG	Tsuchiya & Eulgem, 2013
RPP7_VI_R	TTCTGAATCAAGGGTTGAGAAACGA	Tsuchiya & Eulgem, 2013
ACT8_F	CAGTGTCTGGATTGGTGGTTCTATC	Tsuchiya & Eulgem, 2013
ACT8_R	ATCCCGTCATGGAAACGATGT	Tsuchiya & Eulgem, 2013
ACT8_ChIP_F	CTAAAGAGACATCGTTTCCATGACGG	Tsuchiya & Eulgem, 2013
ACT8_ChIP_R	TCCTTAGACATCTCTCCAAACGC	Tsuchiya & Eulgem, 2013

Chapter 4

The Interacting Arabidopsis Proteins EDM2, EDM3 and IBM2 Mediate Prioritization of Growth Over Immunity via Disturbing ROS Homeostasis

Abstract

Plants have developed growth-defense trade-off mechanisms to survive and successfully reproduce, which is important for their productivity in both nature and agriculture. However, the molecular mechanisms underlying the growth-defense trade-off are still largely unknown. Here, we are using mutants of the *Arabidopsis thaliana* genes *EDM2*, *EDM3* and *IBM2*, which exhibit constitutively elevated basal immunity as well as reduced growth and impaired development, to study mechanisms balancing growth and defense. We demonstrated that EDM2, EDM3 and IBM2 negatively regulate peroxidase activity by downregulating expression levels of multiple peroxidase genes. By inhibiting peroxidase activities in *edm2*, *edm3* and *ibm2* plants, growth defects observed in these mutants were partly rescued, while constitutive immunity was suppressed. Using a set of double mutants compromised in either *EDM2*, *EDM3* or *IBM2*, as well as accumulation of salicylic acid (SA) or signaling processes controlled by this plant defense hormone, we further showed SA to be required for the elevated levels of immunity in all three mutants. Moreover, disruption of

the SA signaling pathway in the *edm2*, *edm3* and *ibm2* mutant backgrounds fully or partly rescued their growth defects. Lastly, the growth defects and enhanced basal immunity in *edm2*, *edm3* and *ibm2* mutants can also be partly rescued by the longer transcript isoform of the *A. thaliana IBM1* gene, expression of which is promoted by EDM2, EDM3 and IBM2. These results show that EDM2, EDM3 and IBM2 balance defense-growth trade-off by regulating peroxidase activity.

Introduction

Constitutive activation of immune responses is often associated with reduced growth in plants, a phenomenon known as defense-growth trade-off. Most of the growth-related trade-offs that have been identified involve incompatible hormones crosstalk (Huot *et al*, 2014), between phytohormones controlling stress responses and development, such as salicylic acid (SA), jasmonate (JA), auxin, brassinosteroids (BR) and gibberellins (GA) etc. SA plays key roles in defense against biotrophic and hemibiotrophic pathogens. In contrast, sustained accumulation of SA can also result in growth inhibition (Clarke *et al*, 2000; Zhang *et al*, 2003; Scott *et al*, 2004), which is likely mediated by antagonistic interaction with signaling pathways triggered by growth-promoting hormones, such as auxin, BR or GA (Huot *et al*, 2014). It has long been believed that the growth-defense trade-off occurs due to limited metabolic resources (Karasov *et al*, 2017). When plants have been attacked, metabolic resources are

preferentially allocated to defense, resulting in enhanced immunity but at the expense of reduced growth. There are many reports showing re-allocation of limited metabolic resources toward defense when plants are under attack (Kempel *et al*, 2011; Züst *et al*, 2015). These observations strongly imply that plants have evolved adaptive mechanisms to optimize growth and defense. Thus, it is essential to understand the underlying mechanisms in order to uncouple or alleviate the trade-off, which could possibly create plants that are able to defend themselves against pathogens and grow well at the same time.

EDM2 is a PHD domain-containing protein. We and other groups (Tsuchiya & Eulgem, 2013; Lei *et al*, 2014) previously found that EDM2 targets the H3K9me2 marked *COPIA-R7* retrotransposon in the first intron of *RPP7*, a gene encoding plant immune receptor that can specifically recognize the Hiks1 isolate of the pathogenic oomycete *Hyaloperonospora arabidopsidis* (*Hpa*). By suppressing proximal transcript polyadenylation at *COPIA-R7*, EDM2 promotes expression of functional RPP7-coding transcripts, while inhibiting expression of a non-coding transcript that is terminated at the 5'LTR of the retrotransposon. This non-coding transcript was termed ECL (Exon1 containing 5'LTR terminated transcript). We further found (Lai *et al*, 2019) that the RRM domain-containing protein, EDM3, also binds to the same area in *RPP7* to suppress proximal polyadenylation causes downregulation of the ECL transcript and upregulation of RPP7-coding transcripts. Another RRM domain-containing protein, IBM2, was also found to be recruited to *COPIA-R7* (Saze *et al*, 2013; Wang *et al*, 2013) and

joining EDM2 and EDM3 in the regulation of *RPP7* expression. Since EDM2, EDM3 and IBM2 co-localized to the same regions within *RPP7*, it is not surprising that physical interactions among them were observed. In fact, both EDM2 and IBM2 directly interact with EDM3 while the interactions between EDM2 and IBM2 seem indirect and require EDM3 as a molecular bridge (Duan *et al*, 2017). EDM2 and IBM2 were also found to target a heterochromatic region within the largest intron of the H3K9me2 demethylase gene *IBM1* (Saze *et al*, 2013; Wang *et al*, 2013; Lei *et al*, 2014). At this locus EDM2 and IBM2 facilitate the expression of the long transcript isoform, IBM1L, while inhibiting the expression of a shorter isoform termed IBM1S. Both EDM2 and IBM2 have positive effects on growth, as their mutants exhibit reduced fresh weight (Tsuchiya & Eulgem, 2010) and/or a smaller rosette area (Tsuchiya & Eulgem, 2010; Coustham *et al*, 2014). It was further observed that abnormal leaf development in *edm2* mutants can be rescued by a genomic *IBM1* clone carrying a deletion of the heterochromatic repeats in its largest intron. In this case wild type levels of IBM1L expression are restored, as no proximal transcript polyadenylation can occur (Lei *et al*, 2014).

Although EDM2, EDM3 and IBM2 positively regulate expression of *RPP7* as well as immunity mediated by this gene, they act also as negative regulators of basal defense. We observed increased basal resistance in their mutants. Possibly this is due to the joint upregulation of large overlapping sets of NLR genes (Lai *et al*, 2020), which are known to activate defense responses, when

overexpressed . It has been known that transcripts of both EDM3 and IBM2 are alternatively spliced. We further showed that only a defined pair of EDM2 and IBM2 splice isoforms (EDM3L and IBM2L) can physically interact (Chapter 2). Only EDM3L or IBM2L, can rescue in *edm3* or *ibm2* mutants the wild type expression levels of at least some of the NLRs that are constitutively upregulated in *edm3* or *ibm2* plants. The same applies to the constitutive basal defense and late flowering time phenotypes observed in these mutants (Chapter 2). We further linked a gradual increase of EDM3L and IBM2L transcript levels to a gradual decrease in basal immunity with the developmental progression of plants immediately prior to the floral transition (Chapter 2). Therefore, EDM3L and IBM2L have critical roles in coordinating the floral transition and basal immunity.

The oxidative burst is an early event among immune responses (Wojtaszek, 1997). Reactive oxygen species (ROS) were observed to be highly induced after pathogen infection or microbe-associated molecular pattern (MAMP) treatment (Daudi *et al*, 2012; Torres *et al*, 2002). In Arabidopsis, NADPH oxidase genes and type III peroxidase genes, the products of which are targeted to plant cell walls, are two main sources of ROS production in the apoplast (Bolwell & Wojtaszek, 1997; Smirnoff & Arnaud, 2019). ROS is not only involved in immune response but also involved in plant growth, as accumulation of ROS can stiffen cell walls, thereby inhibiting plant growth (Schopfer, 1996). Due to its dual effects, ROS is further linked to the defense-growth trade-off as a shared component of both processes (Neuser *et al*, 2019).

Although *edm2* mutants cause stunted growth and altered immune responses, it remains elusive whether and how EDM2 controls the defense-growth trade-off. Here, we report that EDM2 as well as the two RRM domain-containing proteins EDM3 and IBM2 mediate defense-growth trade-off control through their impact on peroxidase activity. We found that EDM2, EDM3 and IBM2 positively regulate plant development. We further demonstrated that EDM2, EDM3 and IBM2 suppress peroxidase activity by downregulating the expression levels of multiple peroxidase genes. Moreover, EDM2, EDM3 and IBM2 promote leaf expansion by inhibiting peroxidase activity. We further observed that the short primary root phenotype we observed in mutants of *EDM2*, *EDM3* and *IBM2* is rescued when immune responses are compromised. Interestingly, restoring wild type expression levels of *IBM1L* in *edm2, edm3* and *ibm2* lines only partly rescued their growth and enhanced basal immunity phenotypes. Overall, we link EDM2, EDM3 and IBM2, three epigenetic regulators which preferentially target genes that contain heterochromatin, to defense-growth trade-off control that is mediated by peroxidase activity.

Results

EDM2/EDM3/IBM2 Positively Regulate Plant Development

Previously, we showed that *edm2* mutants have decreased fresh weight and leaf expansion compared to their wild type parental lines (Tsuchiya & Eulgem, 2010). Here we also observed that fresh weight and leaf expansion are

decreased in mutants of *EDM3* and *IBM2* (Fig 4.1A, 4.1B and 4.2). We further found that *edm2*, *edm3*, and *ibm2* mutants have shorter primary root length (Fig 4.1C and 4.2). Moreover, only the interacting isoforms of EDM3 and IBM2 we previously reported (Chapter 2), EDM3L and IBM2L, can rescue the growth defects in *edm3* and *ibm2* mutants while complementation with the shorter isoforms, EDM3S and IBM2S, failed, as the respective lines exhibit similar phenotypes as the respective parental mutants (Fig 4.2). Overall, these data suggest that EDM2, EDM3L and IBM2L have positive effects on plant development.

EDM2/EDM3/IBM2 Suppress Peroxidase Activity by Down-Regulation of Type III Peroxidase Genes to Promote Leaf Expansion

Although growth defects were observed in all mutants of *EDM2*, *EDM3* and *IBM2*, the underlying mechanism is still unknown. To understand how these genes affect plant development, we re-inspected our previous RNA-seq based transcriptomics analyses of *edm2* plants (Lai *et al*, 2020) and found that twenty-seven type III peroxidase genes and two NADPH oxidase genes, *RbohD* and *RbohF*, are significantly up-regulated in *edm2* mutants compared to their wild type parental line, while the gene encoding the H_2O_2 scavenging enzyme, *CAT1*, is significantly down-regulated. Since over-accumulation of H_2O_2 can reduce cell wall extensibility (Schopfer, 1996), which restricts growth, the joint upregulation of peroxidase and NADPH-oxidase genes may explain why *edm2* mutants exhibit

growth defects. First, we used qRT-PCR to confirm the up-regulation among selected genes in *edm2* plants. We found that all the selected type III peroxidase genes except *PRX31* and *PRX62* are significantly up-regulated in the *edm2-2* mutant as well as in the *edm3-2* and *sg1-3/ibm2* mutants (Fig 4.3A). While we cannot confirm the up-regulation of *RbohD* and *RbohF* (Fig 4.3B), we observed a significant up-regulation of *RbohB,* another member of this family of NADPH oxidase genes (Fig 4.3B). All these data suggest that H_2O_2 is possibly accumulated in mutants of *EDM2*, *EDM3* and *IBM2*. Since many peroxidase genes are up-regulated in *edm2*, *edm3* and *ibm2* plants, we wondered if peroxidase activity is also increased in these mutants. By measuring their peroxidase activity, we found that all the *edm2*, *edm3* and *ibm2* mutants have noticeable increase in peroxidase activity in the ionically bound fraction (Fig 4.3C), while only the tested *ibm2* mutant exhibits a mild increase in peroxidase activity in the soluble fraction (Fig 4.3D). Because type III peroxidases are targeted to the cell wall, it makes sense that an increased peroxidase activity was observed in the ionically bound fraction in mutants of *EDM2*, *EDM3* and *IBM2*.

To test the hypothesis that accumulation of H_2O_2 causes growth defects in *edm2*, *edm3* and *ibm2*, we treated the plants with 20μM SHAM, a peroxidase inhibitor, at day 14 and day 16 and compared their rosette areas at day 25. We observed a significant increase in rosette areas in all tested mutants after SHAM treatment, while there is no difference in wild type after treatment (Fig 4.4).

Overall, these data suggest that accumulation of H_2O_2 and increased peroxidase activity cause growth defects in *edm2*, *edm3* and *ibm2* mutants.

Basal *Hpa*Noco2 Resistance in Mutants of *EDM2*, *EDM3* and *IBM2* is Decreased by Inhibiting Peroxidase Activity

To examine if enhanced basal resistance in *edm2*, *edm3* and *ibm2* mutants is due to increased peroxidase activity, we pre-treated all three mutants with the peroxidase inhibitor, SHAM, 24 hours before infection with *Hpa*Noco2. We observed a larger number of *Hpa*Noco2 spores in all three mutant plants after treatment with SHAM and a mild increase in wild type plants with SHAM treatment (Fig 4.5), suggesting increased peroxidase activity is required for enhanced immunity in all three mutants.

Enhanced Basal Immunity in *edm2*, *edm3* and *ibm2* Suppresses Primary Root Growth

To examine if growth defects in *edm2*, *edm3* and *ibm2* mutants are caused by their constitutively enhanced basal immunity, we used Arabidopsis lines with defects in defense responses controlled by SA. The *sid2-2* mutant is compromised in defense-associated biosynthesis of this phytohormone, while the transgenic *NahG* line cannot accumulate SA, due to the expression of the bacterial salicylic acid hydroxylase gene *NahG*. The *pad4* mutant is deficient in a SA-responsive signaling step. We crossed *edm2*, *edm3* and *ibm2* mutants to each of these three lines and performed experiments with lines homozygous for

each altered component (mutation or transgene). We first examined if enhanced immunity in *edm2*, *edm3* and *ibm2* is reduced by blockage of SA defenses. One week after *Hpa*Noco2 infection, we observed complete loss of the enhanced basal defense phenotype in all double mutants as well as *edm2-2;NahG*, *edm3-2;NahG* and *sg1-3/ibm2;NahG* (Fig 4.6A-D). We further measured the primary root length in all of these lines and observed that the short primary root phenotype of *edm2*, *edm3* and *ibm2* mutants is fully or partly rescued by introducing *sid2-2, NahG* or *pad4* (Fig 4.6E-I). Overall, these findings suggest that enhanced immunity in mutants of *EDM2*, *EDM3* and *IBM2* relies on the SA-dependent basal defense pathway, which is further required for the inhibition of primary root length observed in these mutants.

IBM1L Partly Rescues Growth Defects and Disease Susceptibility in Mutants of EDM2, EDM3 and IBM2

Thus far, we link increased peroxidase activity to EDM2, EDM3 and IBM2-mediated defense-growth trade-off control. However, neither treatment with SHAM nor crossing with mutants of the SA signaling pathway can fully rescue the growth defects in mutants of *EDM2*, *EDM3* and *IBM2*, suggesting that there are other mechanisms that regulate plant growth in these mutants. Because the known EDM2 and IBM2 target gene *IBM1* was shown to rescue leaf abnormalities in *edm2* mutants (Lei *et al*, 2014), we transformed a genomic *IBM1* clone with a deletion of its heterochromatic repeats to mutants of *EDM2*, *IBM2* and *EDM3*. This version of IBM1 can rescue the low expression levels of the

functional *IBM1L* isoform in *edm2* and *ibm2* mutants (Saze *et al*, 2013; Lei *et al*, 2014). We observed that growth defects and *Hpa*Noco2 susceptibility in *edm2*, *edm3* and *ibm2* mutants were partly restored when introducing this version of *IBM1*; with the exception that it fully rescued *Hpa*Noco2 susceptibility in *edm3-2* to wild type levels (Fig 4.7A, 4.7B and 4.8). Overall, these data may at least partly explain why growth defects in mutants of *EDM2*, *EDM3* and *IBM2* are not fully restored when enhanced immunity is suppressed.

Discussion

We previously observed that *edm2* mutants have reduced fresh weight and smaller rosette areas (Tsuchiya & Eulgem, 2010). We further showed that basal immunity is enhanced in *edm2* mutants, which may be due to constitutively elevated expression levels of a large number of NLR genes (Lai *et al*, 2020); Chapter 2). Despite the counter-directional effects on basal immunity and growth, it remained unclear whether and how EDM2 as well as its interacting partners, EDM3 and IBM2 affect defense-growth trade-off. In this study, we found that EDM2, EDM3 and IBM2 mediate the defense-growth trade-off through inhibiting peroxidase activity. Like *edm2* mutants, *edm3* and *ibm2* mutants also exhibit growth defects, such as reduced fresh weight, smaller rosette areas and shorter primary root length. All these findings suggest promoting effects of EDM2, EDM3 and IBM2 on plant growth. We further link these growth defects to increased peroxidase activity in mutants of *EDM2*, *EDM3* and *IBM2*. As type III peroxidases

are commonly targeted to plant cell walls (Smirnoff & Arnaud, 2019) and involved in ROS production in the apoplast, upregulation of type III peroxidase genes and increased peroxidase activity in *edm2*, *edm3* and *ibm2* mutants could possibly result in accumulation of ROS in the apoplast, which reduces cell wall extensibility possibly due to lignin formation and cross linking (Schopfer, 1996; Lee *et al*, 2013), thereby suppressing plant growth. By using a peroxidase inhibitor, SHAM, we observed that smaller rosette areas were partly rescued in mutants of *EDM2*, *EDM3* and *IBM2*. Moreover, peroxidase activity is also found to be required for enhanced resistance in *edm2*, *edm3* and *ibm2* mutants. Thus, increased peroxidase activity is likely linked to the defense-growth trade-off. Oxidative burst is a very early immune response, occurring within minutes when plants are invaded by pathogens (Wojtaszek, 1997). Plant defenses require ROS, which serves as both defensive cytotoxic compounds as well as signaling molecules to prevent spread of invading pathogens (Lorrain *et al*, 2003; Moeder & Yoshioka, 2008). Therefore, although accumulation of ROS can cause growth inhibition, it can also promote immune responses.

That enhanced immunity in *edm2*, *edm3* and *ibm2* plants is the reason for the growth inhibition phenotype in these mutants was further confirmed by crossing them with *sid2-2*, *pad4* and *NahG* lines. The short primary root length in the single mutants was fully or partly restored in the corresponding double mutants. Since neither SHAM treatment nor crossing with mutants in the SA signaling pathway could fully restore the growth defects in all the mutants, we

hypothesized that there should be other mechanisms in the mutants to suppress growth. As the leaf abnormality phenotype in *edm2* mutants can be rescued when *IBM1L* expression is restored to wild type levels or higher, we wondered if downregulation of IBM1L in these mutants could possibly cause some of the observed growth defects. By introducing a genomic *IBM1L* with a deletion of the heterochromatic repeats, growth defects and *Hpa*Noco2 susceptibility were partly rescued in *edm2*, *edm3* and *ibm2* mutant backgrounds. These findings can at least partly explain why growth defects in *edm2*, *edm3* and *ibm2* cannot be fully restored after treatment with SHAM or crossing with the mutants in the SA signaling pathway. Overall, in this study we propose that EDM2, EDM3 and IBM2 control the growth-defense trade-off. Partially this is achieved by modulation of peroxidase activity.

Materials and Methods

Plant Material and Growth Conditions. All the genotypes except specified are in Col-0 background. The following single mutants used in this study: *edm2-2* (Eulgem *et al*, 2007), *edm3-2* (Chapter 2), *sg1-3/ibm2* (Coustham *et al*, 2014), *sid2-2* (Dewdney *et al*, 2000), *pad4* (Jirage *et al*, 1999), and *ibm1-4* (Lai *et al*, 2020). The following double mutants used in this study: *edm2-2;edm3-2, edm2-2;sg1-3/ibm2, edm3-2;sg1-3/ibm2* were described previously (Chapter 2). The following transgenic lines used in this study: *EDM3S^{np}-1*, *EDM3S^{np}-2, EDM3L^{np}-*

1, *EDM3L^{np}-2*, *IBM2S-1* and *IBM2L-1* were described previously (Chapter 2), *NahG* (Delaney *et al*, 1994). Double mutants were made by crossing and F2 seeds were screened by genotyping PCR to select homozygotes. Plants are grown either on ½ MS medium or in soil under long day (16h/8h light-dark cycles).

Primary Root Length Measurement. Plants were grown vertically on ½ MS medium for five or seven days. Primary root length of the indicated genotypes was measured using ImageJ.

Rosette Area Measurement. Seedlings were treated with 20μM SHAM (S607-5G, Sigma) at day 14 and day16. Rosette areas were pictured and measured using ImageJ at day 25.

RNA Extraction and qRT-PCR. Total RNA of the aerial parts of two weeks old plants was extracted using Trizol reagent (Life technologies) according to the instructions of the manufacturer. 1μg of RNA was reversed transcribed into cDNA using Maxima Reverse Transcriptase (Fisher scientific). The cDNA products were used for Real-time PCR with CFX CONNECT detection system (Bio-Rad). All primers used are listed in Table 4.1.

Peroxidase Activity Measurement. Two weeks old seedlings were used for peroxidase activity measurement as described previously (Bindschedler *et al*, 2006).

***Hyaloperonospora arabidopsidis* Infection Assay**. *Hpa*Noco2 infection assays were performed as previously described (McDowell *et al*, 2000).

References

Bindschedler LV, Dewdney J, Blee KA, Stone JM, Asai T, Plotnikov J, Denoux C, Hayes T, Gerrish C, Davies DR, *et al* (2006) Peroxidase-dependent apoplastic oxidative burst in Arabidopsis required for pathogen resistance. *Plant J* 47: 851–863

Bolwell GP & Wojtaszek P (1997) Mechanisms for the generation of reactive oxygen species in plant defence – a broad perspective. *Physiological and Molecular Plant Pathology* 51: 347–366 doi:10.1006/pmpp.1997.0129 [PREPRINT]

Clarke JD, Volko SM, Ledford H, Ausubel FM & Dong X (2000) Roles of salicylic acid, jasmonic acid, and ethylene in cpr-induced resistance in arabidopsis. *Plant Cell* 12: 2175–2190

Coustham V, Vlad D, Deremetz A, Gy I, Cubillos FA, Kerdaffrec E, Loudet O & Bouché N (2014) SHOOT GROWTH1 maintains Arabidopsis epigenomes by regulating IBM1. *PLoS One* 9: e84687

Daudi A, Cheng Z, O'Brien JA, Mammarella N, Khan S, Ausubel FM & Bolwell GP (2012) The apoplastic oxidative burst peroxidase in Arabidopsis is a major component of pattern-triggered immunity. *Plant Cell* 24: 275–287

Dewdney J, Reuber TL, Wildermuth MC, Devoto A, Cui J, Stutius LM, Drummond EP & Ausubel FM (2000) Three unique mutants of Arabidopsis identify eds loci required for limiting growth of a biotrophic fungal pathogen. *Plant J* 24: 205–218

Duan C-G, Wang X, Zhang L, Xiong X, Zhang Z, Tang K, Pan L, Hsu C-C, Xu H, Tao WA, *et al* (2017) A protein complex regulates RNA processing of intronic heterochromatin-containing genes in Arabidopsis. *Proc Natl Acad Sci U S A* 114: E7377–E7384

Eulgem T, Tsuchiya T, Wang X-J, Beasley B, Cuzick A, Tör M, Zhu T, McDowell JM, Holub E & Dangl JL (2007) EDM2 is required for RPP7-dependent disease resistance in Arabidopsis and affects RPP7 transcript levels. *Plant J* 49: 829–839

Huot B, Yao J, Montgomery BL & He SY (2014) Growth–Defense Tradeoffs in Plants: A Balancing Act to Optimize Fitness. *Mol Plant* 7: 1267–1287

Jirage D, Tootle TL, Reuber TL, Frost LN, Feys BJ, Parker JE, Ausubel FM & Glazebrook J (1999) Arabidopsis thaliana PAD4 encodes a lipase-like gene that is important for salicylic acid signaling. *Proc Natl Acad Sci U S A* 96:

13583–13588

Karasov TL, Chae E, Herman JJ & Bergelson J (2017) Mechanisms to Mitigate the Trade-Off between Growth and Defense. *Plant Cell* 29: 666–680

Kempel A, Schädler M, Chrobock T, Fischer M & van Kleunen M (2011) Tradeoffs associated with constitutive and induced plant resistance against herbivory. *Proc Natl Acad Sci U S A* 108: 5685–5689

Lai Y, Cuzick A, Lu XM, Wang J, Katiyar N, Tsuchiya T, Le Roch K, McDowell JM, Holub E & Eulgem T (2019) The Arabidopsis RRM domain protein EDM3 mediates race-specific disease resistance by controlling H3K9me2-dependent alternative polyadenylation of RPP7 immune receptor transcripts. *Plant J* 97: 646–660

Lai Y, Lu XM, Daron J, Pan S, Wang J, Wang W, Tsuchiya T, Holub E, McDowell JM, Slotkin RK, *et al* (2020) The Arabidopsis PHD-finger protein EDM2 has multiple roles in balancing NLR immune receptor gene expression. *PLoS Genet* 16: e1008993

Lee Y, Rubio MC, Alassimone J & Geldner N (2013) A mechanism for localized lignin deposition in the endodermis. *Cell* 153: 402–412

Lei M, La H, Lu K, Wang P, Miki D, Ren Z, Duan C-G, Wang X, Tang K, Zeng L, *et al* (2014) Arabidopsis EDM2 promotes IBM1 distal polyadenylation and regulates genome DNA methylation patterns. *Proc Natl Acad Sci U S A* 111: 527–532

Lorrain S, Vailleau F, Balagué C & Roby D (2003) Lesion mimic mutants: keys for deciphering cell death and defense pathways in plants? *Trends Plant Sci* 8: 263–271

McDowell JM, Cuzick A, Can C, Beynon J, Dangl JL & Holub EB (2000) Downy mildew (Peronospora parasitica) resistance genes in Arabidopsis vary in functional requirements for NDR1, EDS1, NPR1 and salicylic acid accumulation. *Plant J* 22: 523–529

Moeder W & Yoshioka K (2008) Lesion mimic mutants: A classical, yet still fundamental approach to study programmed cell death. *Plant Signal Behav* 3: 764–767

Neuser J, Metzen CC, Dreyer BH, Feulner C, van Dongen JT, Schmidt RR & Schippers JHM (2019) HBI1 Mediates the Trade-off between Growth and Immunity through Its Impact on Apoplastic ROS Homeostasis. *Cell Rep* 28: 1670–1678.e3

Saze H, Kitayama J, Takashima K, Miura S, Harukawa Y, Ito T & Kakutani T (2013) Mechanism for full-length RNA processing of Arabidopsis genes containing intragenic heterochromatin. *Nat Commun* 4: 2301

Schopfer P (1996) Hydrogen peroxide-mediated cell-wall stiffening in vitro in maize coleoptiles. *Planta* 199: 43–49

Scott IM, Clarke SM, Wood JE & Mur LAJ (2004) Salicylate accumulation inhibits growth at chilling temperature in Arabidopsis. *Plant Physiol* 135: 1040–1049

Smirnoff N & Arnaud D (2019) Hydrogen peroxide metabolism and functions in plants. *New Phytol* 221: 1197–1214

Torres MA, Dangl JL & Jones JDG (2002) Arabidopsis gp91phox homologues AtrbohD and AtrbohF are required for accumulation of reactive oxygen intermediates in the plant defense response. *Proc Natl Acad Sci U S A* 99: 517–522

Tsuchiya T & Eulgem T (2010) Co-option of EDM2 to distinct regulatory modules in Arabidopsis thaliana development. *BMC Plant Biology* 10: 203 doi:10.1186/1471-2229-10-203 [PREPRINT]

Tsuchiya T & Eulgem T (2013) An alternative polyadenylation mechanism coopted to the *Arabidopsis RPP7* gene through intronic retrotransposon domestication. *Proceedings of the National Academy of Sciences* 110 doi:10.1073/pnas.1312545110 [PREPRINT]

Wang X, Duan C-G, Tang K, Wang B, Zhang H, Lei M, Lu K, Mangrauthia SK, Wang P, Zhu G, *et al* (2013) RNA-binding protein regulates plant DNA methylation by controlling mRNA processing at the intronic heterochromatin-containing gene IBM1. *Proc Natl Acad Sci U S A* 110: 15467–15472

Wojtaszek P (1997) Oxidative burst: an early plant response to pathogen infection. *Biochem J* 322 (Pt 3): 681–692

Zhang Y, Goritschnig S, Dong X & Li X (2003) A gain-of-function mutation in a plant disease resistance gene leads to constitutive activation of downstream signal transduction pathways in suppressor of npr1-1, constitutive 1. *Plant Cell* 15: 2636–2646

Züst T, Rasmann S & Agrawal AA (2015) Growth–defense tradeoffs for two major anti-herbivore traits of the common milkweed Asclepias syriaca. *Oikos*

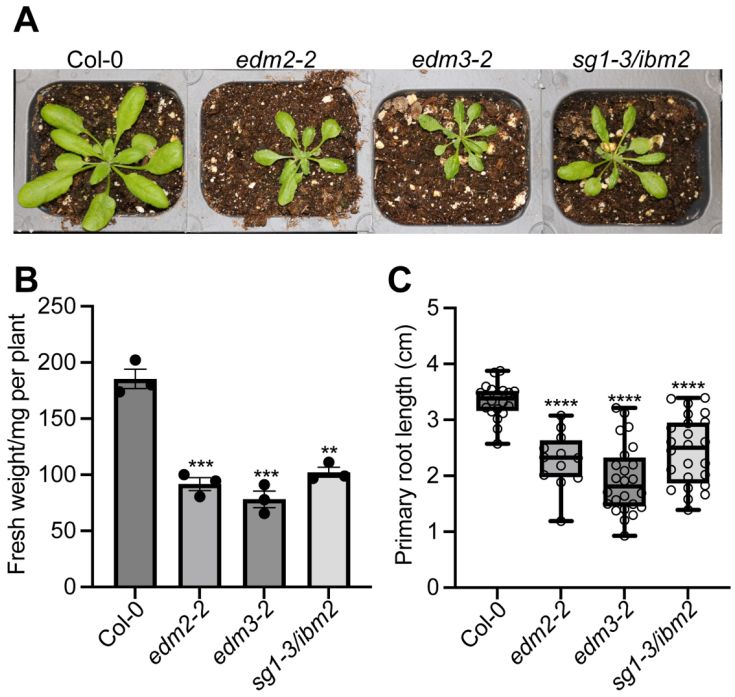

Figure 4.1. EDM2, EDM3 and IBM2 have positive effects on plant development.
A. Representative images of 25 day-old plants grown under long day conditions.
B. Average fresh weight of 25 day-old plants of the indicated genotypes. Error bars represent standard errors from three independent experiments, each with eighteen plants.
C. Primary root length of 7 day-old plants of the indicated genotypes. Primary root length of more than twelve plants of each genotype was measured by ImageJ.
Data information: Asterisks indicate significant differences analyzed by student's t-test. (**, $p < 0.01$; ***, $p < 0.001$; ****, $p < 0.0001$).

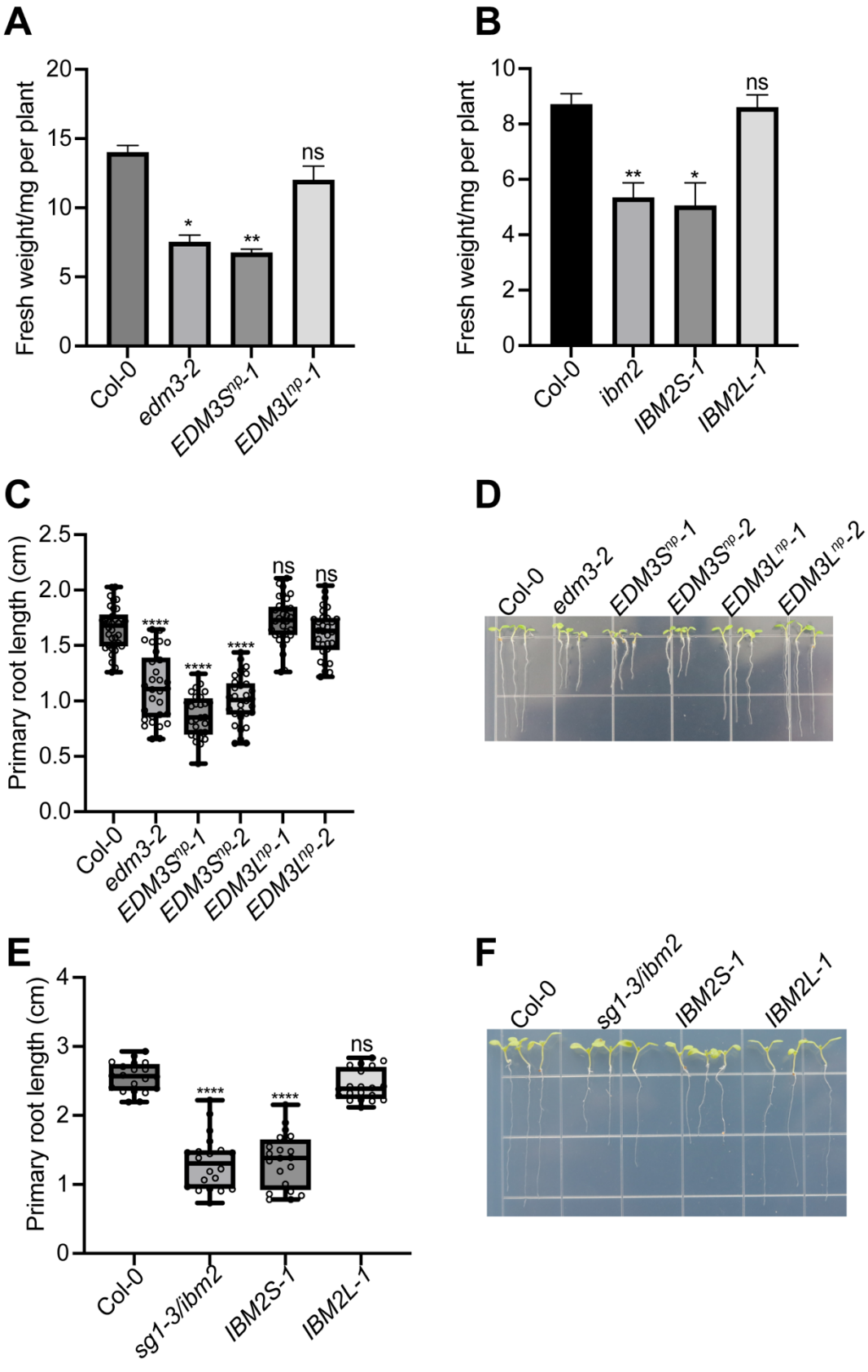
A
Fresh weight/mg per plant
20
15
10
5
0
*
**
ns
Col-0
edm3-2
EDM3S^np-1
EDM3L^np-1
B
Fresh weight/mg per plant
10
8
6
4
2
0
**
*
ns
Col-0
ibm2
IBM2S-1
IBM2L-1
C
Primary root length (cm)
2.5
2.0
1.5
1.0
0.5
0.0
****
****
****
ns
ns
Col-0
edm3-2
EDM3S^np-1
EDM3S^np-2
EDM3L^np-1
EDM3L^np-2
D
Col-0
edm3-2
EDM3S^np-1
EDM3S^np-2
EDM3L^np-1
EDM3L^np-2
E
Primary root length (cm)
4
3
2
1
0
****
****
ns
Col-0
sg1-3/ibm2
IBM2S-1
IBM2L-1
F
Col-0
sg1-3/ibm2
IBM2S-1
IBM2L-1

Figure 4.2. Only longer isoforms of EDM3 and IBM2 can rescue growth defects in *edm3* and *ibm2* mutants.
A & B. Fresh weight of 15 day-old plants of EDM3 isoform-specific complementation lines and 12 days old plants of IBM2 isoform-specific complementation lines, grown under long days.
C & E. Primary root length of 5 day-old plants of EDM3-and IBM2-isoform specific complementation lines.
D & F. Representative images of plants used in panels C and E.
Data information: Error bars represent standard errors from three independent experiments. Asterisks indicate significant differences analyzed by student's t-test. (*, $p < 0.05$; **, $p < 0.01$; ****, $p < 0.0001$; ns, no significance). $n \geq 28$ (C) and $n \geq 20$ (E).

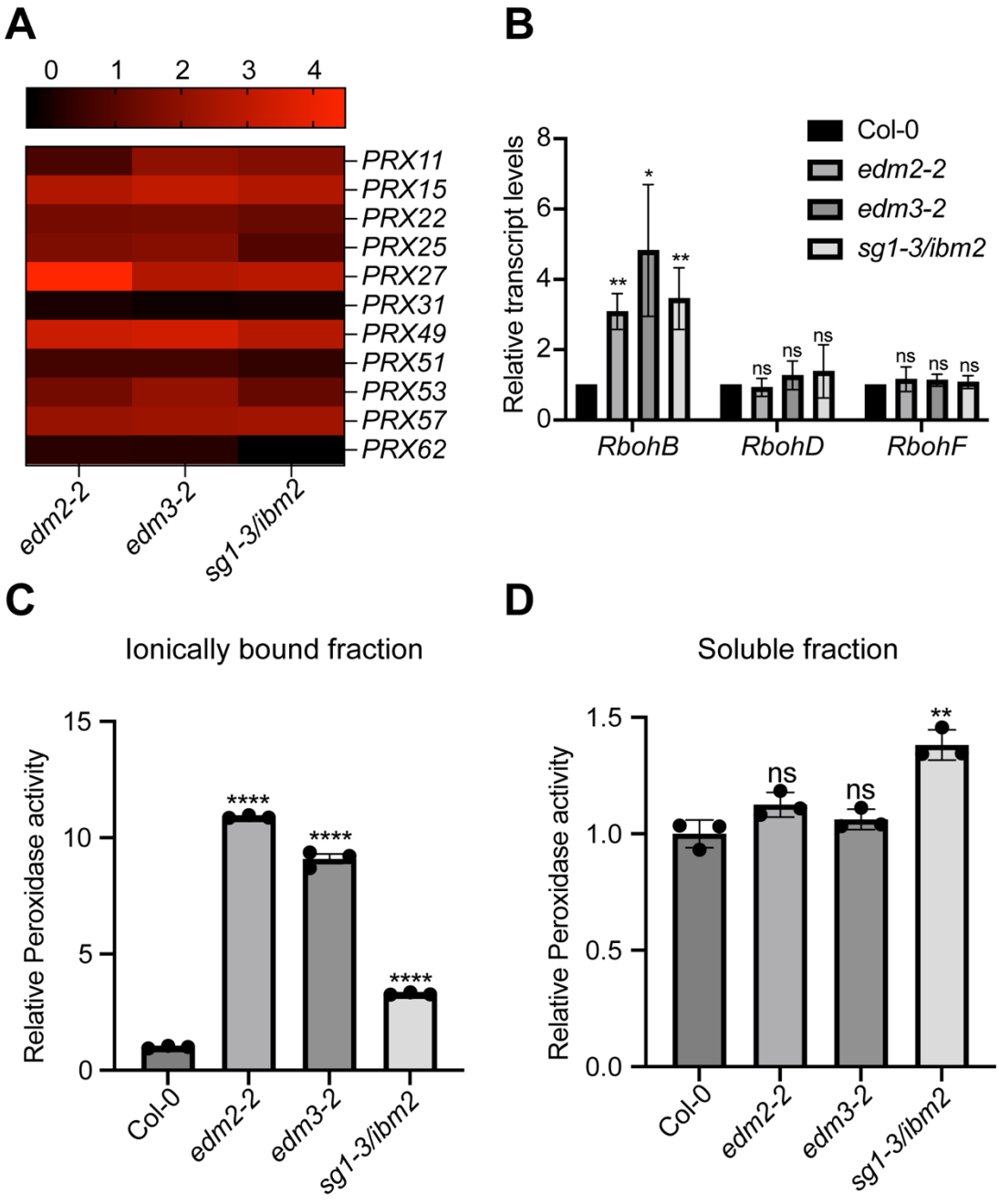
A
0
1
2
3
4
PRX11
PRX15
PRX22
PRX25
PRX27
PRX31
PRX49
PRX51
PRX53
PRX57
PRX62
edm2-2
edm3-2
sg1-3/ibm2
B
Relative transcript levels
Col-0
edm2-2
edm3-2
sg1-3/ibm2
RbohB
RbohD
RbohF
C
Ionically bound fraction
Relative Peroxidase activity
Col-0
edm2-2
edm3-2
sg1-3/ibm2
D
Soluble fraction
Relative Peroxidase activity
Col-0
edm2-2
edm3-2
sg1-3/ibm2

Figure 4.3. EDM2, EDM3 and IBM2 regulate peroxidase activity by down-regulating expression levels of peroxidase genes.

A. The transcript levels of peroxidase genes in mutants of *EDM2*, *EDM3* and *IBM2* in the aerial parts measured by qRT-PCR. Log2-FoldChange (FD) relative to transcript levels in wild type was used to create this heatmap. The bright red color represents the highest increase relative to wild type plants.

B. Transcript levels of NADPH oxidase genes in mutants of *EDM2*, *EDM3* and *IBM2* in the aerial parts measured by qRT-PCR.

C & D. Relative peroxidase activity in mutants of *EDM2*, *EDM3* and *IBM2*. Peroxidase activity was measured in the aerial parts of two-week-old plants, divided by fresh weight and shown relative to the wild type plants.

Data information: Error bars represent standard errors from three independent experiments. Asterisks indicate significant differences analyzed by student's t-test. (*, $p < 0.05$; **, $p < 0.01$; ****, $p < 0.0001$; ns, no significance).

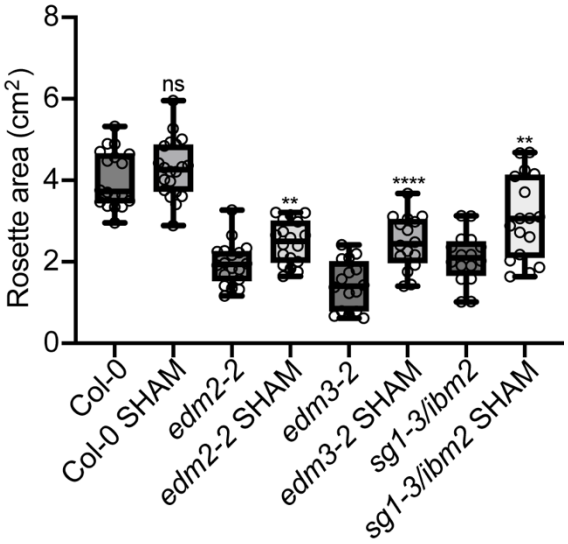

Figure 4.4. Growth defects in mutants of EDM2, EDM3 and IBM2 are partly rescued by inhibiting peroxidase activity.

Rosette areas of 25 day-old plants of the indicated genotypes. 20μM SHAM was applied to soil grown plants at day 14 and day 16. Rosette area ($n \geq 16$) was measured by ImageJ.

Data information: Asterisks indicate significant differences analyzed by student's t-test. (*, $p < 0.05$; **, $p < 0.01$; ****, $p < 0.0001$; ns, no significance).

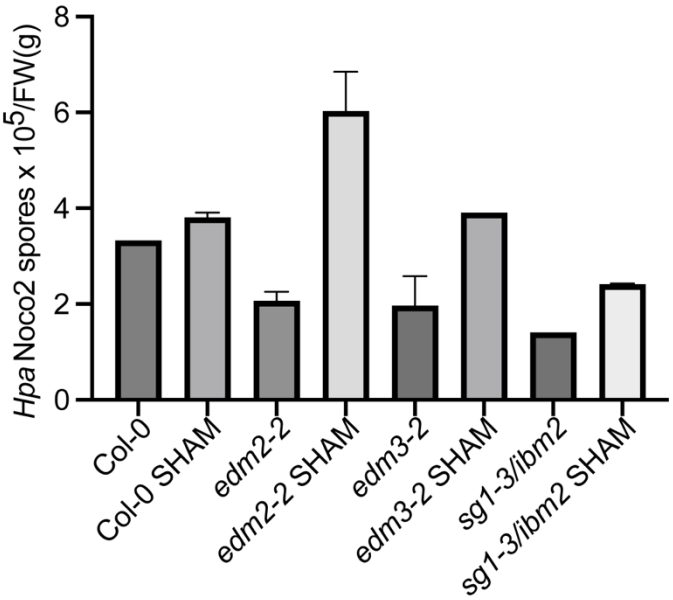

Figure 4.5. Increased basal defense in mutants of *EDM2*, *EDM3* and *IBM2* is dependent on peroxidase activity.
Two week-old plants of the indicated genotypes were pre-treated with 20µM SHAM 24 hours before sprayed-inoculated with 1 x 10^4/ml *Hpa*Noco2 spores. *Hpa*Noco2 spores were counted one week after infection. Spore numbers were normalized to the corresponding fresh weights. Experiment was repeated once.

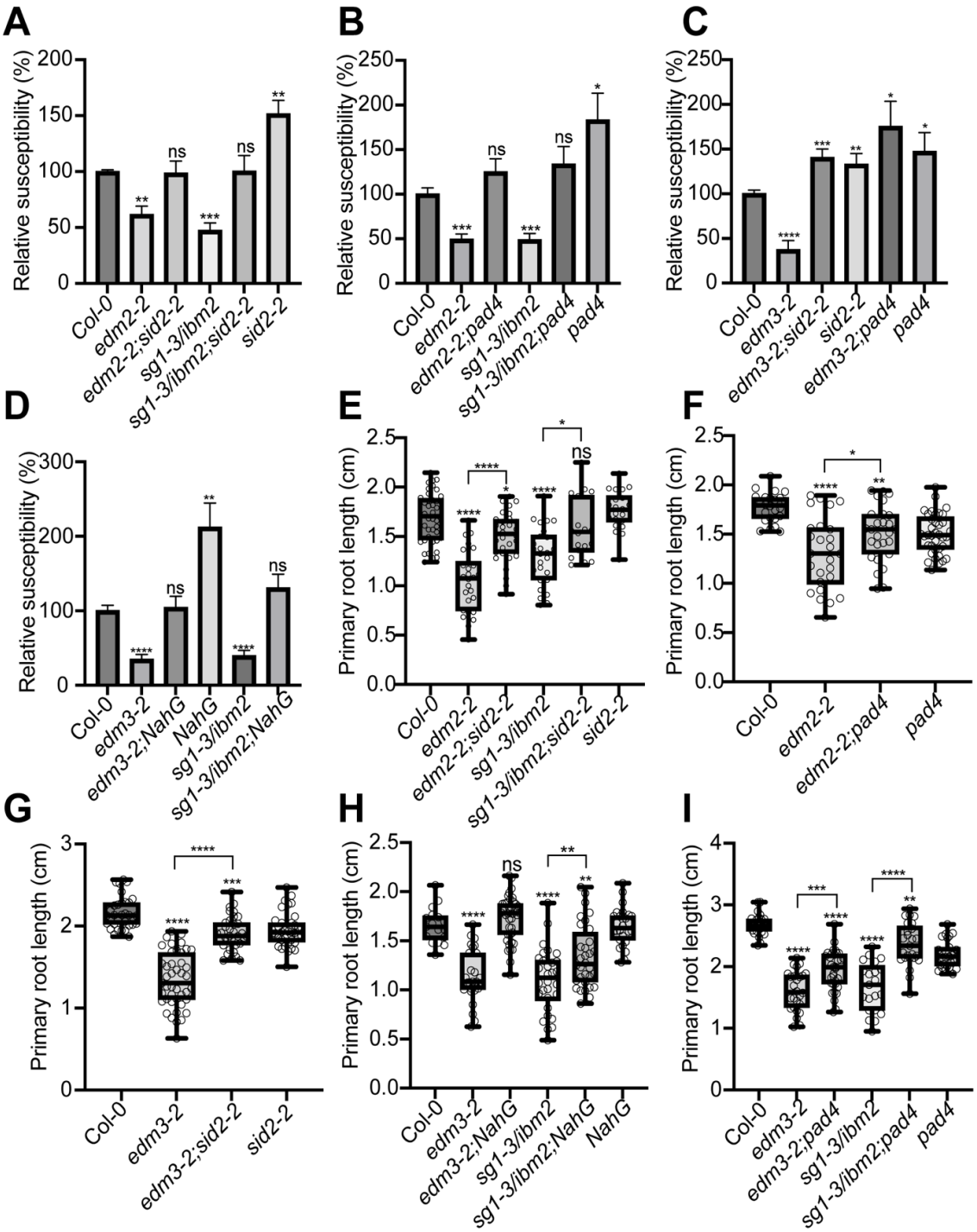
A
Relative susceptibility (%)
Col-0
edm2-2
edm2-2;sid2-2
sg1-3/ibm2
sg1-3/ibm2;sid2-2
sid2-2
B
Relative susceptibility (%)
Col-0
edm2-2
edm2-2;pad4
sg1-3/ibm2
sg1-3/ibm2;pad4
pad4
C
Relative susceptibility (%)
Col-0
edm3-2
edm3-2;sid2-2
sid2-2
edm3-2;pad4
pad4
D
Relative susceptibility (%)
Col-0
edm3-2
edm3-2;NahG
NahG
sg1-3/ibm2
sg1-3/ibm2;NahG
E
Primary root length (cm)
Col-0
edm2-2
edm2-2;sid2-2
sg1-3/ibm2
sg1-3/ibm2;sid2-2
sid2-2
F
Primary root length (cm)
Col-0
edm2-2
edm2-2;pad4
pad4
G
Primary root length (cm)
Col-0
edm3-2
edm3-2;sid2-2
sid2-2
H
Primary root length (cm)
Col-0
edm3-2
edm3-2;NahG
sg1-3/ibm2
sg1-3/ibm2;NahG
NahG
I
Primary root length (cm)
Col-0
edm3-2
edm3-2;pad4
sg1-3/ibm2
sg1-3/ibm2;pad4
pad4

Figure 4.6. Enhanced basal immunity in mutants of *EDM2*, *EDM3* and *IBM2* requires *SID2, PAD4* and SA.

A-D. Enhanced basal immunity in *edm2*, *edm3* and *ibm2* mutants was disrupted by introducing the *sid2-2* or *pad4* mutations as well as the *NahG* transgene. Two week-old seedlings were sprayed-inoculated with 3 x 10^4/ml *Hpa*Noco2 spores. *Hpa*Noco2 spores were counted one week post infection, which were divided by the corresponding fresh weight and shown as percentage relative to wild type.

E-I. Primary root length of 5 day-old plants of the indicated genotypes. Primary root length of the indicated genotypes was measured using ImageJ.

Data information: Error bars represent standard errors from three independent experiments. Asterisks indicate significant differences analyzed by student's t-test. (*, $p < 0.05$; **, $p < 0.01$; ***, $p < 0.001$; ****, $p < 0.0001$; ns, no significance). $n \geq 18$ (E), $n \geq 24$ (F), $n \geq 33$ (G), $n \geq 17$ (H), $n \geq 21$ (I).

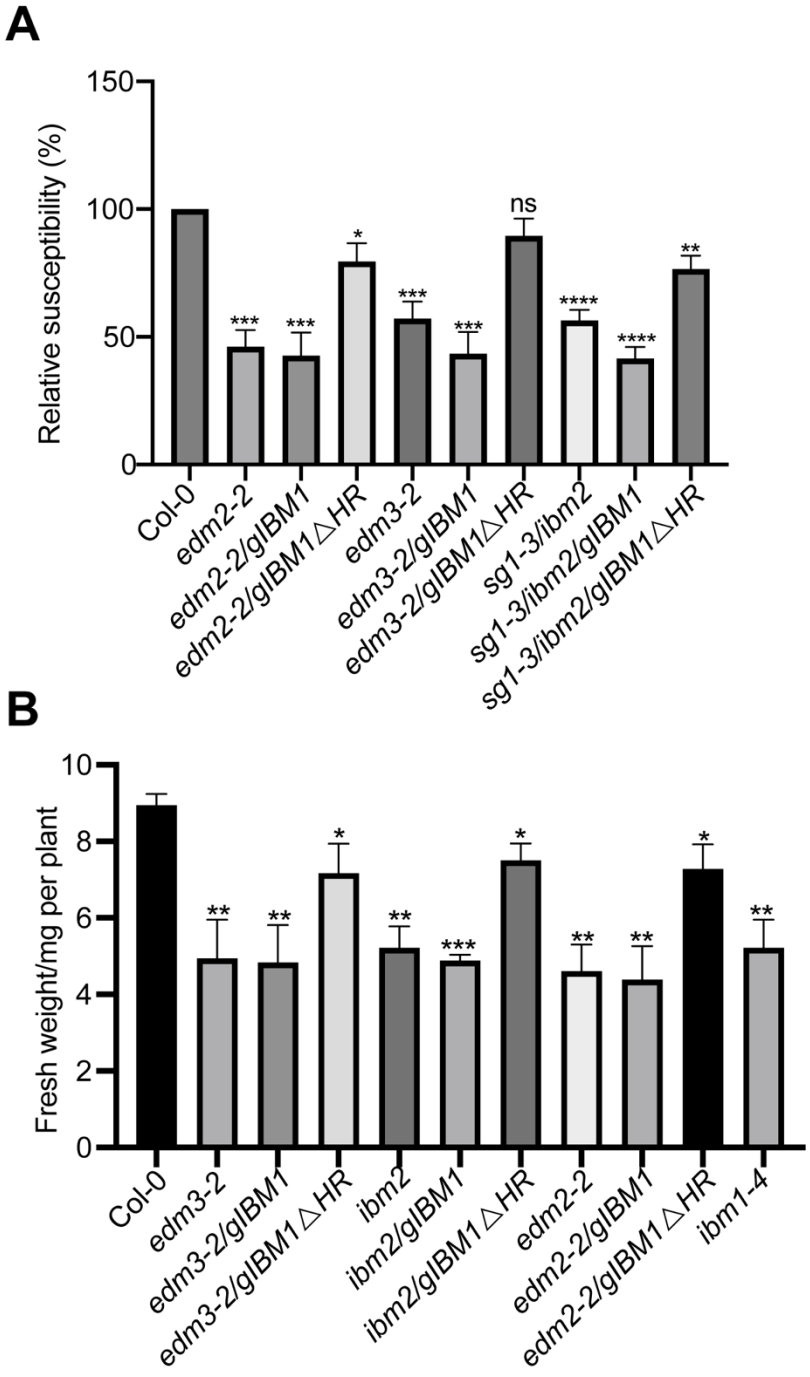
A
Relative susceptibility (%)
150
100
50
0
ns
*
**
***
***
***
***
****
****
Col-0
edm2-2
edm2-2/gIBM1
edm2-2/gIBM1△HR
edm3-2
edm3-2/gIBM1
edm3-2/gIBM1△HR
sg1-3/ibm2
sg1-3/ibm2/gIBM1
sg1-3/ibm2/gIBM1△HR
B
Fresh weight/mg per plant
10
8
6
4
2
0
*
*
*
**
**
**
**
**
***
**
Col-0
edm3-2
edm3-2/gIBM1
edm3-2/gIBM1△HR
ibm2
ibm2/gIBM1
ibm2/gIBM1△HR
edm2-2
edm2-2/gIBM1
edm2-2/gIBM1△HR
ibm1-4

Figure 4.7. Growth defects and *Hpa*Noco2 susceptibility were partly rescued by IBM1L.
A. *Hpa*Noco2 susceptibility was partly rescued in mutants of *EDM2*, *EDM3* and *IBM2* when introducing a genomic *IBM1* with a deletion of its heterochromatic repeats. Two-week old plants were sprayed-inoculated with 3 x 10^4/ml *Hpa*Noco2 spores. *Hpa*Noco2 spores were counted one week post infection. The resulting spore numbers were divided by the respective fresh weight and shown as percentage relative to wild type.
B. Fresh weight of twelve day-old plants of the indicated genotypes.
Data information: Error bars represent standard errors from three independent experiments. Asterisks indicate significant difference analyzed by student's t-test (*, $p < 0.05$; **, $p < 0.01$; ***, $p < 0.001$; ****, $p < 0.0001$).

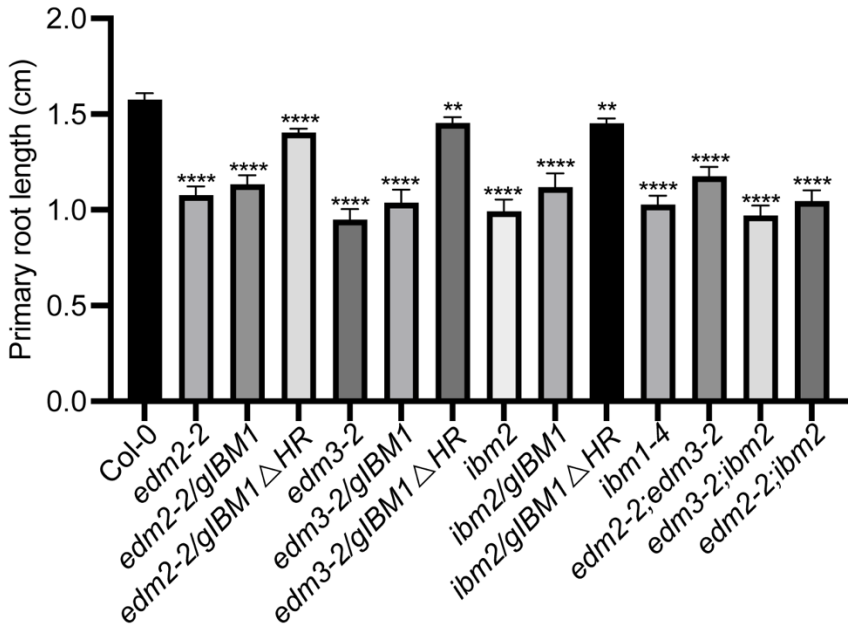

Figure 4.8. Short primary root length in mutants of *EDM2*, *EDM3* and *IBM2* was partly rescued by wild type expression of *IBM1L*.
Primary root lengths of five day-old plants of the indicated genotypes were measured using ImageJ. Error bars represent standard errors. Asterisks indicate significant difference analyzed by student's t-test (****, $p < 0.0001$). $n \geq 20$.

Table 4.1. Primers used in this study

Primer names	Sequence (5'-3')	Notes
PRX11_F	CGGACCAGGAGATGTACACG	
PRX11_R	CCACTGGATCCTCCGCATAC	
PRX15_F	CCAAGGTCTCGATCTCACCG	
PRX15_R	TCTTCCAGCGCTGTTGATGT	
PRX22_F	CCAGACCCAAGTCTGAACCC	
PRX22_R	AAGCATCTGGAGTCACGACA	
PRX25_F	ACCGGAAACTCCGATCCAAC	
PRX25_R	TTCGAACCGTCTCCATTGGG	
PRX27_F	AAAGGAGACAGCGACCCAAG	
PRX27_R	CTAGAGCCGTCGTCGTATCG	
PRX31_F	CGTCGCAACACGTGATCTTC	
PRX31_R	CACCCGACCCACAAACTCTT	
PRX49_F	AGCTCGTGGGTTTGACGTAG	
PRX49_R	AGTGTTGTTTGGTGCAGGGA	
PRX51_F	AGATGGACTTTCGTCGTCGG	
PRX51_R	ATCCTAATGTGTGTGCCCCG	
PRX53_F	TTTCGGCTGTCGGGCTTAAT	
PRX53_R	GGATTTCCTGTCCCGCTGAA	
PRX57_F	ACGGAAGCGTCAGGGAATTT	
PRX57_R	CCAGAGACGGAGATCGTTGG	
PRX62_F	GACTTTGTCCCCAAAACGGC	
PRX62_R	GTCCCCGTCTTCACACCAAT	
ACT8_F	CAGTGTCTGGATTGGTGGTTCTATC	Tsuchiya & Eulgem, 2013
ACT8_R	ATCCCGTCATGGAAACGATGT	Tsuchiya & Eulgem, 2013
RbohB_F	GTAAGTCGTTCGGTGCTATGT	
RbohB_R	CAAACCTCATTGCAACCTCATC	
RbohD_F	CCGGAGACGATTACCTGAGC	
RbohD_R	CGTCGATAAGGACCTTCGGG	
RbohF_F	CTTGGCATTGGTGCAACTCC	
RbohF_R	TCTTTCGTCTTGGCGTGTCA	

Chapter 5

General Conclusions

EDM2, EDM3 and IBM2 are three epigenetic regulators in Arabidopsis that preferentially target genes associated with heterochromatin (Tsuchiya & Eulgem, 2013; Lei *et al*, 2014; Wang *et al*, 2013; Saze *et al*, 2013; Lai *et al*, 2019; Zhang *et al*, 2021). One of their target genes, *RPP7*, encodes a plant immune receptor that specifically recognizes *Hyaloperonospora arabidopsidis* (*Hpa*) Hiks1 (Slusarenko & Schlaich, 2003). EDM2, EDM3 and IBM2 positively regulate *RPP7*-mediated disease resistance against *Hpa*Hiks1 directly by promoting the expression of full-length RPP7-coding transcripts (Tsuchiya & Eulgem, 2013; Lei *et al*, 2014; Saze *et al*, 2013; Lai *et al*, 2019; Duan *et al*, 2017). In contrast, EDM2 is also a negative regulator of basal immunity; likely by suppressing expression of numerous NLR-type immune receptor genes (Lai *et al*, 2020). Overexpression of NLR genes has been shown to result in growth retardation and developmental abnormalties. Thus, EDM2 seems to downregulate a set of NLR genes, to compensate for potential growth penalties caused by promoting *RPP7* expression. Although *edm2* mutants are known to cause growth retardation (Tsuchiya & Eulgem, 2010), is still unknown whether and how EDM2 as well as its interacting partners, EDM3 and IBM2 affect the trade-off between growth and defense. In my dissertation, I not only clearly demonstrate the roles

of specific isoforms of EDM3-and IBM2 in coordinating basal defense and the floral transition, but also show that EDM2, EDM3 and IBM2 likely mediate growth-defense trade-off via modulating levels of reactive oxygen species (ROS). Our findings strongly suggest that EDM2, EDM3 and IBM2 play essential roles in coordinating defense responses and plant development.

The alternative splice isoforms of EDM3 and IBM2 I described in chapter 2 perform differently in defense and flowering time control. Only the longer isoforms, EDM3L and IBM2L, that strongly interact with each other in our yeast two-hybrid assays, are able to promote the floral transition by downregulating expression of the floral suppressor gene *Flowering Locus C* (*FLC*). Moreover, only EDM3L and IBM2L rescue the decline of *FLC* expression during the progression of development prior to the floral transition. This decline is perfectly negatively correlated with the gradual increase of EDM3L and IBM2L transcript levels. Like EDM2, the RRM domain proteins EDM3 and IBM2 were also found to act as negative regulators of basal immunity in my dissertation research. EDM3 and IBM2 not only suppress many NLR genes directly or indirectly but also directly target other defense-associated genes. I further showed for the first time that basal immunity is gradually decreased with plant age prior to the floral transition. My results clearly implicate EDM3L, IBM2L and EDM2 in the regulation of this dynamic change. Overall, the increase of EDM3L and IBM2L expression likely causes a gradual suppression of *FLC* and defense-associated genes, which promotes flowering and concomitantly inhibits basal immunity,

respectively. Coordination of the timing of the floral transition with a decline in basal defense may be critical due limitations in available metabolic resources. Thus, plants preferentially re-allocate such limited resources toward reproductive growth, resulting in a suppression of immune responses.

I showed in Chapter 3 that isoforms of EDM3 and IBM2 selectively bind to the retrotransposon at the first intron of *RPP7* gene. While only the longer isoform IBM2L binds to chromatin in this area, both isoforms of EDM3 bind to it. Consistent with our ChIP-qPCR, IBM2L but not IBM2S rescued the expression of the full-length RPP7-coding transcripts and *Hpa*Hiks1 susceptibility. These findings further support the importance of the interplay of different IBM2 and EDM3 isoforms in defense and developmental processes. An interesting question that needs to be answered in future study is how EDM3 and IBM2 isoforms are regulated to control *RPP7* gene expression.

We previously showed that EDM2 is a negative regulator of basal immunity and its mutants exhibit growth retardation-related phenotypes (Tsuchiya & Eulgem, 2010; Lai *et al*, 2020). We further showed in Chapter 2 that both EDM3 and IBM2 are also negative regulators of basal immunity. However, whether and how EDM2, EDM3 and IBM2 mediate the trade-off between growth and defense remains unknown. In Chapter 4, we showed that EDM2, EDM3 and IBM2 regulate peroxidase activity and ROS homeostasis by down-regulating the expression levels of type III peroxidase genes and one NADPH oxidase gene, RbohB. As type III peroxidases and NADPH oxidases are two main sources of

ROS production (Bolwell & Wojtaszek, 1997; Smirnoff & Arnaud, 2019), it is necessary to quantify H_2O_2 in future to see if H_2O_2 is accumulated in the mutants of EDM2, EDM3 and IBM2. Accumulation of H_2O_2 is known to reduce cell wall extensibility, which restricts plant growth (Schopfer, 1996). Thus, I treated plants with the peroxidase inhibitor, SHAM, to examine if the growth defects observed in *edm2*, *edm3* and *ibm2* mutants can be rescued. As expected, inhibiting peroxidase activity resulted in partial recovery of growth defects in *edm2*, *edm3* and *ibm2* mutants. We further found that peroxidase activity is required for the enhanced immune response in mutants of *EDM2*, *EDM3* and *IBM2*. Therefore, these findings suggest that EDM2, EDM3 and IBM2 mediate the trade-off between defense and growth via modulating ROS homeostasis. Because growth defects can only be partly rescued by inhibiting peroxidase activity, I wondered if there are other mechanisms that affect immunity and growth in *edm2*, *edm3* and *ibm2* mutants. Interestingly, I found that the growth defects in all of these mutants were fully or partly restored when separately crossed with the *sid2-2* and *pad4*, and *NahG* Arabidopsis lines, each of which is deficient in SA mediated immunity. We further found that growth defects and *Hpa*Noco2 susceptibility were partly rescued when *IBM1L* expression levels were restored. Overall, these findings suggest critical and complex effects of EDM2, EDM3 and IBM2 on defense and plant development. One of the most interesting questions that needs to be answered in future is how EDM2, EDM3 and IBM2 regulate type III peroxidase genes. Since EDM2 contains an N^6-adenine methyltransferase-like domain

(Eulgem *et al*, 2007), which suggests possible functions on m^6A modification of RNAs, methylated RNA immunoprecipitation associated with sequencing (MeRIP-seq) can be used to dissect the transcriptomic m^6A levels in mutants of EDM2, EDM3 and IBM2. This is likely to reveal some critical target genes of these regulators and may allow to uncover regulatory mechanisms controlled by them.

References

Bolwell GP & Wojtaszek P (1997) Mechanisms for the generation of reactive oxygen species in plant defence – a broad perspective. *Physiological and Molecular Plant Pathology* 51: 347–366 doi:10.1006/pmpp.1997.0129 [PREPRINT]

Duan C-G, Wang X, Zhang L, Xiong X, Zhang Z, Tang K, Pan L, Hsu C-C, Xu H, Tao WA, *et al* (2017) A protein complex regulates RNA processing of intronic heterochromatin-containing genes in Arabidopsis. *Proc Natl Acad Sci U S A* 114: E7377–E7384

Eulgem T, Tsuchiya T, Wang X-J, Beasley B, Cuzick A, Tör M, Zhu T, McDowell JM, Holub E & Dangl JL (2007) EDM2 is required for RPP7-dependent disease resistance in Arabidopsis and affects RPP7 transcript levels. *Plant J* 49: 829–839

Lai Y, Cuzick A, Lu XM, Wang J, Katiyar N, Tsuchiya T, Le Roch K, McDowell JM, Holub E & Eulgem T (2019) The Arabidopsis RRM domain protein EDM3 mediates race-specific disease resistance by controlling H3K9me2-dependent alternative polyadenylation of RPP7 immune receptor transcripts. *Plant J* 97: 646–660

Lai Y, Lu XM, Daron J, Pan S, Wang J, Wang W, Tsuchiya T, Holub E, McDowell JM, Slotkin RK, *et al* (2020) The Arabidopsis PHD-finger protein EDM2 has multiple roles in balancing NLR immune receptor gene expression. *PLoS Genet* 16: e1008993

Lei M, La H, Lu K, Wang P, Miki D, Ren Z, Duan C-G, Wang X, Tang K, Zeng L, *et al* (2014) Arabidopsis EDM2 promotes IBM1 distal polyadenylation and regulates genome DNA methylation patterns. *Proc Natl Acad Sci U S A* 111: 527–532

Saze H, Kitayama J, Takashima K, Miura S, Harukawa Y, Ito T & Kakutani T (2013) Mechanism for full-length RNA processing of Arabidopsis genes containing intragenic heterochromatin. *Nat Commun* 4: 2301

Schopfer P (1996) Hydrogen peroxide-mediated cell-wall stiffening in vitro in maize coleoptiles. *Planta* 199

Slusarenko AJ & Schlaich NL (2003) Downy mildew of Arabidopsis thaliana caused by Hyaloperonospora parasitica (formerly Peronospora parasitica). *Mol Plant Pathol* 4: 159–170

Smirnoff N & Arnaud D (2019) Hydrogen peroxide metabolism and functions in

plants. *New Phytol* 221: 1197–1214

Tsuchiya T & Eulgem T (2010) Co-option of EDM2 to distinct regulatory modules in Arabidopsis thaliana development. *BMC Plant Biology* 10: 203 doi:10.1186/1471-2229-10-203 [PREPRINT]

Tsuchiya T & Eulgem T (2013) An alternative polyadenylation mechanism coopted to the *Arabidopsis RPP7* gene through intronic retrotransposon domestication. *Proceedings of the National Academy of Sciences* 110 doi:10.1073/pnas.1312545110 [PREPRINT]

Wang X, Duan C-G, Tang K, Wang B, Zhang H, Lei M, Lu K, Mangrauthia SK, Wang P, Zhu G, *et al* (2013) RNA-binding protein regulates plant DNA methylation by controlling mRNA processing at the intronic heterochromatin-containing gene IBM1. *Proc Natl Acad Sci U S A* 110: 15467–15472

Zhang Y-Z, Lin J, Ren Z, Chen C-X, Miki D, Xie S-S, Zhang J, Chang Y-N, Jiang J, Yan J, *et al* (2021) Genome-wide distribution and functions of the AAE complex in epigenetic regulation in Arabidopsis. *J Integr Plant Biol* 63: 707–722